Topological Phases of Matter

Lecture Notes • Summer Term 2021

Nicolai Lang*

Institute for Theoretical Physics III
University of Stuttgart

Updated June 26, 2023

*nicolai.lang@itp3.uni-stuttgart.de

Contents

Preliminaries

Requirements

For this course, we assume that students are familiar with the following concepts:

- Non-relativistic quantum mechanics and second quantization (fermions, bosons, spins, …)
- Basics of condensed matter theory (band theory, quasi particles, …)
- Basics of quantum information (qubits, quantum gates, …)
- Basics of group theory ((non-)abelian groups, linear representations, …)
- For some exercises, basic programming skills are useful (Python, Julia, Mathematica, …)

If you think that you lack knowledge in one of these fields, you may still participate in the course if you close the gaps as we go along.

Literature

A dedicated list with literature is given for each topic; this includes both original research and textbooks (see sections of this script).

Goals

The goal of this course is to explore the realm of "topological quantum phases"—quantum phases that cannot be characterized by the paradigm of spontaneous symmetry breaking. This field is a very active domain of research with potential applications in quantum information processing. I plan to cover topics such as …

- Integer- and [fractional quantum Hall effects]
- Symmetry protected topological phases
- Classification of non-interacting fermionic topological phases
- Topological band structures, Berry phases and Chern numbers
- Classification of interacting bosonic topological phases
- [Projective representations, group cohomology and symmetry fractionalization]
- [Topological order and topological quantum field theories]
- [Anyonic statistics and fusion categories]
- [Topological quantum memories and quantum computation]

As an in-depth review of the these topics would require a dedicated course for each bullet point alone, our goal shall be a bit more modest: At the end of this course you should know the various key concepts that allow for topological characterizations of phases of matter, and you should be aware of their relations and differences (i.e. we aim more for the "big picture" than the details). The topics in [...] may be covered in a follow-up course (due to time constraints).

Note

This script is **not** an extension of the material covered in the lectures but contains the notes I use to prepare them. Please have a look at the given references in each section for more comprehensive coverage.

Key

- The content of this script is color-coded as follows:
    - Text in black is written to the blackboard.
    - Notes in red should be mentioned in the lecture to prevent misconceptions.
    - Notes in blue can be mentioned/noted in the lecture if there is enough time.
    - Notes in green are hints for the lecturer.
- One page of the script corresponds roughly to one covered panel of the blackboard.
- Only equations that are later refered to are numbered.
- Enumerated lists are used for more or less rigorous chains of thought:
  1 leads to 2 leads to 3 ...
- "$\lhd$" reads "consider"
- "$\to$" reads "therefore"
- "➋" reads "see"
- "$\stackrel{\circ}{=}$" denotes a non-trivial equality that requires lengthy, but straightforward calculations
- "$\stackrel{*}{=}$" denotes a non-trivial equality that cannot be derived without additional input
- "$\stackrel{\circ}{\to}$" reads "it is easy to show" (not the Russian style, really easy ...)
- "$\stackrel{*}{\to}$" reads "it is *not* easy to show"
- "$\Rightarrow$" denotes a logical implication
- "$\land$" denotes a logical conjunction
- "$\lor$" denotes a logical disjunction
- "$\square$" denotes a repeated expression
- "w/o" reads "without"
- "w/" reads "with"
- "➋": Internal forward reference ("see below")
- "➌": Internal backward reference ("see above")

0 The Big Picture

> ◉ **Goals of this lecture**
>
> 1. Introduce our objects of interest: Quantum phases and phase transitions
> 2. Sketch the Landau paradigm: Spontaneous symmetry breaking
> 3. Concepts beyond the Landau paradigm: Topological phases
> 4. Sketch different types of topological phases

0.1 Quantum phases and quantum phase transitions

- Phases at $T = 0 \rightarrow$ Groundstate(s) of local Hamiltonians
- Quantum phase transitions driven by *quantum fluctuations*
  (due to non-commuting terms in the Hamiltonian)
- Phase diagrams wrt. *parameters* of the Hamiltonian (e.g. magnetic field)
  (and not temperature)

Examples (that exist in nature and/or can be experimentally realized):

- Superconductors
- Superfluids (e.g. superfluid Helium …)
- Bose-Einstein condensates
- Fermi liquids
- quantum Hall states

Paradigmatic example: the transverse field Ising model

◁ Periodic 1D chain of L spin-1/2:

$$H = -J \sum_{i=1}^{L} \sigma_i^z \sigma_{i+1}^z - h \sum_{i=1}^{L} \sigma_i^x \quad \text{Transverse field Ising model (TIM)} \quad (0.1)$$

with ferromagnetic coupling $J > 0$ and transverse field $h > 0$
(*transverse* since h points in x-direction which is transverse to the z-direction of the interactions)

Observation: $[\sigma_i^z \sigma_{i+1}^z, \sigma_i^x] \neq 0 \rightarrow$ quantum fluctuations

$\rightarrow$ Ground state(s) = (entangled) superpositions of eigenstates of $\sigma_i^z \sigma_{i+1}^z$ for $h \neq 0$

$\rightarrow$ Two qualitatively different parameter regimes:

↑ Notes

- $J \ll h$ ($J \approx 0$): *gapped* phase *unique* ground state

$$|G_+\rangle = |+ + \cdots +\rangle \quad \Rightarrow \quad \langle G_+ | \sigma_i^z \sigma_j^z | G_+ \rangle \xrightarrow{|i-j| \to \infty} 0 \tag{0.2}$$

  $\to$ *Paramagnetic phase* (*disordered* phase)

- $J \gg h$ ($h \approx 0$): *gapped* phase with *2-fold degenerate* ground state

$$|G_\uparrow\rangle = |\uparrow\uparrow \ldots \uparrow\rangle \quad \text{and} \quad |G_\downarrow\rangle = |\downarrow\downarrow \ldots \downarrow\rangle \tag{0.3}$$

$$\Rightarrow \quad \langle G | \sigma_i^z \sigma_j^z | G \rangle \xrightarrow{|i-j| \to \infty} 1 \tag{0.4}$$

$$\text{with} \quad |G\rangle = \alpha |G_\uparrow\rangle + \beta |G_\downarrow\rangle \quad \text{arbitrary} \tag{0.5}$$

  $\to$ *Ferromagnetic phase* (*ordered* phase)
  (It is *not* topologically ordered since σ_i^z is a local observable.)

σ_i^z is a *local order parameter* for the ferromagnetic phase since …

- $\lim_{|i-j| \to \infty} \langle \sigma_i^z \sigma_j^z \rangle = 0$ in the paramagnetic (disordered) phase
- $\lim_{|i-j| \to \infty} \langle \sigma_i^z \sigma_j^z \rangle \neq 0$ in the ferromagnetic (ordered) phase

Note that $[H, \sigma_i^z] \neq 0$, i.e. correlations of the observable at two distant points are a non-trivial phenomenon!

0.2 Spontaneous symmetry breaking

What happends between the two gapped phases for $J \ll h$ and $J \gg h$?

Since the degeneracy in the two gapped phases is different, the gap must close at some critical ratio $g_c = h/J$. $\to$

Schematic spectrum:
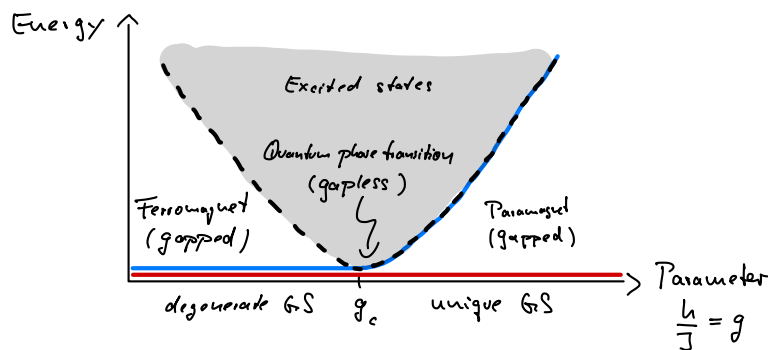
We (or you) will solve this model exactly in this course (➲ Problemset ?).

Long range order:
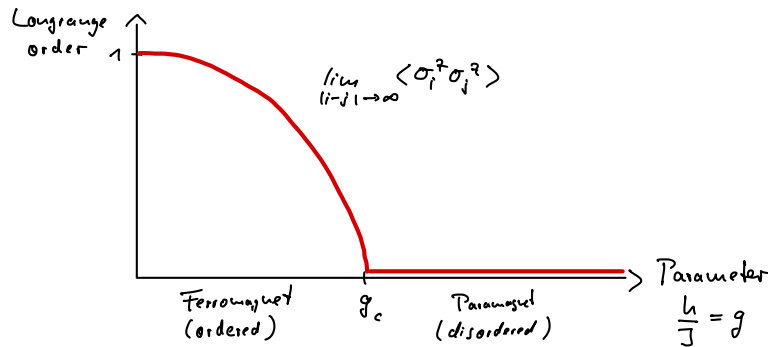
→ Order parameter continuous at phase transition
→ *Continuous (2nd order) phase transition*:
This is the most typical situation with the following features

- gap closes at phase transition

- long-range fluctuations and self-similarity (= quantum fluctuations on all length scales)

- effective conformal field theory (CFT) description

- algebraic decay of correlations (as compared to exponential decay in gapped phases)

What happens at the phase transition?
LEV LANDAU: *Spontaneous symmetry breaking*!

◁ Symmetry group of the TIM *Hamiltonian*:
$G_S = \mathbb{Z}_2 = \{\mathbb{1}, X\}$ with $X = \prod_i \sigma_i^x$ (global spin flip)
Check that $[H, X] = 0$.

◁ Symmetry groups of the TIM *ground states*:

- Paramagnetic phase: $G_E^{(p)} = \{\mathbb{1}, X\} = G_S$ since $X|G_+\rangle = |G_+\rangle$
  → *Symmetric phase*

- Ferromagnetic phase: $G_E^{(f)} = \{\mathbb{1}\} \subsetneq G_S$ since $X|G_\uparrow\rangle = |G_\downarrow\rangle$
  → *Symmetry-broken phase*

> ⁑ **Important**
>
> In the ferromagnetic phase, the ground states $|G_{\uparrow/\downarrow}\rangle$ *spontaneously break* the symmetry G_S of the Hamiltonian → *Spontaneous symmetry breaking (SSB)*

This concept extends to many quantum phases and their phase transitions (e.g. superconductors/superfluids where the particle number symmetry $G_S = \mathrm{U}(1)$ is spontaneously broken) and is also applicable to classical phases and phase transitions (e.g. the transition from liquid to solid where rotation and translation symmetry are broken down to subgroups).

Landau's paradigm (Spontaneous symmetry breaking)

Symmetric ┊		Symmetry-broken		
$G_E = G_S$	$G_E^{(1)}$	$G_E^{(2)}$	$G_E^{(3)}$	$\cdots$

Labels of phases = Subgroups $G_E^{(i)}$ of symmetry group G_S

This concept covers many (quantum and classical) phases and phase transitions, but in the realm of quantum mechanics there is more than just symmetry breaking—there is entanglement!

A few notes before we move on:

- We stress that the SSB of the TIM in 1D is *not* forbidden by the *Mermin-Wagner theorem* since the broken symmetry is discrete ($\mathbb{Z}_2$).

- In 1D, the SSB (and the ferromagnetic phase) does *not* survive at finite temperatures $T > 0$ (recall that the *classical* Ising model does not have a phase transition in 1D).

- By contrast, in 2D (and above) the SSB (and the ferromagnetic phase) *does* survive at finite temperatures $T > 0$.

- A note on "symmetry breaking" in the quantum case:

  The groundstate (for $h = 0$)

  $$|G\rangle = |\uparrow\uparrow \ldots \uparrow\rangle + |\downarrow\downarrow \ldots \downarrow\rangle \tag{0.6}$$

  is clearly *symmetric* under global spin-flips X. So what about the symmetry *breaking*? (Note that this is something without analog in a classical setting where you cannot superimpose arbitrary ground states to form new ground states.) Mathematically, the two symmetry-breaking states $|G_\uparrow\rangle$ and $|G_\downarrow\rangle$ belong to different *superselection sectors* in the thermodynamic limit. As a consequence, the "symmetric state" $|G\rangle$ is not a state in the Hilbert space of the infinite system (strictly speaking, this is the mathematical manifestation of SSB). Physically, the symmetry-broken states $|G_{\uparrow/\downarrow}\rangle$ behave very differently than the symmetry-invariant states $|G_\uparrow\rangle \pm |G_\downarrow\rangle$: Local measurements (of σ_i^z) immediately collapse the latter into a mixture of the former. I.e. the symmetric states are extremely *fragile* (in contrast to the symmetry-broken states). Thus, in an experiment, one would always observe the *symmetry-broken* states so that the notion of "spontaneous symmetry-breaking" effectively carries over to the quantum realm.

0.3 Extending Landau's paradigm: Topological phases

To understand the deficits of Landau's paradigm and the conceptual possibility of topological phases, we first need a …
Formal definition of quantum phases: (Without spontaneous symmetry breaking!)

★ **Definition: Quantum Phases**

◁ Gapped, local Hamiltonians H_a and H_b with unique ground states $|\Omega_a\rangle$ and $|\Omega_b\rangle$.

They belong to the same quantum phase iff there is a family of *gapped* and *local* Hamiltonians $\hat{H}(\alpha)$

↑ Notes

that depends continuously on $\alpha \in [0, 1]$ such that $H_a = \hat{H}(0)$ and $H_b = \hat{H}(1)$.

The two constraints *gapped* and *local* ensure that the macroscopic properties of the ground states only change gradually along the path (which precludes the traversal of phase boundaries).

◁ Parameterspace of local Hamiltonians (without SSB, $G_E = G_S$):
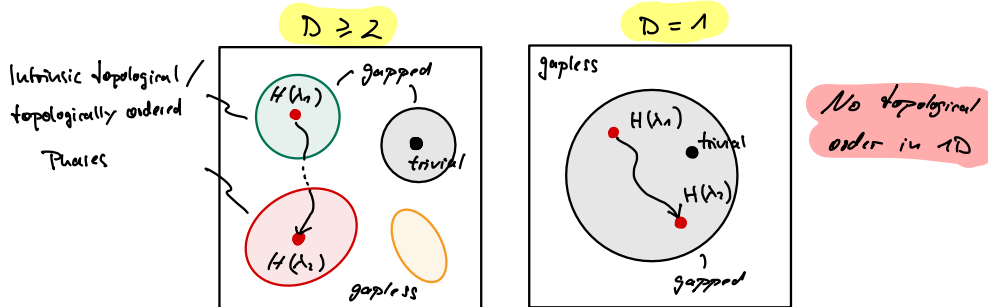
- *Trivial phase:* Ground state = disentangled product state (e.g. $|+\rangle \otimes |+\rangle \otimes \cdots$)
- *Topological phase:* Ground state = long-range entangled state
  (different patterns of long-range entanglement = different topological phases)

This splitting can also occur for Hamiltonians *with* SSB and a fixed subgroup G_E. We will not discuss this case in this course.

---

† Note: Constant depth quantum circuits [1]

There is an alternative (but equivalent) definition of quantum phases in terms of local unitary circuits with constant depth:
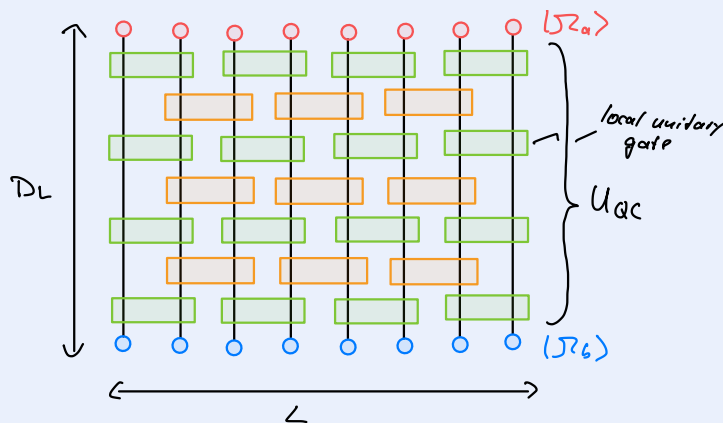
Then, $|\Omega_a\rangle$ and $|\Omega_b\rangle$ belong to the same quantum phase, iff

$$|\Omega_a\rangle = U_{\mathrm{QC}}|\Omega_b\rangle \tag{0.7}$$

where U_{QC} is a local quantum circuit of constant depth $D_L = \mathrm{const}$ for $L \to \infty$.

This definition can be shown to be equivalent to the one given above [1]. It formalizes the notion that two states belong to the same quantum phase if they share the same "pattern of long-range entanglement."

Some consequences:

- A ground state $|\Omega_a\rangle$ is long-range entangled (= topologically ordered) iff it cannot be transformed into a trivial product state $|\uparrow\uparrow\uparrow\ldots\rangle$ by a constant-depth quantum circuit that is local wrt. the geometry of the system.
- This makes the preparation of topologically ordered states challenging for quantum computers / quantum simulators with locality constraints.

First extension of Landau's paradigm: (Intrinsic) Topological order

---
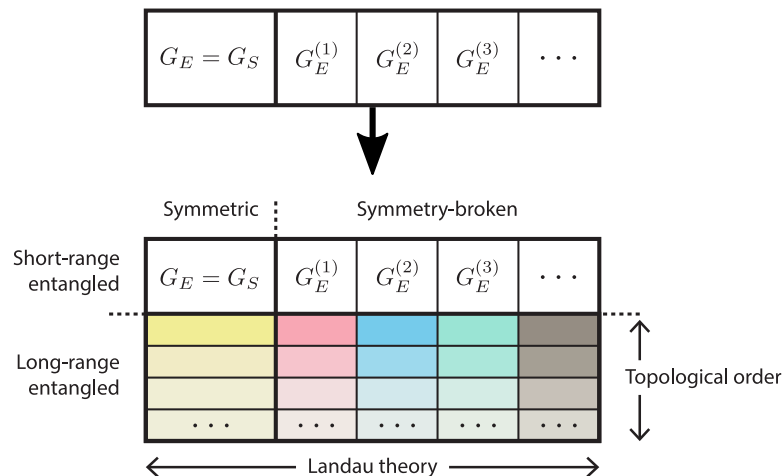
⁂ **Important**

Topological order = Patterns of long-range entanglement

Depending on time, we might discuss this concept at the end of this course: ➋ Chapter 3

Examples (existing in nature): Fractional quantum Hall liquids
Yes, this is all we actually know of! There is a plethora of theoretical models, but none of them has been realized so far …

But wait! There is more …

Adding patterns of long-range entanglement to our labeling scheme produces a more fine-grained classification of quantum phases. However, it can be useful to make this classification even more fine-grained by adding additional symmetry constraints. Let us motivate this concept by a classical system:

↓ **Interlude: Restrictions on perturbations**

◁ Phase diagram of water:
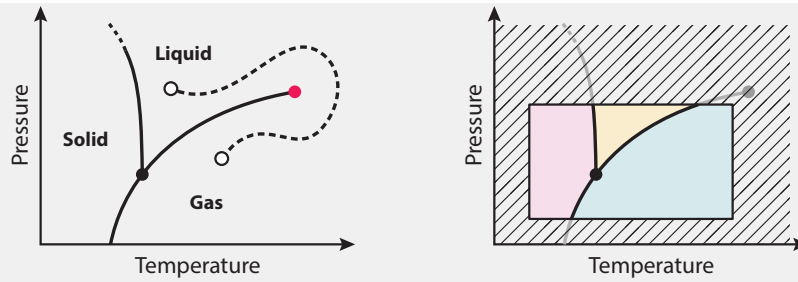
(This argument draws inspiration from classical thermodynamic phases, not quantum phases.)

$\rightarrow$ Restrictions on allowed paths can be useful! (depending on the system …)

Here we will restrict Hamiltonians by *(protecting) symmetries* $G_P \subseteq G_S$:

★ **Definition: Symmetry-protected Quantum Phases**

◁ Gapped, local Hamiltonians H_a and H_b with unique ground states $|\Omega_a\rangle$ and $|\Omega_b\rangle$ and a symmetry group G_P (represented by unitaries U_g on the Hilbert space) with $[H_{a/b}, U_g] = 0$ for all $g \in G_P$.

They belong to the same *symmetry-protected topological (SPT)* phase iff there is a family of *gapped* and *local* Hamiltonians $\hat{H}(\alpha)$ that depends continuously on $\alpha \in [0, 1]$ such that $H_a = \hat{H}(0)$ and $H_b = \hat{H}(1)$ and $[\hat{H}(\alpha), U_g] = 0$ for all $g \in G_P$ and $\alpha \in [0, 1]$.

$\rightarrow$ Phases with the same entanglement pattern can *split* further:
In particular short-range entangled phases that belong to the trivial phase!
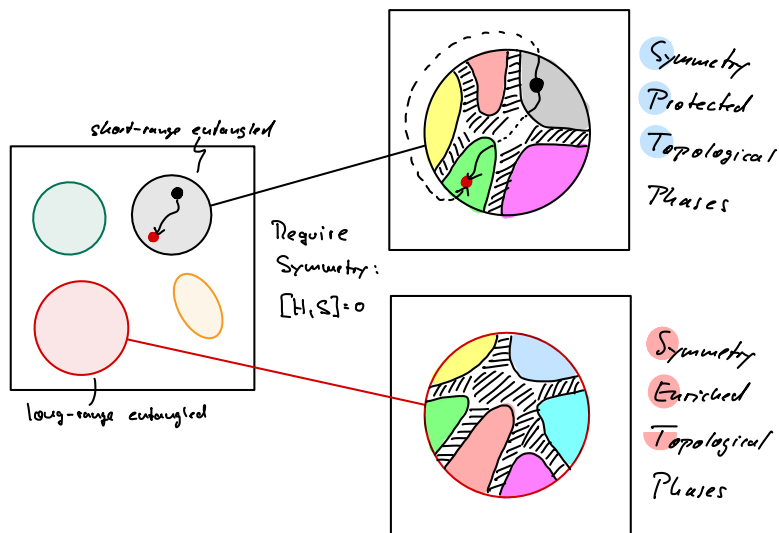
Possible SPTs depend on the protecting symmetry G_P:
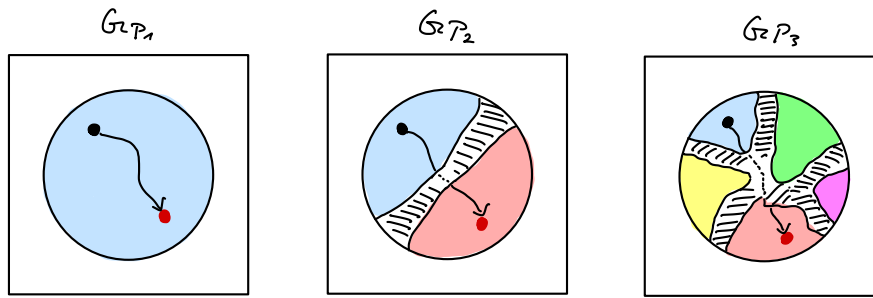
Second extension of Landau's paradigm: Symmetry-protected topological order
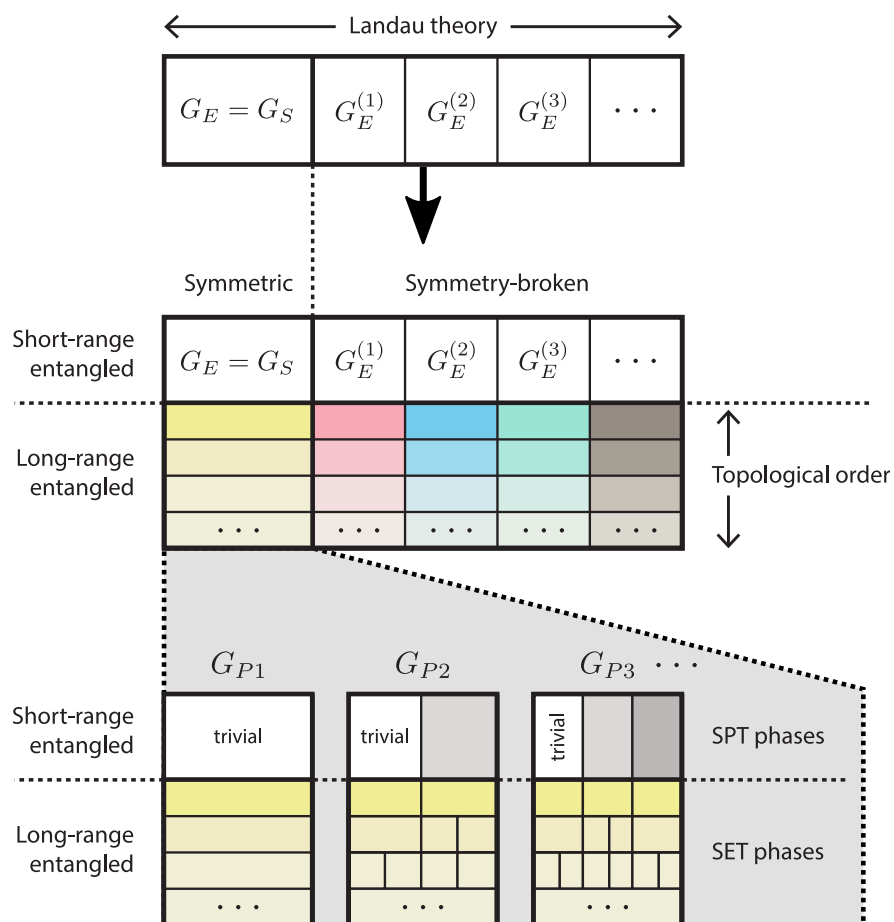
(In this course we focus on phases without SSB.)

How to characterize SPT phases?
(They have no long-range entanglement nor do they break any symmetry!)

- Non-interacting fermions ➔ Chapter 1
- Interacting bosons (in 1D) ➔ Chapter 2

Here a few answers to questions that might come up at this point:

↑ Notes

- Why not *interacting* fermions?
  In 1D, this classification derives from the classification of interacting bosons (also in 1D). In higher dimensions, there are approaches how to classify interacting fermions (this is ongoing research), but this goes beyond the scope of this course.

- Why not *non-interacting* bosons?
  Because non-interacting bosons form a Bose-Einstein condensate (which is a well-understood non-topological quantum phase). Thus topological phases for bosons require interactions.

- Why not interacting bosons in *higher dimensions*?
  This can be done with a generalization of the mathematical methods that we will discuss for the 1D case. We will not discuss these generalizations in this course.

0.4 Summary and Outlook

We can combine all these concepts into a flowchart:
Highlight the three classes that we will discuss in this course.
(A few important original references are given that establish the various concepts.)

↑ Notes
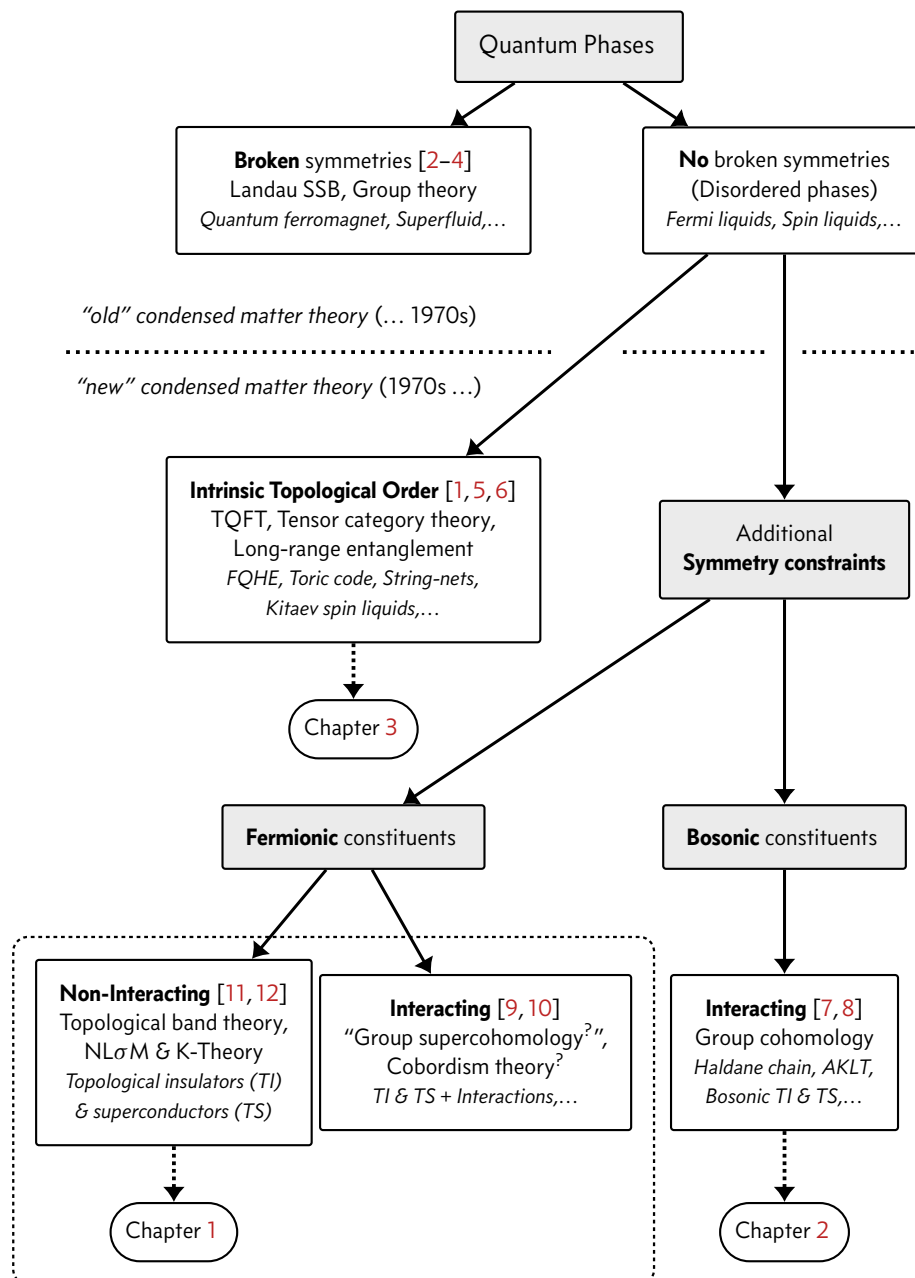
★ **Definition: Nomenclature**

In this course, quantum phases that (1) do not break symmetries and are either (2a) *topologically ordered (TO)* (with and without additional protecting symmetries) or (2b) *symmetry-protected (SPT)* will jointly be refered to as *topological phases (TP)*.

Note the difference between "topologically ordered phases" (which are long-range entangled) and "topological phases" (which can also refer to short-range entangled SPT phases)!

So far, we discussed topological phases on an abstract level. To further motivate these concepts, let us briefly list a few features of these intriguing phases of matter. Note that not every topological phase exhibits all these features! Some of them necessarily require long-range entanglement, some don't. Conversely, long-range entanglement does not necessarily imply all these features. It is quite a mess and we will study various models in this course to to shed light on these features and their origins.

Hallmarks of topological phases:

- TPs cannot be characterized by local order parameters (correlations of local operators decay exponentially, cf. our discussion of the TIM).

- For some TPs, the ground state degeneracy on closed manifolds depends on their topology (whether it is a sphere, a torus, etc.) and is robust in the presence of perturbations [13].

- Some TPs feature exponentially localized excitations (*quasiparticles*) that obey neither fermionic nor bosonic statistics—they are *anyons* and obey *fractional* or *anyonic statistics* [14, 15].

- These quasiparticles can carry fractionalized charges (e.g. a fraction of the electron charge) [16].

- In some TPs, (lattice) defects can exhibit anyonic statistics as well (under continuous deformations of the Hamiltonian).

- Some TPs feature robust, gapless edge states on manifolds with boundaries that allow for scattering-free transport [17].

- The linear response of TPs can be *quantized* to a remarkable degree (even in the presence of disorder!).

- Some TPs have an effective low-energy description in terms of a *topological quantum field theory (TQFT)* [18] (a quantum field theory defined by an action that is a topological invariant).

1 Topological phases of non-interacting fermions

1.1 The integer quantum Hall effect

1.1.1 From the classical to the quantum Hall effect

◁ 2D electron gas (2DEG) in perpendicular magnetic field $\boldsymbol{B} = B\boldsymbol{e}_z$:
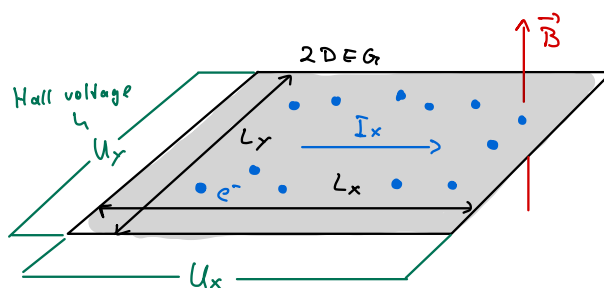
Drude model: (= Electrons as billard balls)

$$m\frac{\mathrm{d}\boldsymbol{v}}{\mathrm{d}t} = -e\boldsymbol{E} - e\,\boldsymbol{v}\times\boldsymbol{B} - \frac{m}{\tau}\boldsymbol{v} \tag{1.1}$$

τ: scattering time

With current density $\boldsymbol{J} = -ne\boldsymbol{v}$ (n: electron density) and $\frac{\mathrm{d}\boldsymbol{v}}{\mathrm{d}t} = 0$ (equilibrium) $\overset{\circ}{\to}$
(Note that $I_x = L_y J_x$ and $U_y = L_y E_y$.)

$$\underbrace{\boldsymbol{J} = \sigma\boldsymbol{E}}_{\text{Ohm's law}} \quad \text{with} \quad \underbrace{\sigma = \begin{bmatrix} \sigma_{xx} & \sigma_{xy} \\ -\sigma_{xy} & \sigma_{yy} \end{bmatrix} = \frac{\sigma_0}{1+\omega_B^2\tau^2}\begin{bmatrix} 1 & -\omega_B\tau \\ \omega_B\tau & 1 \end{bmatrix}}_{\text{Conductivity tensor}} \tag{1.2}$$

with

$$\boxed{\omega_B = \frac{eB}{m} \quad \text{the \textit{cyclotron frequency}}} \tag{1.3}$$

and $\sigma_0 = ne^2\tau/m$ the *DC conductivity* (conductivity w/o magnetic field).

$\overset{\circ}{\to}$ *Resistivity tensor:*

$$\rho \equiv \begin{bmatrix} \rho_{xx} & \rho_{xy} \\ -\rho_{xy} & \rho_{yy} \end{bmatrix} := \sigma^{-1} = \frac{1}{\sigma_0}\begin{bmatrix} 1 & \omega_B\tau \\ -\omega_B\tau & 1 \end{bmatrix} \tag{1.4}$$

Note that Hall *resistance* and Hall *resistivity* are (up to a sign depending on convention) the same:

$$R_{xy} := \frac{U_y}{I_x} = \frac{L_y E_y}{L_y J_x} = \frac{E_y}{J_x} = -\rho_{xy} \tag{1.5}$$

This is *not* true for longitudinal resistance and resistivity:

$$R_{xx} := \frac{U_x}{I_x} = \frac{L_x E_x}{L_y J_x} = \frac{L_x}{L_y} \rho_{xx} \tag{1.6}$$

→ In particular:

$$\rho_{xy} = \frac{\omega_B \tau}{\sigma_0} = \frac{B}{ne} \qquad \text{Independent of } \tau \text{ (= no dissipation) !} \tag{1.7}$$

$$\rho_{xx} = \frac{m}{ne^2\tau} \tag{1.8}$$

→ Classical prediction:
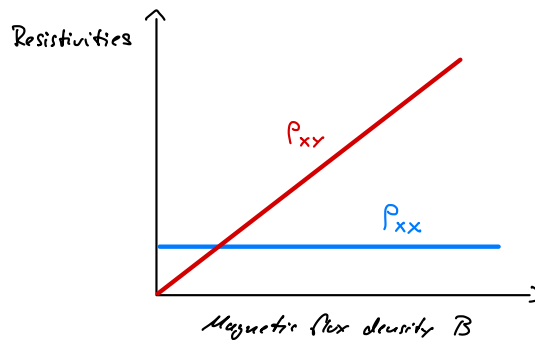
Experimentally valid for high temperatures & weak magnetic fields ($\hbar\omega_B \ll k_B T$).

But *not* for low temperatures & strong magnetic fields ($\hbar\omega_B \gg k_B T$):
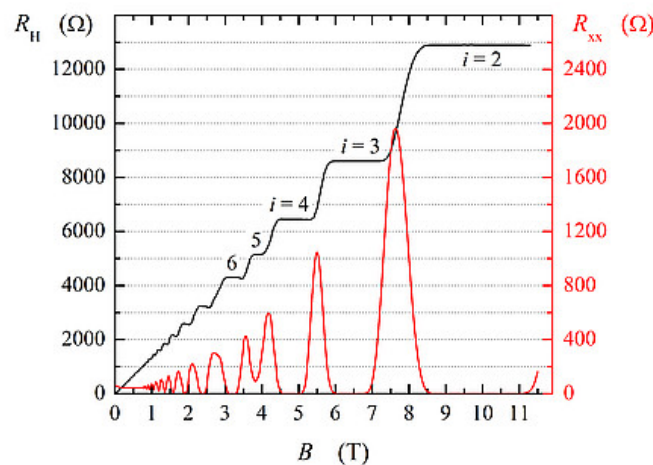
These results are from the electrical quantum metrology division of the PTB (the national metrology institute of Germany) and taken from https://www.ptb.de/cms/en/

`ptb/fachabteilungen/abt2/fb-26/ag-262/the-quantum-hall-resistance.html`; here $R_H = R_{xy} = L_y/L_y \cdot \rho_{xy} = \rho_{xy}$ and $R_{xx} = L_x/L_y \cdot \rho_{xx}$ and $i = \nu$ (see below). This phenomenon was first observed by VON KLITZING in [19] for which he was awarded the 1985 Nobel Prize in Physics.

$\rightarrow$ *Quantized* plateaus for Hall resistivity:

$$\rho_{xy} = \underbrace{\frac{2\pi\hbar}{e^2}}_{R_K} \frac{1}{\nu} \quad \text{with} \quad \nu \in \{1, 2, 3, \dots\} \tag{1.9}$$

R_K: *von Klitzing constant* or *quantum of resistivity* ($R_K \approx 25.8\,\mathrm{k\Omega}$)

By the revision of the SI system of units in 2019, the numerical values of h and e are now fixed. Consequently, the value of the von Klitzing constant R_K is also fixed by definition and does not have to be measured. The integer quantum Hall effect can then be used as a universal (and defining) resistance measurement device (that's why the BTP is measuring the Hall resistance, see above). In particular, the quantization of the first LL is perfect by definition: $\nu = 1.000\dots$. (Using your ohmmeter to measure this quantization would be as if using your balance to measure the weight of the primary kilogram in Paris before the revision of the SI. With one big difference: the primary kilogram was a unique artifact. By contrast, the integer quantum Hall effect is a universal phenomenon that can be reproduced everywhere with the right equipment. Thus "bootstrapping" universal units for measurement is much easier when artifacts are not involved. This was the motivation behind the 2019 revision of the SI system in the first place.)

> ⚛ **Important**
>
> The *exact quantization* of the (macroscopic) Hall response in *disordered samples* is a remarkable and unexpected feature that demands for an explanation!

Historically, the miracle of the quantized Hall response and its "topological explanation" [20] (see below) kick-started the study of topological phases in the first place.

With "exact quantization" one refers to the extraordinary precision to which the experimentally measured Hall resistivity of *different* samples coincides: the relative variations are of order 10^{-10}! A miracle indeed.

1.1.2 Landau levels

> ⚛ **Important**
>
> The *integer* quantum Hall effect can be understood in the context of *non-interacting fermions*. Thus we will focus on *single-particle wavefunctions* in the following.

(This is *not* true for the *fractional* quantum Hall effect ➋ Chapter 3.)

◁ Same setup as before, but now we qantize the system!

Single-particle Hamiltonian of an electron in a magnetic field:

$$H = \frac{1}{2m} \underbrace{(\boldsymbol{p} + e\boldsymbol{A})}_{\boldsymbol{\pi}}{}^2 \tag{1.10}$$

$\boldsymbol{\pi}$: kinetic momentum (gauge independent)
$\boldsymbol{p}$: canonical momentum (gauge dependent)
$\boldsymbol{A}$: gauge potential with $\nabla \times \boldsymbol{A} = B\boldsymbol{e}_z$ (we do not yet fix a gauge!)

Canonical quantization:

$$\left[x_i, p_j\right] = i\hbar\delta_{ij} \tag{1.11}$$

$\to [\pi_x, \pi_y] \stackrel{\circ}{=} -ie\hbar B$

The magnetic field couples the movement in x- and y-direction so that the kinetic momenta form a pair of conjugate observables. This immediately suggests the introduction of ladder operators.

With

$$a := \frac{1}{\sqrt{2e\hbar B}}(\pi_x - i\pi_y) \quad \text{and} \quad a^\dagger = \frac{1}{\sqrt{2e\hbar B}}(\pi_x + i\pi_y) \tag{1.12}$$

we find $[a, a^\dagger] = 1$ and

$$H \stackrel{\circ}{=} \hbar\omega_B \left(a^\dagger a + \frac{1}{2}\right). \tag{1.13}$$

$\to$ Discrete spectrum $E_n = \hbar\omega_B(n + 1/2)$ with $n = 0, 1, 2, \ldots$
$\to$ *Landau levels*

Eigenstates? Degeneracy?

Note that we only used one degree of freedom (= one harmonic oscillator) while we started with two independent degrees of freedom (an electron moving in the plane). The Landau levels must be extensively degenerate to harbour all the needed states! So see this, we must fix a gauge …

We stress that here the gauge field $\boldsymbol{A}$ is *not* a dynamical degree of freedom (like when you quantize the electromagnetic field). Thus gauge fixing is really just a classical inconvenience and does not lead to fundamental problems like negative norm states etc.

Landau gauge

Gauge choice: $\boldsymbol{A} := xB\boldsymbol{e}_y$
(This gauge breaks translation symmetry in x-direction and rotation symmetry in the plane.)

$\to$ Hamiltonian

$$H = \frac{1}{2m}\left[p_x^2 + (p_y + eBx)^2\right] \tag{1.14}$$

Translation symmetry in y-direction (if we consider periodic boundaries in y-direction or take the limit $L_y \to \infty$)
$\to$ Ansatz: $\Psi_k(x, y) = e^{iky}f_k(x)$

$\rightarrow$ *Shifted harmonic oscillator*

$$H \stackrel{\circ}{=} \frac{1}{2m}p_x^2 + \frac{m\omega_B^2}{2}(x + kl_B^2)^2 \tag{1.15}$$

with the *magnetic length*

$$l_B = \sqrt{\frac{\hbar}{eB}} \tag{1.16}$$

The magnetic length is the relevant length scale for electrons in a magnetic field (it is the length scale of their cyclotron orbits).

$\rightarrow$ *Eigenfunctions:*

$$\Psi_{n,k}(x,y) = \mathcal{N} \underbrace{e^{iky}}_{\text{Plane wave in } y\text{-direction}} \underbrace{H_n(x + kl_B^2)\, e^{-\frac{(x+kl_B^2)^2}{2l_B^2}}}_{\text{Harmonic oscillator wavefunctions in } x\text{-direction}} \tag{1.17}$$

with $n = 0, 1, 2, \ldots$ the Landau level index and $k = \frac{2\pi}{L_y}\mathbb{Z}$ the y-momentum

Note that the eigenspaces of H (and the eigenfunctions) are *physical* and therefore gauge independent. What is *unphysical* is the choice of a basis (and the labeling of the basis wavefunctions by "good" quantum numbers). Since the Landau gauge preserves translation symmetry in y-direction, the basis above can be labeled by momenta in y-direction. In other gauges (see below), this is not the case. However, the eigenspaces that are spanned by these wavefunctions are the same for all gauges (of course) and you can linearly combine basis functions of one gauge with basis functions of another.

$\rightarrow$ *Spectrum:* $E_n = \hbar\omega_B(n + 1/2)$ (degenerate in k quantum number!)
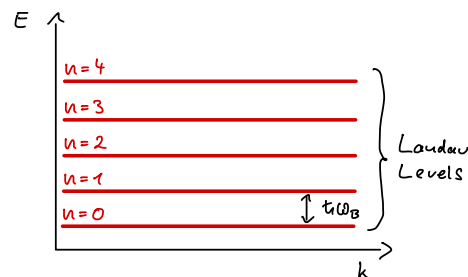
The Landau levels are prototypes for *perfectly flat bands*. If a LL is only partially filled, the many-body properties of the electrons that occupy this level are then determined by their (Coulomb) interactions. This will be important for the *fractional quantum Hall effect* $\bullet$ Chapter 3.

Degeneracy: $0 \leq x \leq L_x \rightarrow$ Allowed k: $-L_x/l_B^2 \leq k \leq 0$
(Since wavefunctions are exponentially localized around $x_k = -kl_B^2$.)

$\rightarrow$ Number of states in each Landau level:

$$N = \frac{L_x/l_B^2 - 0}{2\pi/L_y} = \frac{L_x L_y}{2\pi l_B^2} = \frac{AB}{\Phi_0} = \frac{\Phi}{\Phi_0} \tag{1.18}$$

$\Phi_0 = 2\pi\hbar/e$: *quantum of flux* (recall $R_K = 2\pi\hbar/e^2$ the *quantum of resistivity*)
$A = L_x L_y$: area of the sample

$\rightarrow$ Extensive degeneracy of each Landau level (as expected)

The number of electrons N than can be crammed into each Landau level increases with the magnetic flux through the sample (one electron per quantum of flux). This implies that if we fix the electron density and increase the magnetic flux density, fewer and fewer Landau levels will be needed to distribute all electrons, until for very large B all electrons fit into the lowest Landau level (LLL). Conversely, at "every day" weak-field conditions, Landau levels up to very large indices n are occupied by fermions.

Aside: Symmetric gauge

You will do these calculations in ➜ Problemset 1.

The symmetric gauge breaks translational invariance in both directions but retains the two-dimensional rotation invariance of the system. Instead of k we should expect a basis labeled by angular momentum quantum numbers m.

Gauge choice: $\boldsymbol{A} := -\frac{1}{2}\boldsymbol{r} \times \boldsymbol{B} = -\frac{yB}{2}\boldsymbol{e}_x + \frac{xB}{2}\boldsymbol{e}_y$

Hamiltonian:

$$\text{Eq. (1.13)} \quad \rightarrow \quad H = \frac{\pi^2}{2m} = \hbar\omega_B\left(a^\dagger a + \frac{1}{2}\right). \qquad (1.19)$$

with $a, a^\dagger$ defined via π_x and π_y (this procedure does not depend on the gauge choice since the kinetic momentum is a gauge independent quantity).

Define additional "momentum": (which does not show up in the Hamiltonian!)

$$\tilde{\boldsymbol{\pi}} := \boldsymbol{p} - e\boldsymbol{A} \quad \Rightarrow \quad \left[\tilde{\pi}_x, \tilde{\pi}_y\right] \stackrel{\circ}{=} ie\hbar B \qquad (1.20)$$

(Recall that $\boldsymbol{\pi} = \boldsymbol{p} + e\boldsymbol{A}$.)

Importantly, in Landau gauge the two momenta are independent: $[\pi_i, \tilde{\pi}_j] \stackrel{\circ}{=} 0$
This is violated in other gauges!

$\rightarrow$ Additional ladder operators:

$$b := \frac{1}{\sqrt{2e\hbar B}}(\tilde{\pi}_x + i\tilde{\pi}_y) \quad \text{and} \quad b^\dagger = \frac{1}{\sqrt{2e\hbar B}}(\tilde{\pi}_x - i\tilde{\pi}_y) \qquad (1.21)$$

$\rightarrow [b, b^\dagger] = 1$ and $[a, b] = 0$
$\rightarrow$ *Eigenstates:*

$$|n, m\rangle := \frac{a^{\dagger n} b^{\dagger m}}{\sqrt{n!m!}}|0, 0\rangle \quad \text{with} \quad a|0, 0\rangle = b|0, 0\rangle = 0 \qquad (1.22)$$

$n = 0, 1, 2, \ldots$: Landau level index
$m = 0, 1, 2, \ldots$: Angular momentum index (see below)
m replaces k and generates now the degeneracy of the Landau levels!

Introduce complex coordinates
(the unconventional sign makes the functions below holomorphic instead of antiholomorphic)

$$z := x - iy \quad \text{and} \quad \bar{z} := x + iy \qquad (1.23)$$

and the corresponding Wirtinger derivatives

$$\partial := \frac{1}{2}(\partial_x + i\,\partial_y) \quad \text{and} \quad \bar{\partial} := \frac{1}{2}(\partial_x - i\,\partial_y) \qquad (1.24)$$

Then $\partial z = \bar{\partial}\bar{z} = 1$ and $\partial \bar{z} = \bar{\partial} z = 0$. A function of complex variables is then holomorphic (= satisfies the Cauchy-Riemann equations) if and only if $\bar{\partial} f = 0$, i.e., $f = f(z)$.

Using $p_i = -i\hbar\partial_i$ and the symmetric gauge for $A \to$

$$a = -i\sqrt{2}\left(l_B\bar{\partial} + \frac{z}{4l_B}\right) \quad \text{and} \quad a^\dagger = -i\sqrt{2}\left(l_B\partial - \frac{\bar{z}}{4l_B}\right) \qquad (1.25)$$

$$b = -i\sqrt{2}\left(l_B\partial + \frac{\bar{z}}{4l_B}\right) \quad \text{and} \quad b^\dagger = -i\sqrt{2}\left(l_B\bar{\partial} - \frac{z}{4l_B}\right) \qquad (1.26)$$

$\to$ Lowest Landau level wavefunctions $\Psi_0(z,\bar{z})$:

$$a\Psi_0 = 0 \quad \Leftrightarrow \quad \bar{\partial}\Psi_0 = -\frac{z}{4l_B^2}\Psi_0 \quad \Leftrightarrow \quad \Psi_0(z,\bar{z}) = f(z)e^{-z\bar{z}/4l_B^2} \qquad (1.27)$$

with an arbitrary holomorphic function $f(z)$

The unique state with $m = 0$ is given by

$$b\Psi_0 = 0 \quad \Leftrightarrow \quad \partial\Psi_0 = -\frac{\bar{z}}{4l_B^2}\Psi_0 \quad \Leftrightarrow \quad \partial f(z) = 0 \quad \Leftrightarrow \quad f(z) = \text{const} \qquad (1.28)$$

so that $\Psi_{0,0}(z,\bar{z}) \propto e^{-|z|^2/4l_B^2}$

Other states in the LLL can be constructed with $b^\dagger$:

$$\Psi_{0,m} \propto b^{\dagger m}\Psi_{0,0} \propto \left(l_B\bar{\partial} - \frac{z}{4l_B}\right)^m e^{-z\bar{z}/4l_B^2} \propto \left(\frac{z}{l_B}\right)^m e^{-|z|^2/4l_B^2} \qquad (1.29)$$

$\to$ Holomorphic monomials $\times$ Gaussian

$\to$ In the LLL, m is an angular momentum quantum number:

$$J\Psi_{0,m} = \hbar m\Psi_{0,m} \quad \text{with} \quad J = i\hbar(x\partial_y - y\partial_x) = \hbar(z\partial - \bar{z}\bar{\partial}) \qquad (1.30)$$

with $m = 0, 1, 2, \dots$

Note: In 2D there is only one generator of angular momentum $J = J_z$ and the Lie algebra that generates the rotation group $\mathrm{SO}(2) \simeq U(1)$ (namely $\mathfrak{u}(1) \simeq \mathbb{R}$) is abelian. Consequently there is no algebraic reason for spin to be quantized (as in 3D where spin can take only half-integer values) and all irreducible representations are one-dimensional. Thus there is only *one* spin quantum number needed (to label the irrep) but none to label distinct basis states of an irrep, i.e., $J = m$. So Eq. (1.30) is all there is to say about spin in this context. Note that the abelian "angular momentum algebra" in 2D has also consequences for particles with anyonic statistics which do not only feature "fractional charges" and "fractional statistic" but also "fractional spin" (as in the fractional quantum Hall effect ➲ Chapter 3).

1.1.3 Berry connection and Berry holonomy

The following concepts are very fundamental and will be important throughout this course. The application to the quantized Hall conductivity below is only one example.

Setting: ◁

- Continuous family of gapped Hamiltonians $H(\mathbf{\Gamma})$ with k parameters $\mathbf{\Gamma} = (\Gamma_1, \Gamma_2, \ldots, \Gamma_k)$ and n-fold degenerate ground state space $\mathcal{V}(\mathbf{\Gamma}) \equiv \mathcal{V}(H(\mathbf{\Gamma}))$
  Since $H(\mathbf{\Gamma})$ is continuous and gapped, the dimension of $\mathcal{V}(\mathbf{\Gamma})$ is constant!
  We set $H(\mathbf{\Gamma})|\Psi\rangle = 0$ for $|\Psi\rangle \in \mathcal{V}(\mathbf{\Gamma})$ and all Γ, i.e., the ground state energy is zero.

- Slow variation of parameters $\mathbf{\Gamma}(t)$ for $0 \leq t \leq T$
  "Slow" compared to the (inverse) of the smallest energy gap along the path $\mathbf{\Gamma}(t)$.

- Initial ground state $|\Psi_0\rangle \in \mathcal{V}(\mathbf{\Gamma}(0))$

Question: What happens with $|\Psi_0\rangle$ as $H(\mathbf{\Gamma}(0))$ evolves to $H(\mathbf{\Gamma}(T))$?

We use the following well-known fact:

> ⁂ **Important: Adiabatic theorem [21]**
>
> A physical system remains in its instantaneous eigenstate if a given perturbation is acting on it slowly enough and if there is a gap between the eigenvalue and the rest of the Hamiltonian's spectrum.
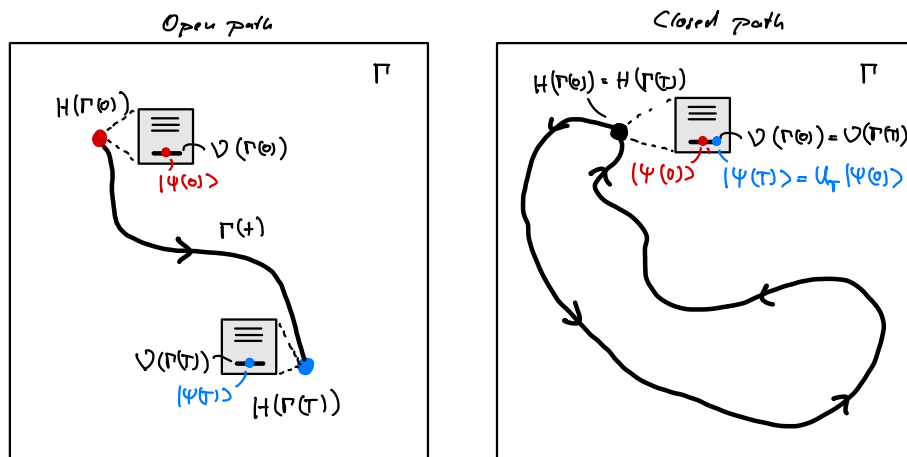
1. Pick a basis $|v_i(\mathbf{\Gamma})\rangle$ of $\mathcal{V}(\mathbf{\Gamma})$ for every $\mathbf{\Gamma}$ $(i = 1, 2, \ldots, n)$
   This choice is not unique and leads to a U(n) gauge degree of freedom, see below. Here we assume that the choice is differentiable (and therefore continuous) along the path $\mathbf{\Gamma}$. This makes it less arbitrary but leaves a lot arbitrariness to choose from. Note that a choice that is globally continuous is often impossible. Then one follows the arguments below on local patches in parameter space on which such a choice is possible.

2. Time-dependent Schrödinger equation (recall that we set the energy to zero):

$$i\hbar\partial_t|\Psi(t)\rangle = H(\mathbf{\Gamma}(t))|\Psi(t)\rangle = 0 \tag{1.31}$$

3. Adiabatic theorem $\rightarrow$ $|\Psi(t)\rangle = \sum_{i=0}^{n} \Psi_i(t)|v_i(\mathbf{\Gamma}(t))\rangle \rightarrow$ (Einstein notation)

$$\partial_t|\Psi(t)\rangle = (\partial_t\Psi_i(t))|v_i(\mathbf{\Gamma}(t))\rangle + \Psi_i(t)(\partial_{\Gamma_l}|v_i(\mathbf{\Gamma}(t))\rangle)(\partial_t\Gamma_l(t)) \tag{1.32}$$

4. Apply $\langle v_j(\mathbf{\Gamma}(t))|$ and use Eq. (1.31):

$$\partial_t \Psi_j(t) = -\Psi_i(t) \langle v_j(\mathbf{\Gamma}(t))|\partial_{\Gamma_l}|v_i(\mathbf{\Gamma}(t))\rangle (\partial_t \Gamma_l(t)) \tag{1.33}$$

5. Define the

$$\boxed{\textit{Berry connection} \quad (\mathcal{A}_l(\mathbf{\Gamma}))_{ji} := -i \langle v_j(\mathbf{\Gamma})|\partial_{\Gamma_l}|v_i(\mathbf{\Gamma})\rangle \quad \in \mathfrak{u}(n)} \tag{1.34}$$

Think of the $\mathcal{A}_l$ as $\mathbf{\Gamma}$-dependent Hermitian $n \times n$-matrices, one for each parameter.

6. Then

$$\partial_t \mathbf{\Psi}(t) = -i(\partial_t \Gamma_l(t))\mathcal{A}_l(\mathbf{\Gamma}(t))\mathbf{\Psi}(t) \tag{1.35}$$

can be solved with the *time- ($\mathcal{T}$) or path-ordered ($\mathcal{P}$) exponential*

$$\mathbf{\Psi}(T) = \mathcal{T} \exp\left[-i \int_0^T \mathcal{A}_l(\mathbf{\Gamma}(t)) \, \partial_t \Gamma_l(t) \, dt\right] \mathbf{\Psi}_0 \tag{1.36}$$

$$= \underbrace{\mathcal{P} \exp\left[-i \int_{\Gamma} \mathbf{\mathcal{A}} \, d\mathbf{\Gamma}\right]}_{=:U_{\Gamma}} \mathbf{\Psi}_0 \tag{1.37}$$

$\mathbf{\mathcal{A}} = (\mathcal{A}_l)$ should be seen as a $\mathfrak{u}(n)$-valued vector field on the parameter space (a 1-form). I.e., $\mathbf{\mathcal{A}}$ can be integrated along parameter paths which, after (path ordered) exponentiation, produces a unitary $U(n)$ that describes the geometric part of the adiabatic evolution on the ground state space.

7. Change local basis by unitary $\Omega(\mathbf{\Gamma}) \in U(n)$: $|v_i'(\mathbf{\Gamma})\rangle := \Omega_{ij}(\mathbf{\Gamma})|v_j(\mathbf{\Gamma})\rangle$
   Note that the choice of basis is a gauge choice: it cannot have physical significance!

$\overset{\circ}{\rightarrow}$

$$\mathcal{A}_l' = \Omega \mathcal{A}_l \Omega^\dagger - i \frac{\partial \Omega}{\partial \Gamma_l} \Omega^\dagger \tag{1.38}$$

If you attended a course on quantum field theory, you might recognize this as the gauge transformation of a non-abelian $U(n)/SU(n)$ Yang-Mills gauge theory (like QCD). The difference is that here the gauge (Berry) connection $\mathcal{A}_l$ does not live on Minkowski spacetime but on an abstract parameterspace. Gauge transformations arise from "parameter-local" basis transformations in the degenerate ground state space of a Hamiltonian (family).

$\overset{\circ}{\rightarrow}$ (use differential calculus to show this)

$$U_\Gamma' = \Omega(\mathbf{\Gamma}(T)) \, U_\Gamma \, \Omega^\dagger(\mathbf{\Gamma}(0)) \tag{1.39}$$

$\rightarrow$ For an open path Γ, U_Γ is gauge dependent and does not contain physical information!

To see this let $\Omega(\mathbf{\Gamma}(0)) = \mathbb{1}$. Then $U_\Gamma' = \Omega(\mathbf{\Gamma}(T)) \, U_\Gamma$ can be chosen (almost) *arbitrary* since $U(n)$ is a group and $\Omega(\mathbf{\Gamma}(T))$ can be chosen (almost) arbitrary (just connect it smoothly to the identity, i.e., its determinant must be one). This means that U_Γ cannot contain physical information as it can be transformed into any other unitary U_Γ' (with the same determinant) by parameter-local basis transformations.

$\uparrow$ Notes

→ ◁ Closed loops Γ in parameter space

I.e., $H(\mathbf{\Gamma}(0)) = H(\mathbf{\Gamma}(T))$ and $\mathcal{V}(\mathbf{\Gamma}(0)) = \mathcal{V}(\mathbf{\Gamma}(T))$ such that U_Γ is an automorphism on $\mathcal{V}(\mathbf{\Gamma}(0))$ and described the geometric transformation of ground states due to cyclic (and adiabatic) deformations of the Hamiltonian.

8. The

$$\boxed{\textit{Berry holonomy}\quad U_\Gamma = \mathcal{P}\exp\left[-i\oint_\Gamma \mathbfcal{A}\,d\mathbf{\Gamma}\right]\quad \in \mathrm{U}(n)} \tag{1.40}$$

is *gauge covariant*:

$$U'_\Gamma = \Omega(\mathbf{\Gamma}(0))\,U_\Gamma\,\Omega^\dagger(\mathbf{\Gamma}(0)) \tag{1.41}$$

Note that the argument from above breaks down since both unitaries $\Omega(\mathbf{\Gamma}(T)) = \Omega(\mathbf{\Gamma}(0))$ are necessarily the same (since the parameter path is closed). U_Γ can still be changed, but not arbitrarily: It is unique up to unitary basis transformations (for instance, its spectrum is independent of basis changes!). This quantity *can* encode physical properties of the system. We stress the difference between *gauge invariant* ($U'_\Gamma = U_\Gamma$) and *gauge covariant* [Eq. (1.41)].

9. There is another important *gauge covariant* quantity (that we will use below): The Non-abelian field strength or

$$\boxed{\textit{Berry curvature}\quad \mathcal{F}_{lm} := \frac{\partial \mathbfcal{A}_l}{\partial \Gamma_m} - \frac{\partial \mathbfcal{A}_m}{\partial \Gamma_l} - i\,[\mathbfcal{A}_l, \mathbfcal{A}_m]\quad \in \mathfrak{u}(n)} \tag{1.42}$$

is *gauge covariant* as well:

$$\mathcal{F}'_{ij}(\mathbf{\Gamma}) \overset{\circ}{=} \Omega(\mathbf{\Gamma})\,\mathcal{F}_{ij}(\mathbf{\Gamma})\,\Omega^\dagger(\mathbf{\Gamma}) \tag{1.43}$$

This is the field strength tensor known from non-abelian Yang-Mills gauge theories. The Yang-Mills Lagrangian takes the trace of the field strength tensor, thereby converting a gauge *covariant* quantity into a gauge *invariant* quantity: $\mathrm{Tr}[F_{\mu\nu}F^{\mu\nu}]$ (Note that the summing over μ and ν is not related to gauge but Lorentz invariance for YM theories; as we do not have generic symmetries on the *parameter space*, we do not have an analog of this symmetry in the current situation.).

We now want to focus on the special case w/o degeneracy, $n = 1$. In this case we can make use of the Berry curvature to calculate the Berry holonomy (which is for $n = 1$ just a phase known as *Berry phase*).

Berry phase and Chern number

$\lhd$ Special case $n = 1$: $\mathcal{V}(\boldsymbol{\Gamma}) = \text{span}\{|v(\boldsymbol{\Gamma})\rangle\}$ (= systems w/o ground state degeneracy)
$\rightarrow$ Ground state can only change by a phase!

Berry connection	$\mathcal{A}_l(\boldsymbol{\Gamma}) = -i\langle v(\boldsymbol{\Gamma})|\partial_{\Gamma_l}|v(\boldsymbol{\Gamma})\rangle$	$\in \mathfrak{u}(1) \simeq \mathbb{R}$	(1.44)
Berry holonomy	$U_\Gamma = \exp\left[-i\oint_\Gamma \boldsymbol{\mathcal{A}}\, d\boldsymbol{\Gamma}\right] \equiv e^{i\gamma(\Gamma)}$	$\in \mathrm{U}(1)$	(1.45)
Berry curvature	$\mathcal{F}_{lm} = \dfrac{\partial \mathcal{A}_l}{\partial \Gamma_m} - \dfrac{\partial \mathcal{A}_m}{\partial \Gamma_l}$	$\in \mathfrak{u}(1) \simeq \mathbb{R}$	(1.46)

Gauge transformation: $\Omega(\boldsymbol{\Gamma}) = e^{i\xi(\boldsymbol{\Gamma})} \rightarrow$

$$\boldsymbol{\mathcal{A}}' = \boldsymbol{\mathcal{A}} + \nabla_{\boldsymbol{\Gamma}}\xi \tag{1.47}$$
$$U'_\Gamma = U_\Gamma \qquad \text{(gauge \textit{invariant})} \tag{1.48}$$
$$\mathcal{F}'_{lm} = \mathcal{F}_{lm} \qquad \text{(gauge \textit{invariant})} \tag{1.49}$$

★ **Definition: Berry phase [22]**

For $n = 1$, the exponent of the Berry holonomy is called *Berry phase*:

$$\gamma(\Gamma) = -\oint_\Gamma \boldsymbol{\mathcal{A}}\, d\boldsymbol{\Gamma} = i\oint_\Gamma \langle v(\boldsymbol{\Gamma})|\partial_{\Gamma_l}|v(\boldsymbol{\Gamma})\rangle\, d\Gamma_l \qquad \in \mathbb{R} \tag{1.50}$$

Nomenclature is sometimes a bit vague here: $\gamma(\Gamma)$ and $e^{i\gamma(\Gamma)}$ are both referred to as "Berry phase."

Examples of systems with non-trivial Berry phase:

- Spin-$\frac{1}{2}$ in a variable magnetic field ($\circleddot$ Problemset 1 and $\circleddot$ [22])
- Aharonov-Bohm effect ($\circleddot$ [22])
- Focault pendulum ($\circleddot$ [23, 24])
  The concept of parallel transport with non-trivial holonomies is not restricted to quantum mechanical systems!

Gauge transformation:

$$\gamma'(\Gamma) = -\oint_\Gamma \boldsymbol{\mathcal{A}}'\, d\boldsymbol{\Gamma} = -\oint_\Gamma (\boldsymbol{\mathcal{A}} + \nabla_{\boldsymbol{\Gamma}}\xi)\, d\boldsymbol{\Gamma} = \gamma(\Gamma) - [\xi(\boldsymbol{\Gamma}(T)) - \xi(\boldsymbol{\Gamma}(0))] \tag{1.51}$$

Continuity of the gauge transformation: $\Omega(\boldsymbol{\Gamma}(0)) = \Omega(\boldsymbol{\Gamma}(T)) \rightarrow$

$$\xi(\boldsymbol{\Gamma}(T)) - \xi(\boldsymbol{\Gamma}(0)) = 2\pi m \quad \text{for} \quad m \in \mathbb{Z} \tag{1.52}$$
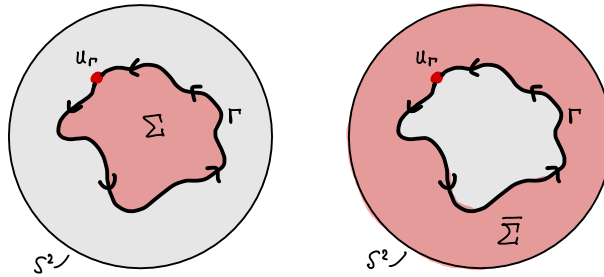
$\rightarrow \gamma(\Gamma)$ is gauge invariant *up multiples of 2π*
In particular for $\gamma(\Gamma) \notin 2\pi\mathbb{Z}$, the Berry phase *cannot* be gauged away!

Computation of the Berry phase for $k = 2$ on a compact manifold $\mathcal{M}$ (sphere, torus):
This is the most important case for us where the parameter space will be the 2D Brillouin zone (which is a torus).

◁ Closed path Γ on sphere $\mathcal{M} = S^2$ and submanifolds with $\Sigma \cup \bar{\Sigma} = \mathcal{M}$ and $\partial\Sigma = \Gamma = \partial\bar{\Sigma}$:

> ⁂ **Important**
>
> In general it is *not* possible to choose a gauge that is continuous (= non-singular) everywhere on $\mathcal{M}$!

◁ Continuous gauge $\mathcal{A}_1$ on $\Sigma \rightarrow$ Stokes' theorem valid on $\Sigma \rightarrow$

$$\oint_\Gamma \mathcal{A}_1 \, d\Gamma \stackrel{\text{Stokes}}{=} \int_\Sigma \mathcal{F}_{lm} \, d\sigma^{lm} \tag{1.53}$$

σ^{lm} is the differential area element (a 2-form that is antisymmetric in l and m, just as $\mathcal{F}_{lm}$).

◁ Continuous gauge $\mathcal{A}_2$ on $\bar{\Sigma} \rightarrow$ Stokes' theorem valid on $\bar{\Sigma} \rightarrow$

$$\oint_\Gamma \mathcal{A}_2 \, d\Gamma \stackrel{\text{Stokes}}{=} -\int_{\bar{\Sigma}} \mathcal{F}_{lm} \, d\sigma^{lm} \tag{1.54}$$

The sign is due to the opposite orientation of the boundary for $\bar{\Sigma}$!

Using Eq. (1.52) $\wedge$ Eq. (1.53) $\wedge$ Eq. (1.54) $\rightarrow$

$$\int_\mathcal{M} \mathcal{F}_{lm} \, d\sigma^{lm} = \oint_\Gamma \mathcal{A}_1 \, d\Gamma - \oint_\Gamma \mathcal{A}_2 \, d\Gamma = 2\pi m \quad \text{with} \quad m \in \mathbb{Z} \tag{1.55}$$

This motivates the following definition:

> ★ **Definition: Chern number**
>
> For a compact, closed two-dimensional parameter space $\mathcal{M}$ with Berry curvature $\mathcal{F}$, the *(first)* *Chern number* is an integer and defined as
>
> $$C = \frac{1}{2\pi} \int_\mathcal{M} \mathcal{F}_{lm} \, d\sigma^{lm} \quad \in \mathbb{Z} \tag{1.56}$$
>
> This is our first example of a *topological invariant*.

We will meet the Chern number again in the next section where we compute the Hall conductivities!

Following the argument above, it is clear that whenever there exists a gauge that is non-singular on the complete parameter space, the Chern number is necessarily zero. Conversely, whenever

the Chern number does not vanish, there must be singularities in all gauges! You will encounter an example of this in ➡ Problemset 1.

Aside I: Differential forms

The proper way to formulate the application of Stokes' theorem is in terms of *differential forms*. In this framework

$$\mathcal{A} = \sum_{l=1}^{k} \mathcal{A}_l \, d\,\Gamma_l \tag{1.57}$$

is a *1-form* that can be integrated along paths:

$$\gamma(\Gamma) = -\oint_\Gamma \mathcal{A} \,. \tag{1.58}$$

The Berry curvature is then the *2-form* given by the exterior derivative of $\mathcal{A}$ (this is only true for $n = 1$, i.e., abelian gauge fields):

$$\mathcal{F} := d\,\mathcal{A} = \sum_{1 \leq l,m \leq k} \underbrace{(\partial_m \mathcal{A}_l - \partial_l \mathcal{A}_m)}_{\mathcal{F}_{lm}} \underbrace{\frac{1}{2} d\,\Gamma_m \wedge d\,\Gamma_l}_{d\sigma^{lm}} = \mathcal{F}_{lm} \, d\sigma^{lm} \tag{1.59}$$

where the last expression is just a shorthand notation.

Finally, Stoke's theorem for differential forms states that

$$\oint_{\Gamma = \partial\Sigma} \mathcal{A} = \int_\Sigma d\,\mathcal{A} = \int_\Sigma \mathcal{F} \,. \tag{1.60}$$

Aside II: Observation of the Berry phase

◁ Spin-polarized particles on beam splitter in magnetic field with constant amplitude:
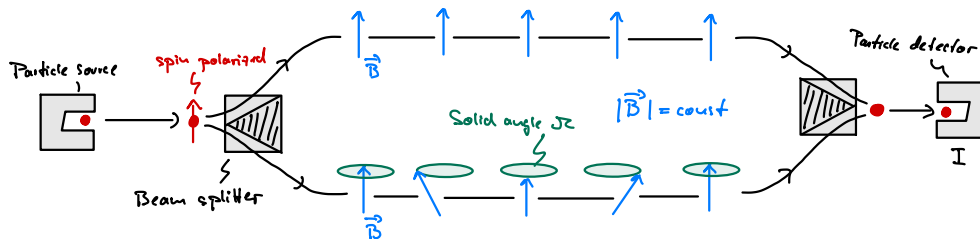
→ Interference pattern: $I = |1 + e^{i\gamma(\Gamma)}|^2$ where $e^{i\gamma(\Gamma)} = e^{i\Omega/2}$ with solid angle $0 \leq \Omega \leq 4\pi$.

You will calculate the dependency of the Berry phase on the solid angle traced out by the magnetic field in ➡ Problemset 1.

Aside III: Geometric interpretation of the Berry curvature

↑ Notes

(In general, the parameter space can be multi-dimensional. For obvious reasons we only draw two of them.)

The Berry holonomy can be compared to the rotation of a vector when carried ("parallel transported") around a closed curve on a curved space (like the shown sphere). The analog to the spatial curvature in parameter space is the Berry curvature. The Chern number equals the Euler characteristic of a compact 2D manifold and the relation that gives the Chern number in terms of the Berry curvature is then known as *Gauss-Bonnet theorem*. The "real space analog" may be known from your lectures on general relativity.

1.1.4 Quantization of the Hall conductivity

> **† Note**
>
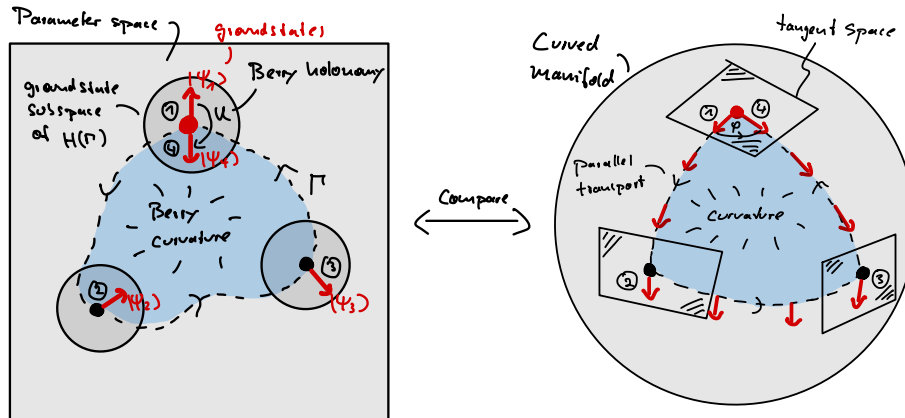> The following discussion is based on David Tong's lecture notes on the quantum Hall effect [25]. For a more detailed (and much more technical) discussion, see Chapter 3 of Bernevig's textbook [26]; another account can be found in Chapter 9 of Fradkin's textbook [27]. You might also want to have a look at the original manuscript by TKNN [20] and the follow-up [28].

The Kubo formula

Goal: Compute linear response of a quantum mechanical system at $T = 0$ for a time-dependent, external perturbation. Here we will focus on the special case where the perturbation is a time-dependent electric field and the response is a current of charged particles. The approach is quite general and is valid for general (in particular: interacting) Hamiltonians.

1. ◁ Unperturbed Hamiltonian H_0 with Eigenstates $|m\rangle$ and Eigenenergies E_m
   ◁ Time-dependent perturbation $\Delta H(t)$
   → $H = H_0 + \Delta H(t)$ (Schrödinger picture!)

2. *Interaction picture:*

$$\Delta H_I(t) = U_0^\dagger(t)\Delta H(t)U_0(t) \quad \text{and} \quad |\Psi(t)\rangle_I = U(t, t_0)|\Psi(t_0)\rangle_I \qquad (1.61)$$

with $U_0(t) = e^{-\frac{i}{\hbar}H_0 t}$ and

$$U(t, t_0) = \mathcal{T}\exp\left[-\frac{i}{\hbar}\int_{t_0}^t \Delta H_I(t')\,dt'\right] \qquad (1.62)$$

3. Prepare system for $t_0 \to -\infty$ in ground state $|0\rangle$ of H_0 (or some other eigenstate)

4. ◁ Expectation value of arbitrary operator $\mathcal{O}_I(t) = U_0^\dagger \mathcal{O} U_0$:

$$\langle \mathcal{O}(t) \rangle = \langle 0| U^\dagger(t, -\infty) \mathcal{O}_I(t) U(t, -\infty)|0\rangle \tag{1.63}$$

$$\approx \langle 0| \left\{ \mathcal{O}_I(t) + \frac{i}{\hbar} \int_{-\infty}^t \left[\Delta H_I(t'), \mathcal{O}_I(t) \right] dt' \right\} |0\rangle \tag{1.64}$$

This linearization is the core of *linear response* theory.
Note that time ordering is not important in linear order (only one time integral!)

$\to$

> *Kubo formula:* $\hspace{10cm}$ (1.65)
>
> $$\delta\langle \mathcal{O}(t) \rangle \equiv \langle \mathcal{O}(t) \rangle - \langle \mathcal{O} \rangle = \frac{i}{\hbar} \int_{-\infty}^t \langle 0| \left[\Delta H_I(t'), \mathcal{O}_I(t) \right] |0\rangle \, dt' \tag{1.66}$$

This is the linear response of the system to the perturbation ΔH. Note that $\langle \mathcal{O} \rangle = \langle 0|\mathcal{O}|0\rangle$ is not a dynamic response but the static expectation value of $\mathcal{O}$ in the initial state. In the following, we will set it to zero.

5. ◁ Coupling to electric field $\boldsymbol{E}(t) = \boldsymbol{E} e^{-i\omega t}$
Choose gauge such that $\boldsymbol{E}(t) = -\partial_t \boldsymbol{A}(t)$ (i.e. $A_t = \phi = \text{const}$)
$\to \boldsymbol{A}(t) = \boldsymbol{E} e^{-i\omega t}/(i\omega)$:

$$\Delta H_I(t) = -\boldsymbol{J}(t) \cdot \boldsymbol{A}(t) \tag{1.67}$$

with *current operator* $\boldsymbol{J}(t)$ (a Heisenberg/Dirac operator)
This is a linearized version of the true coupling Hamiltonian (linearized in $\boldsymbol{A}$). There is also a quadratic term $\boldsymbol{A}^2$ which does not contribute to the Hall conductance (so we can safely drop it).

6. ◁ Current as observable: $\mathcal{O} = J_i \to$

$$\langle J_i(t) \rangle = -\frac{1}{\hbar\omega} \int_{-\infty}^t \langle 0| \left[J_j(t'), J_i(t) \right] |0\rangle E_j e^{-i\omega t'} \, dt' \tag{1.68}$$

Time-translation invariance of H_0; Substitution $t'' = t - t'$

$$= \underbrace{\left\{ -\frac{1}{\hbar\omega} \int_0^\infty \langle 0| \left[J_j(0), J_i(t'') \right] |0\rangle \, e^{i\omega t''} \, dt'' \right\}}_{=:\sigma_{ij}(\omega)} E_j e^{-i\omega t} \tag{1.69}$$

with *conductivity tensor* $\sigma_{ij}(\omega)$

7. *Hall conductivity:* (still frequency dependent; this is the AC Hall conductivity)

$$\sigma_{xy}(\omega) = -\frac{1}{\hbar\omega} \int_0^\infty \langle 0| \left[J_y(0), J_x(t) \right] |0\rangle \, e^{i\omega t} \, dt \tag{1.70}$$

8. Use $U_0(t) = \sum_n e^{-iE_n t/\hbar}|n\rangle\langle n|$ and $J_i(t) = U_0^\dagger(t) J_i U_0(t)$:

$$\sigma_{xy}(\omega) = -\frac{1}{\hbar\omega}\int_0^\infty \sum_n \left\{ \begin{array}{l} \langle 0|J_y|n\rangle\langle n|J_x|0\rangle e^{i(E_n-E_0)t/\hbar} \\ -\langle 0|J_x|n\rangle\langle n|J_y|0\rangle e^{i(E_0-E_n)t/\hbar} \end{array} \right\} e^{i\omega t}\, dt \qquad (1.71)$$

Integrate (using a regularization $\omega + i\varepsilon$ to make the integral convergent)

$$= \frac{i}{\omega}\sum_{n\neq 0}\left\{ \frac{\langle 0|J_y|n\rangle\langle n|J_x|0\rangle}{\hbar\omega + E_n - E_0} - \frac{\langle 0|J_x|n\rangle\langle n|J_y|0\rangle}{\hbar\omega + E_0 - E_n} \right\} \qquad (1.72)$$

9. Take DC limit $\omega \to 0$ and use $\frac{1}{\hbar\omega+E_n-E_0} = \frac{1}{E_n-E_0} - \frac{\hbar\omega}{(E_n-E_0)^2} + \mathcal{O}(\omega^2)$:
   (Note the i/ω that must be cancelled to render the expression finite!)

$$\boxed{\sigma_{xy} \doteq -i\hbar \sum_{n\neq 0} \frac{\langle 0|J_y|n\rangle\langle n|J_x|0\rangle - \langle 0|J_x|n\rangle\langle n|J_y|0\rangle}{(E_n-E_0)^2}} \qquad (1.73)$$

Note that

$$\sum_{n\neq 0} \frac{\langle 0|J_y|n\rangle\langle n|J_x|0\rangle + \langle 0|J_x|n\rangle\langle n|J_y|0\rangle}{E_n - E_0} = 0 \qquad (1.74)$$

which makes the constant terms of the Taylor expansion cancel (this avoids the divergence for $\omega \to 0$!).

One way to see this is from rotation invariance of the system in the x-y-plane (a quantum Hall system should be rotation invariant about the axis of the magnetic field). In particular, σ_{xy} should be invariant under the $\pi/2$-rotation $J_x \mapsto J_y$ and $J_y \mapsto -J_x$ (note that $\boldsymbol{J}$ is a vector operator). In particular

$$\sum_{n\neq 0} \frac{\langle 0|J_y|n\rangle\langle n|J_x|0\rangle + \langle 0|J_x|n\rangle\langle n|J_y|0\rangle}{E_n - E_0} \overset{!}{=} -\sum_{n\neq 0} \frac{\langle 0|J_x|n\rangle\langle n|J_y|0\rangle + \langle 0|J_y|n\rangle\langle n|J_x|0\rangle}{E_n - E_0} \qquad (1.75)$$

which implies Eq. (1.74) so that only the antisymmetric part of σ_{xy} survives.

Note that this is a quite general argument: If we decompose the 2D conductivity tensor into symmetric and antisymmetric parts, $\sigma = \sigma_s + \sigma_a$, and demand rotational invariance of the tensor, i.e., $\sigma = R\sigma R^T$ for a 2D rotation matrix R, we have $\sigma_s = R\sigma_s R^T$ and $\sigma_a = R\sigma_a R^T$ separately. The only *symmetric* matrix invariant under rotations is proportional to the identity, $\sigma_s = \sigma_{xx} \cdot \mathbb{1}$, so that there cannot be a symmetric contribution to the off-diagonals (that is, the Hall conductivity σ_{xy}). Thus the most general form of a *rotation invariant* conductivity tensor is

$$\sigma = \begin{pmatrix} \sigma_{xx} & \sigma_{xy} \\ -\sigma_{xy} & \sigma_{xx} \end{pmatrix}. \qquad (1.76)$$

The TKNN invariant

Goal: Here we want to connect the Hall conductivity (given by the Kubo formula) to the Chern number and thereby explain the quantization of the former. To do this, we consider non-interacting electrons in a two-dimensional periodic potential, so that the momentum space becomes a torus.

1. ◁ Single electron in a periodic potential with Hamiltonian H_0:
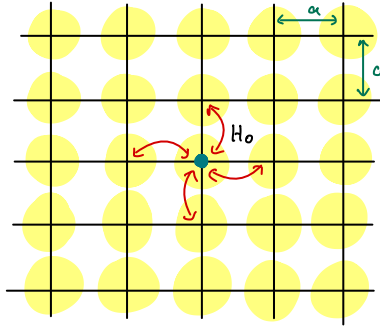
2. *Bloch theorem:*

   - Eigenfunctions $\Psi_{nk} = e^{ikx} u_{nk}(x)$
     with $u_{nk}(x + R) = u_{nk}(x)$ for lattice vectors R and band index $n = 1, 2, \ldots$

   - Eigenenergies $\varepsilon_n(k)$ continuous in $k \to$ "Bands"

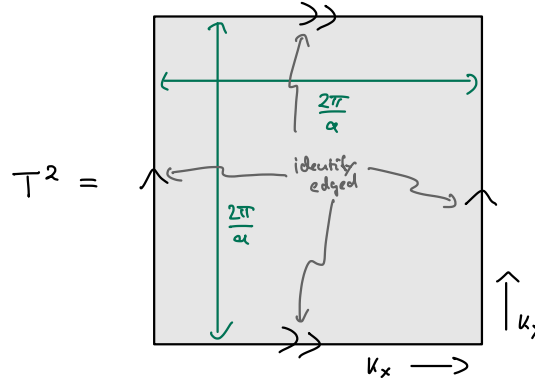   - $\Psi_{nk+K} = \Psi_{nk}$ for reciprocal lattice vectors K
     $\to$ Brillouin zone = Torus T^2

3. *Many-body Fock states* with Fermi energy E_F:

$$\text{Ground state} = |0\rangle \;\mapsto\; \mathbf{|0\rangle} = \text{Filled Fermi sea} \tag{1.77}$$

$$\text{Excited states} = |n\rangle \;\mapsto\; \mathbf{|n\rangle} = \text{Fermi sea with particle-hole excitations} \tag{1.78}$$

$$\text{Current operator} = J_i \;\mapsto\; \mathfrak{J}_i = \text{Second-quantized current operator} \tag{1.79}$$

Henceforth, bold states live in the fermionic Fock space whereas states with normal weight live in the single-particle Hilbert space.

$\to$

$$\sigma_{xy} \overset{\circ}{=} -i\hbar \sum_{\mathbf{n} \neq \mathbf{0}} \frac{\langle \mathbf{0}|\mathfrak{J}_y|\mathbf{n}\rangle \langle \mathbf{n}|\mathfrak{J}_x|\mathbf{0}\rangle - \langle \mathbf{0}|\mathfrak{J}_x|\mathbf{n}\rangle \langle \mathbf{n}|\mathfrak{J}_y|\mathbf{0}\rangle}{(E_{\mathbf{n}} - E_{\mathbf{0}})^2} \tag{1.80}$$

Note that the sum goes over all possible excited many-body states (which are all states except the Fermi sea ground state). However, below we will see that only states with a single particle-hole excitation contribute.

4. Current operator = Single-particle operator:

$$\mathfrak{I}_i = \sum_{n\boldsymbol{k},m\boldsymbol{q}} \langle \Psi_{n\boldsymbol{k}} | J_i | \Psi_{m\boldsymbol{q}} \rangle\, c^\dagger_{n\boldsymbol{k}} c_{m\boldsymbol{q}} \tag{1.81}$$

$c^\dagger_{n\boldsymbol{k}}$: Creation operator for fermion in Bloch state $|\Psi_{n\boldsymbol{k}}\rangle$

$\rightarrow$

$$\sum_{n\neq 0} \frac{\langle 0|\mathfrak{I}_y|n\rangle\langle n|\mathfrak{I}_x|0\rangle}{(E_n - E_0)^2} = \sum_{n\boldsymbol{k}',m\boldsymbol{q}'} \sum_{n\boldsymbol{k},m\boldsymbol{q}} \langle \Psi_{n\boldsymbol{k}}|J_y|\Psi_{m\boldsymbol{q}}\rangle \langle \Psi_{n\boldsymbol{k}'}|J_x|\Psi_{m\boldsymbol{q}'}\rangle \tag{1.82}$$

$$\underbrace{\sum_{n\neq 0} \frac{\langle 0|c^\dagger_{n\boldsymbol{k}}c_{m\boldsymbol{q}}|n\rangle \langle n|c^\dagger_{n\boldsymbol{k}'}c_{m\boldsymbol{q}'}|0\rangle}{(E_n - E_0)^2}}_{\dfrac{\delta_{n\boldsymbol{k}=m\boldsymbol{q}'}\,\delta_{m\boldsymbol{q}=n\boldsymbol{k}'}\,\delta_{\varepsilon_m(\boldsymbol{q})>E_F}\,\delta_{\varepsilon_n(\boldsymbol{k})<E_F}}{(\varepsilon_m(\boldsymbol{q})-\varepsilon_n(\boldsymbol{k}))^2}}$$

$$= \sum_{\substack{n\boldsymbol{k},m\boldsymbol{q} \\ \varepsilon_n(\boldsymbol{k})<E_F<\varepsilon_m(\boldsymbol{q})}} \frac{\langle \Psi_{n\boldsymbol{k}}|J_y|\Psi_{m\boldsymbol{q}}\rangle \langle \Psi_{m\boldsymbol{q}}|J_x|\Psi_{n\boldsymbol{k}}\rangle}{(\varepsilon_m(\boldsymbol{q}) - \varepsilon_n(\boldsymbol{k}))^2} \tag{1.83}$$

$\rightarrow$ (Note that the Fermi energy is assumed to be in the gap between two bands!)

$$\sigma_{xy} \doteq -i\hbar \sum_{\substack{n,m \\ \varepsilon_n<E_F<\varepsilon_m}} \int_{T^2} \frac{d^2k\ d^2q}{(2\pi)^4} \frac{\left\{ \begin{matrix} \langle \Psi_{n\boldsymbol{k}}|J_y|\Psi_{m\boldsymbol{q}}\rangle \langle \Psi_{m\boldsymbol{q}}|J_x|\Psi_{n\boldsymbol{k}}\rangle \\ -\langle \Psi_{n\boldsymbol{k}}|J_x|\Psi_{m\boldsymbol{q}}\rangle \langle \Psi_{m\boldsymbol{q}}|J_y|\Psi_{n\boldsymbol{k}}\rangle \end{matrix} \right\}}{(\varepsilon_m(\boldsymbol{q}) - \varepsilon_n(\boldsymbol{k}))^2} \tag{1.84}$$

(In the thermodynamic limit, the sum over momenta becomes an integral over the Brillouin zone T^2.)

5. a) Define the *single-particle current operator*

$$\boldsymbol{J} := e\dot{\boldsymbol{x}} = i\frac{e}{\hbar}[H_0, \boldsymbol{x}] \tag{1.85}$$

Here we use the Heisenberg equation of motion to express the velocity operator in terms of a commutator.

b) $\lhd$ Translation operator $T_{\boldsymbol{R}}$ with lattice vector $\boldsymbol{R}$:

$$T_{\boldsymbol{R}} \boldsymbol{x} T_{\boldsymbol{R}}^{-1} = \boldsymbol{x} + \boldsymbol{R}, \quad T_{\boldsymbol{R}} H_0 T_{\boldsymbol{R}}^{-1} = H_0 \tag{1.86}$$

and $\quad T_{\boldsymbol{R}} |\Psi_{n\boldsymbol{k}}\rangle = e^{i\boldsymbol{k}\boldsymbol{R}} |\Psi_{n\boldsymbol{k}}\rangle \tag{1.87}$

- The commutativity with the Hamiltonian follows from the discrete translational invariance of the system.

- The energy eigenstates of such a Hamiltonian are Bloch states $|\Psi_{n\boldsymbol{k}}\rangle$ which are also eigenstates of these lattice translations (this is just the statement of Bloch's theorem).

↑ Notes

DRAFT

c) Consequently

$$T_{\boldsymbol{R}} \boldsymbol{J} T_{\boldsymbol{R}}^{-1} = i\frac{e}{\hbar}[H_0, \boldsymbol{x} + \boldsymbol{R}] = i\frac{e}{\hbar}[H_0, \boldsymbol{x}] = \boldsymbol{J} \tag{1.88}$$

d) Thus

$$\sigma_{xy} \overset{\circ}{=} -i\hbar \sum_{\substack{n,m \\ \varepsilon_n < E_F < \varepsilon_m}} \int_{T^2} \frac{d^2k}{(2\pi)^2} \frac{\begin{Bmatrix} \langle \Psi_{n\boldsymbol{k}} | J_y | \Psi_{m\boldsymbol{k}} \rangle \langle \Psi_{m\boldsymbol{k}} | J_x | \Psi_{n\boldsymbol{k}} \rangle \\ -\langle \Psi_{n\boldsymbol{k}} | J_x | \Psi_{m\boldsymbol{k}} \rangle \langle \Psi_{m\boldsymbol{k}} | J_y | \Psi_{n\boldsymbol{k}} \rangle \end{Bmatrix}}{(\varepsilon_m(\boldsymbol{k}) - \varepsilon_n(\boldsymbol{k}))^2} \tag{1.89}$$

6.   a) Use $|\Psi_{n\boldsymbol{k}}\rangle = e^{i\boldsymbol{k}\boldsymbol{x}}|u_{n\boldsymbol{k}}\rangle$ (Bloch theorem!) and define $\tilde{\boldsymbol{J}}(\boldsymbol{k}) := e^{-i\boldsymbol{k}\boldsymbol{x}} \boldsymbol{J} e^{i\boldsymbol{k}\boldsymbol{x}}$ so that

$$\langle \Psi_{n\boldsymbol{k}} | J_i | \Psi_{m\boldsymbol{k}} \rangle = \langle u_{n\boldsymbol{k}} | \tilde{J}_i(\boldsymbol{k}) | u_{m\boldsymbol{k}} \rangle \tag{1.90}$$

Note that in $e^{i\boldsymbol{k}\boldsymbol{x}}$, $\boldsymbol{x}$ is the position *operator*!

b) Define $\tilde{H}_0(\boldsymbol{k}) := e^{-i\boldsymbol{k}\boldsymbol{x}} H_0 e^{i\boldsymbol{k}\boldsymbol{x}}$ so that

$$H_0|\Psi_{n\boldsymbol{k}}\rangle = \varepsilon_n(\boldsymbol{k})|\Psi_{n\boldsymbol{k}}\rangle \;\Leftrightarrow\; \tilde{H}_0(\boldsymbol{k})|u_{n\boldsymbol{k}}\rangle = \varepsilon_n(\boldsymbol{k})|u_{n\boldsymbol{k}}\rangle \tag{1.91}$$

c) Then

$$\tilde{J}_i \overset{\circ}{=} \frac{e}{\hbar}\tilde{\partial}_i \tilde{H}_0 \quad \text{with} \quad \tilde{\partial}_i := \frac{\partial}{\partial k_i} \tag{1.92}$$

d) Thus

$$\sigma_{xy} \overset{\circ}{=} -i\frac{e^2}{\hbar} \sum_{\substack{n,m \\ \varepsilon_n < E_F < \varepsilon_m}} \int_{T^2} \frac{d^2k}{(2\pi)^2} \frac{\begin{Bmatrix} \langle u_{n\boldsymbol{k}} | \tilde{\partial}_y \tilde{H}_0 | u_{m\boldsymbol{k}} \rangle \langle u_{m\boldsymbol{k}} | \tilde{\partial}_x \tilde{H}_0 | u_{n\boldsymbol{k}} \rangle \\ -\langle u_{n\boldsymbol{k}} | \tilde{\partial}_x \tilde{H}_0 | u_{m\boldsymbol{k}} \rangle \langle u_{m\boldsymbol{k}} | \tilde{\partial}_y \tilde{H}_0 | u_{n\boldsymbol{k}} \rangle \end{Bmatrix}}{(\varepsilon_m(\boldsymbol{k}) - \varepsilon_n(\boldsymbol{k}))^2}$$

$$\tag{1.93}$$

7. Use

$$\langle u_{n\boldsymbol{k}} | \tilde{\partial}_y \tilde{H}_0 | u_{m\boldsymbol{k}} \rangle = \langle u_{n\boldsymbol{k}} | \tilde{\partial}_y \left(\tilde{H}_0 | u_{m\boldsymbol{k}} \rangle \right) - \langle u_{n\boldsymbol{k}} | \tilde{H}_0 | \tilde{\partial}_y u_{m\boldsymbol{k}} \rangle \tag{1.94a}$$

$$= [\varepsilon_m(\boldsymbol{k}) - \varepsilon_n(\boldsymbol{k})] \langle u_{n\boldsymbol{k}} | \tilde{\partial}_y u_{m\boldsymbol{k}} \rangle \tag{1.94b}$$

$$= [\varepsilon_n(\boldsymbol{k}) - \varepsilon_m(\boldsymbol{k})] \langle \tilde{\partial}_y u_{n\boldsymbol{k}} | u_{m\boldsymbol{k}} \rangle \tag{1.94c}$$

The first line is just the product rule, in the second line we used that $\tilde{H}_0 = \tilde{H}_0^\dagger$ and that $\langle u_{n\boldsymbol{k}} | u_{m\boldsymbol{k}} \rangle = 0$ for $n \neq m$ (which is the case in our expression for the Hall conductivity). The last line follows if in the first line the derivative acts on the bra to the left instead on the ket to the right.

$\rightarrow$

$$\sigma_{xy} \overset{\circ}{=} -i\frac{e^2}{\hbar} \sum_{\substack{n,m \\ \varepsilon_n < E_F < \varepsilon_m}} \int_{T^2} \frac{d^2k}{(2\pi)^2} \begin{Bmatrix} \langle \tilde{\partial}_y u_{n\boldsymbol{k}} | u_{m\boldsymbol{k}} \rangle \langle u_{m\boldsymbol{k}} | \tilde{\partial}_x u_{n\boldsymbol{k}} \rangle \\ -\langle \tilde{\partial}_x u_{n\boldsymbol{k}} | u_{m\boldsymbol{k}} \rangle \langle u_{m\boldsymbol{k}} | \tilde{\partial}_y u_{n\boldsymbol{k}} \rangle \end{Bmatrix} \tag{1.95}$$

8. Use

$$\sum_m |u_{mk}\rangle\langle u_{mk}| = \mathbb{1} \tag{1.96}$$

$$\Rightarrow \sum_{m:\varepsilon_m > E_F} |u_{mk}\rangle\langle u_{mk}| = \mathbb{1} - \sum_{m:\varepsilon_m < E_F} |u_{mk}\rangle\langle u_{mk}| \tag{1.97}$$

These statements are true on the subspace spanned by the Bloch functions $|u_{nk}\rangle$ for fixed k. More rigorously, one should replace $\mathbb{1}$ by the projector P_k onto states with lattice momentum k and do the derivatives in the expression for σ_{xy} properly; the result will be the same, though.

$\rightarrow$

$$\sigma_{xy} \overset{\circ}{=} -i\frac{e^2}{\hbar} \sum_{n:\varepsilon_n < E_F} \int_{T^2} \frac{d^2k}{(2\pi)^2} \left\{ \langle \tilde{\partial}_y u_{nk}|\tilde{\partial}_x u_{nk}\rangle - \langle \tilde{\partial}_x u_{nk}|\tilde{\partial}_y u_{nk}\rangle \right\} \tag{1.98}$$

Only the term with $\mathbb{1}$ survives. The second term vanishes as it replaces the sum over empty bands by a sum over filled bands. But then the sum in the expression for the Hall conductance vanishes identically if one shifts the derivatives to the states with mk in the first term (using Eq. (1.94)) and substitutes $n \leftrightarrow m$ in the sums (the last step only works because m and n now run over the same range of filled bands).

9.   a) Define the *Berry connection* of band n:

$$\mathcal{A}_i^{[n]}(k) = -i\langle u_{nk}|\tilde{\partial}_i u_{nk}\rangle \tag{1.99}$$

This is a U(1) connection on the Brillouin zone which is the compact 2D manifold T^2. The parameters are the momenta ($\Gamma = k$) and the local Hilbert spaces are one dimensional: $\mathcal{V}^{[n]}(k) = \text{span}\{|u_{nk}\rangle\}$; these are the non-degenerate eigenspaces (no band crossings!) of the Hamiltonian family $\tilde{H}_0(k)$ with discrete spectrum $\varepsilon_n(k)$ (fix k as a parameter!). Thus $n = 1$ and $k = 2$ (these are the parameters that we introduced in our discussion of the Berry curvature; here the n denotes not the band index).

b) *Berry curvature* of band n:

$$\mathcal{F}_{ij}^{[n]}(k) = \tilde{\partial}_j \mathcal{A}_i^{[n]} - \tilde{\partial}_i \mathcal{A}_j^{[n]} \tag{1.100}$$

$$= -i\langle \tilde{\partial}_j u_{nk}|\tilde{\partial}_i u_{nk}\rangle + i\langle \tilde{\partial}_i u_{nk}|\tilde{\partial}_j u_{nk}\rangle \tag{1.101}$$

(The cross terms cancel!)

c) $\rightarrow$ *Chern number* of band n:

$$C^{[n]} = \frac{1}{2\pi} \int_{T^2} \mathcal{F}_{ij}\, d\sigma^{ij} = -\frac{1}{2\pi} \int_{T^2} \mathcal{F}_{xy}\, d^2k \tag{1.102}$$

$$= \frac{i}{2\pi} \int_{T^2} \left\{ \langle \tilde{\partial}_y u_{nk}|\tilde{\partial}_x u_{nk}\rangle - \langle \tilde{\partial}_x u_{nk}|\tilde{\partial}_y u_{nk}\rangle \right\} d^2k \tag{1.103}$$

The integral ist best evaluated with differential forms where $\mathcal{F} = \mathrm{d}\mathcal{A}$ is a 2-form and $\mathcal{A} = A_x \mathrm{d}k_x + A_y \mathrm{d}k_y$ is a 1-form. Then

$$C = \frac{1}{2\pi} \int_{T^2} \mathcal{F} = \frac{1}{2\pi} \int_{T^2} \left(\tilde{\partial}_y A_x \, \mathrm{d}k_y \wedge \mathrm{d}k_x + \tilde{\partial}_x A_y \, \mathrm{d}k_x \wedge \mathrm{d}k_y \right) \quad (1.104)$$

$$= -\frac{1}{2\pi} \int_{T^2} \underbrace{\left(\tilde{\partial}_y A_x - \tilde{\partial}_x A_y \right)}_{\mathcal{F}_{xy}} \underbrace{\mathrm{d}k_x \wedge \mathrm{d}k_y}_{d^2k} \quad (1.105)$$

where we used $\mathrm{d}k_i \wedge \mathrm{d}k_j = -\mathrm{d}k_j \wedge \mathrm{d}k_i$.

10. Eq. (1.98) $\wedge$ Eq. (1.103) $\rightarrow$

> ⁂ **Important: TKNN formula [20]**
>
> $$\sigma_{xy} = -\frac{e^2}{2\pi\hbar} \sum_{n:\varepsilon_n < E_F} C^{[n]} = -\frac{e^2 \nu}{2\pi\hbar} \quad \text{with} \quad \nu := \sum_{n:\varepsilon_n < E_F} C^{[n]} \in \mathbb{Z} \quad (1.106)$$

The Hall conductivity of a system with non-degenerate bands that are either completely filled or completely empty is an integer multiple ν of $e^2/2\pi\hbar$ where ν is the sum of the Chern numbers of the filled bands. This quantization is robust and independent of microscopic details because the Chern numbers are topological invariants that are necessarily integer as long as they are well-defined (= no gaps close).

The salient feature of the integer quantum Hall effect is that a quantity that describes a macroscopic response of system (the Hall conductivity) is exactly quantized and hence impervious to microscopic disorder. This magic turns into comprehension when we go back (to Eq. (1.73)) and realize that we only showed that the *antisymmetric* part of the conductivity tensor has a topological character (remember that we argued the symmetric part away to evade a divergence in the DC limit). Note that in a conventional conductor (w/o magnetic field) the conductivity tensor is *not* antisymmetric but symmetric. So in generality we should start with the decomposition

$$\sigma = \sigma_s + \sigma_a \quad (1.107)$$

with $\sigma_s^T = \sigma_s$ and $\sigma_a^T = -\sigma_a$. w/o magnetic field σ_a vanishes (this is an example of an *Onsager relation* [29]). Strictly speaking, we have only shown that the contribution of this antisymmetric part is topologically quantized. But this contribution is also special in another way. The current $\boldsymbol{J}$ is the response due to an external electric field: $\boldsymbol{J} = \sigma \boldsymbol{E}$. The power that is dissipated in a equilibrium setting (through bumps of the charge carriers with the crystal structure) is then $P = \boldsymbol{J} \cdot \boldsymbol{E}$ (if $\boldsymbol{J}$ is the current *density* this is of course the power *density*); this is known as *Joule's law*. Putting everything together, we find

$$P = \boldsymbol{E}^T \sigma \boldsymbol{E} = \boldsymbol{E}^T \sigma_s \boldsymbol{E} \quad (1.108)$$

since $(\boldsymbol{E}^T \sigma_a \boldsymbol{E})^T = \boldsymbol{E}^T \sigma_a^T \boldsymbol{E} = -\boldsymbol{E}^T \sigma_a \boldsymbol{E} = 0$. Thus only the *symmetric* part of the conductivity tensor plays a role for dissipation! But we didn't show that this part is quantized, only the "non-dissipative" contribution σ_a is. So our intuition that a *dissipative* quantity should depend on microscopic details and hence *not* be quantized was right, after all. What we missed

is that not everything about the conductivity *tensor* is dissipative; there is also a topological (or geometric) contribution that has nothing to do with microscopic physics. It is this contribution that gives rise to the integer quantum Hall effect.

There is much more to be said about the physics of the integer quantum Hall effect. Since this a course on the broader topic of topological phases, we should not linger too long, though. However, there are three last topics that must be mentioned to prevent misconceptions and embed the IQHE into the Big Picture. For students that want to dig deeper into quantum Hall physics, I can highly recommend the lecture notes by David Tong [25].

1.1.5 The role of disorder

The above derivation is based on *non-interacting* fermions in a translational invariant potential (= *w/o disorder*). However, the quantization of the Hall response is more general than that and prevails in the presence of disorder and/or interactions that do not close the spectral gap above the many-body ground state [28]. This statement is based on a more general expression for the Hall conductivity that does not rely on the Brillouin zone (and therefore translational invariance). This approach can also be used to compute the Hall conductivity of the Landau levels of a continuum system on a torus, see Chapter 9.7 of Fradkin's textbook [27].

However, even if we take these statements for granted, there is still a problem that is sometimes swept under the rug in superficial discussions of the IQHE:

1. ◁ System with fixed electron density n (= fixed chemical potential)
   Recall: Number of states per LL: $N = AB/\Phi_0$
   → Lowest $\nu \in \mathbb{N}$ LLs *exactly* filled for $B_\nu = \Phi_0 n/\nu$

   → Only for the *discrete* B_ν the Hall response σ_{xy} is topological and thus quantized:
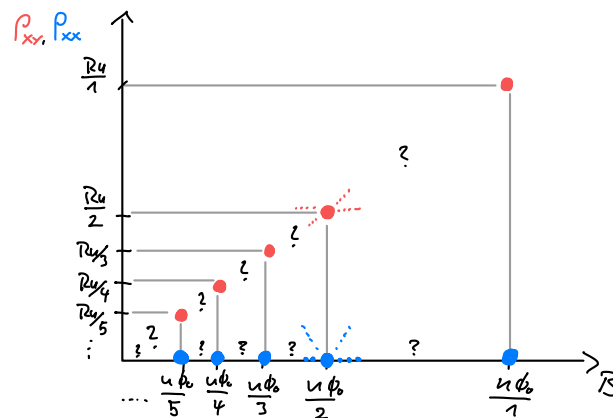
   → This does *not* explain the observed plateaus!
   Recall the experimental data shown in the first lecture on the IQHE.
   The situation is a bit strange: Our hard-earned result (the TKNN formula) explains the quantization of the *height* of the plateaus, but not their *existence* (= finite width).

   Solution: *Disorder …*

2. *First* effect of *disorder*: LLs are broadened:

$\rightarrow$ This does *still not* explain the observed plateaus!
The problem stays the same, whether the LLs are perfectly flat or not.

3. *Second* effect of *disorder*:

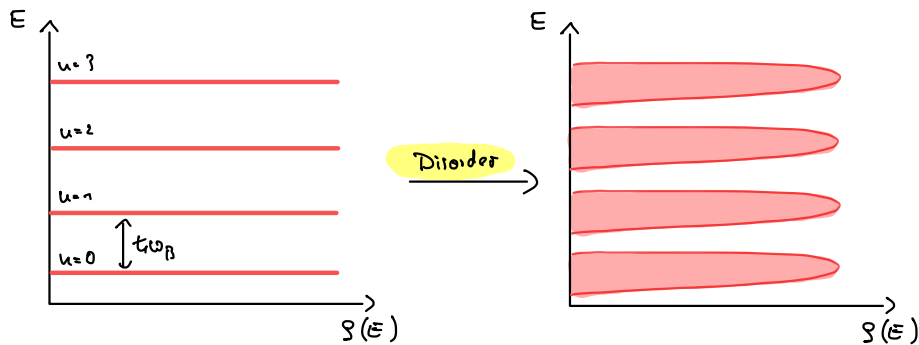   - (Most) single-electron states are *localized* and *pinned* at local potential peaks/dips
     $\rightarrow$ Do *not* contribute to conductivity

   - At least one mode along the edge cannot be localized
     $\rightarrow$ Contributes to conductivity
     (The existence of the edge states is a topological consequence of the non-zero Chern number of the LLs: the chirality makes backscattering along the edge impossible and prevents the edge modes from aquiring a gap [see note below].)

$\rightarrow$ *Mobility gap*:
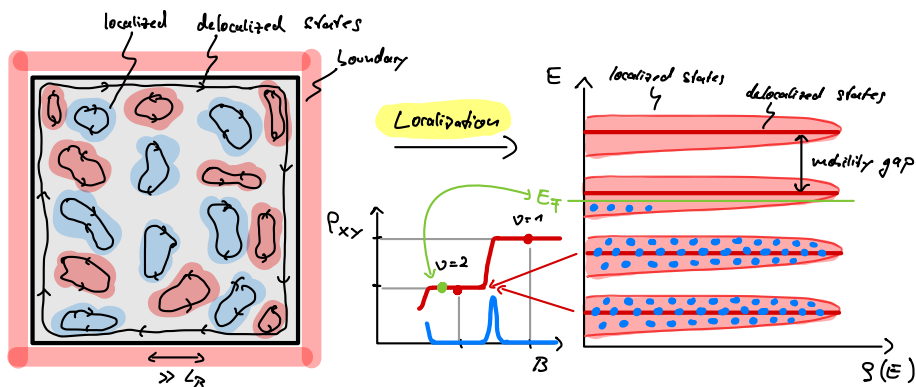
$\rightarrow$ Filling/depletion of broadened LLs for $B \lessgtr B_\nu$ does *not* affect conductivity as long as E_F is in the mobility gap
$\rightarrow$ Explains *extended* Hall plateaus around B_ν with quantized height R_K / ν

In a nutshell:

- *Topology* fixes the height of the plateaus but

- *disorder* gives them their finite width (= makes them visible).

This implies that in a (hypothetical) perfectly clean sample, the Hall plateaus cannot be observed!

1.1.6 Edge states

So far, we focused on the Hall conductivity σ_{xy}, a linear response function of the system; it is a property of the *bulk* and does not depend on the presence or absence of boundaries.

Above we have argued that in systems with boundary, there are delocalized single-particle modes running along the boundary in one direction (determined by the sign of the magnetic field and the sign of the charge carriers). These *edge states* on the 1D "surface" of the 2D system cannot be removed by disorder—they are topologically protected. We will encounter this phenomenon again in our discussion of topological insulators.

1. *Classical picture:*
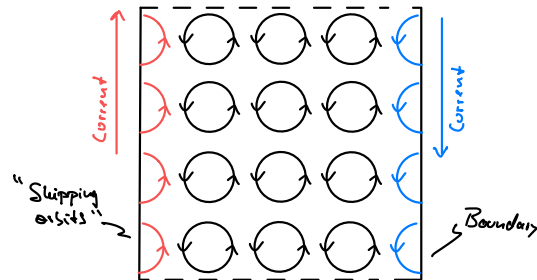
→ *Skipping orbits* → Chiral currents along edges

2. *Quantum picture:*

   a) ◁ Strip geometry:
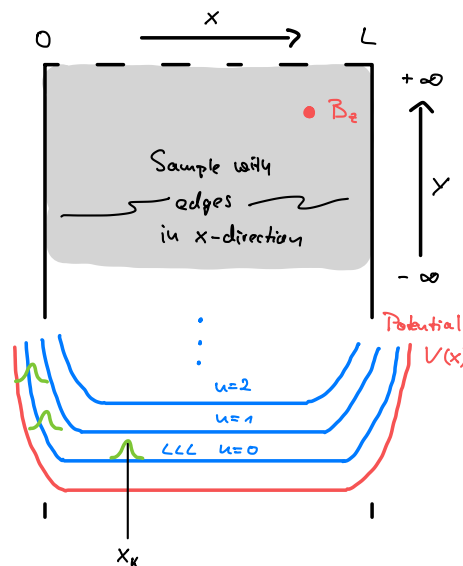
   b) Hamiltonian in *Landau gauge:*

$$H = \frac{1}{2m}p_x^2 + \frac{m\omega_B^2}{2}(x + kl_B^2)^2 + V(x) \tag{1.109}$$

   $V(x)$: Potential that varies on length scales $\gg l_B$

   c) LL wavefunctions $\Psi_{n,k}$ still eigenfunctions (with shifted energies)

      ◁ Lowest Landau Level:

$$\Psi_{0,k}(x,y) = \mathcal{N}\, e^{iky}\, e^{-\frac{(x+kl_B^2)^2}{2l_B^2}} \tag{1.110}$$

   y-momentum k → localized at $X_k = -kl_B^2$
   → Eigenenergy $E_k = \frac{1}{2}\hbar\omega_B + V(X_k)$

d) Group velocity in y-direction:

$$v_g^y(X) = \frac{1}{\hbar}\frac{\partial E_k}{\partial k} = \frac{1}{\hbar}\frac{\partial E_k}{\partial X_k}\frac{\partial X_k}{\partial k} = -\frac{l_B^2}{\hbar}\frac{\partial V(X)}{\partial X} = -\frac{1}{eB}\frac{\partial V(X)}{\partial X} \qquad (1.111)$$

$\rightarrow$ Current density $I_y(x) = -e\, v_g^y(x)\, \rho(x)$

$\rho(x)$: density of occupied states for fixed Fermi energy E_F

Note that the system is gapped with $\hbar\omega_B$ in the bulk but *gapless* on the edges!

$\rightarrow$ Gapless, chiral *edge modes*

- The existence of these edge modes is deeply rooted in topology and a consequence of the non-zero Chern number of the Landau levels. The general statement that topologically non-trivial bulk insulators give rise to gapless modes on their boundary is known as *bulk-boundary correspondence* [30–32] and one of the striking features of systems with topological bands.
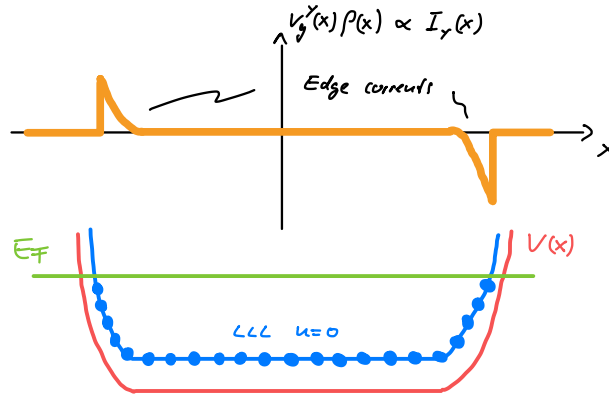
- The *chirality* of these modes (i.e., the fact that electrons can move only in one direction along the edge) is a consequence of time-reversal symmetry breaking and makes the charge transport robust because backscattering is impossible (there are just no counterpropagating modes in which to scatter).

- This robustness prevents the generation of a gap on the edge (even in the presence of disorder and/or weak interactions). In the language of field theory, the low-energy physics on the edge is described by a *chiral Luttinger liquid*. Due to the missing counterpropagating modes, there are no relevant operators that could open a gap.

$\rightarrow$ Vanishing current along the strip (at $T = 0$):

$$I_y = \int_{-\infty}^{\infty} I_y(x)\, dx = -e\int_{-\infty}^{\infty}\frac{1}{\hbar}\frac{\partial E_k}{\partial k}\rho(k)\frac{dk}{2\pi} \qquad (1.112)$$

$$= -\frac{e}{2\pi\hbar}\int_{\mu_L}^{\mu_R} dE = -\frac{e}{2\pi\hbar}(\mu_R - \mu_L) \stackrel{\mu_R = \mu_L}{=} 0 \qquad (1.113)$$

That's good news because there is no voltage applied!

e) *Hall conductivity:*

Apply electric field in x-direction: $\mu_R - \mu_L = eV_x$
V_x: Hall voltage between left and right boundary
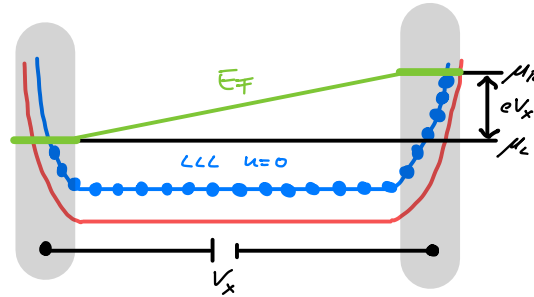
→ Hall current:

$$I_y = -\frac{e}{2\pi\hbar}(\mu_R - \mu_L) = -\frac{e^2}{2\pi\hbar}V_x \tag{1.114}$$

→ Hall conductivity per filled LL:

$$\sigma_{xy} = -\frac{e^2}{2\pi\hbar} \tag{1.115}$$

If the ν lowest Landau levels are filled, each contributes Eq. (1.115) to the total conductivity such that

$$\sigma_{xy} = -\frac{e^2}{2\pi\hbar}\nu\,. \tag{1.116}$$

3. *Disorder:*

   For weak disorder in the potential $V(x)$ that does not cross the local Fermi erengy, the above calculation of the Hall current remains correct as it only depends on the chemical potential at the left and right boundary but not the behaviour of E_k (or, equivalently, $V(x)$) inbetween:
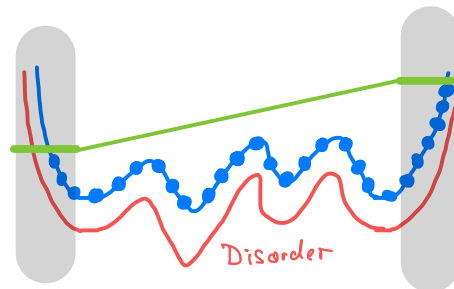
   → The result for the Hall conductivity Eq. (1.115) is robust to disorder!

4. *Chiral* edge modes are special:

   † **Note: Nielsen-Ninomiya-Theorem in 1D [33, 34]**

   ◁ Non-interacting fermions on a lattice in 1D:

→ Brillouin zone = Circle S^1 (i.e., bands must be periodic!)
→ Equal number of left (ψ_L) and right movers (ψ_R) in low-energy theory of lattice models

There is a higher-dimensional (and more important) generalizations of this statement in 3+1 dimensions. Then, the fact that every chiral Weyl fermion must have a partner when discretized on a lattice is known as *fermion doubling problem* which is inherent to lattice formulations of quantum field theories (like QCD).

→ Chiral edge modes can only appear *on the boundary* of a 2D bulk material!

Strictly speaking, the argument above applies only to *lattice formulations* of the IQHE (e.g., the Hofstadter model, ❷ Problemset 3) which, however, feature similar chiral edge modes as the IQHE in its continuum formulation. In the continuum, the proper line of arguments uses the concept of *gauge anomalies* (see Chapters 5 and 6 of Ref. [25]).

This is an observation that goes deep with far-reaching ramifications: Effective low-energy theories that describe the gapless $D-1$-dimensional boundaries of gapped D-dimensional systems can have properties that are—under reasonable assumptions—impossible for "true" $D-1$-dimensional systems (i.e., systems that are *not* the boundary of some larger system).

The magnetic field *spatially separates* left- and right movers:
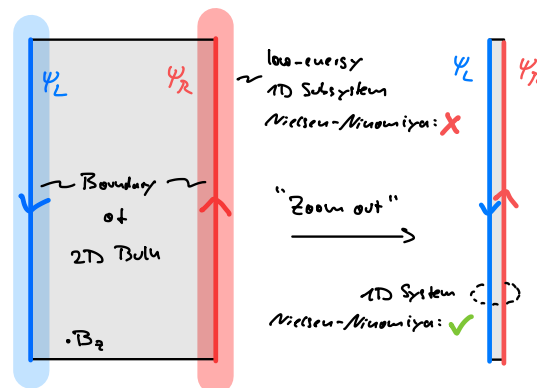
Some additional facts:

- In bands with non-zero Chern number, no single-particle basis exists where *all* wavefunctions are localized (this is kown as a *topological obstruction* [35, 36]).
  → Delocalized edge modes

- To proper way to show the existence (and robustness) of the chiral edge modes is to construct a low-energy effective quantum field theory (QFT). This QFT turns out to be a gauge theory known as *Chern-Simons (CS) theory* (of the "abelian variety" and with "integer level"). In the presence of a boundary, the gauge invariance of the CS theory *requires* the existence of gapless physical degrees of freedom at the edge of the sample (gauge invariance demands a "chiral Luttinger liquid" on the boundary).
  $\rightarrow$ Robust edge modes

 The neat thing about the QFT approach is that it can be directly generalized to the *fractional* quantum Hall effect (then the CS theory can become "non-abelian" and is of "fractional level").

1.1.7 Notes on classification

The IQHE is an important corner stone in the theory of topological phases, both historically and conceptually. Starting from the IQHE, there are (at least) two directions to explore:
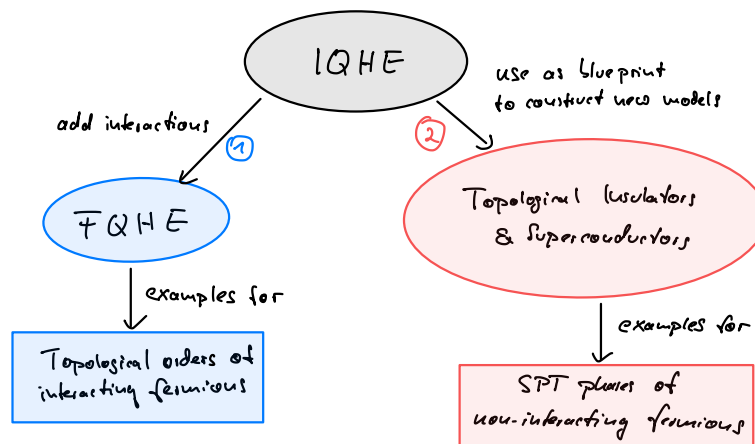
1. Keep the QHE setting but consider fractionally filled Landau levels:
   $\rightarrow$ Interactions become important (flat bands!)
   $\rightarrow$ Fractional quantum Hall Effect (FQHE)
   $\rightarrow$ Different *topologically ordered states*
   with anyonic excitations and fractional charges (depending on the filling)

2. Leave the QHE setting but stay in the realm of non-interacting fermions (on the lattice):
   $\rightarrow$ Construct lattice models with topological bands …

   - …w/o magnetic fields (?)

   - …w/o breaking time reversal symmetry (?)

   - …w/o particle-number conservation (?)

   $\rightarrow$ Topological insulators & superconductors
   [(mostly) SPT phases of non-interacting fermions]

In the following we will pursue path 2, which will eventually lead us to the "periodic table of topological insulators and superconductors."

Note: The IQH states themselves are part of the classification of topological phases of non-interacting fermions that we will introduce [37]. However, they are also long-range

entangled [38] but this long-range entanglement is of a special "boring" kind in that it does not give rise to fancy anyonic statistics of excitations. (Such topological orders are sometimes refered to as *invertible* [38–40] since they can be deformed into trivial product states by gluing "inversely" ordered states on top. According to another naming scheme [different from the one I introduced], IQH states are short-range entangled because they lack anyonic excitations and their *topological entanglement entropy* vanishes [41, 42]. Because of the time-reversal symmetry breaking and the chiral nature of their edge modes, some call IQH states simply *chiral phases* [43, 44].) It is noteworthy that symmetry *does* play a role for the IQHE, namely the U(1) symmetry that describes the conservation of charge. It does neither protect the entanglement structure nor the chiral edge states but is necessary for the quantization of the Hall response [38, 43, 44]. (Which makes sense: in a material where charge can randomly enter or leave the sample, there is no reason for a conductivity to be quantized.)

1.2 Topological bands without magnetic fields: The quantum anomalous Hall effect

1.2.1 Preliminaries

We seek for models with the following properties:

- Lattice model (of non-interacting fermions)
- Band insulator
- Non-zero Chern number
- No magnetic field (!)

The first three conditions are satisfied by the Hofstadter model (➲ Problemset 3). However, the Hofstadter model is a complex multiband model due to the enlarged magnetic unit cell. This motivates the question:

> *Are there non-magnetic models with Chern bands?*

- Chern band = Bands with non-zero Chern number

- Note that the sum of Chern numbers of all bands is always zero (➲ Problemset 2). Thus, if the answer to this question is affirmative, the model must have at least 2 bands. This can be achieved either with an internal degree of freedom (spin) or, alternatively, with sublattice degrees of freedom (i.e., a unit cell with more than one site).

Before we proceed, let us fix the nomenclature:

★ **Definition: Chern insulator**

$$
\text{Chern insulator* (CI*)} := \begin{cases} \text{Lattice model} \\ \text{Band insulator} \\ \text{Non-zero Chern number} \end{cases} \tag{1.117}
$$

Prototype: Hofstadter model

$$
\text{Chern insulator (CI)} := \begin{cases} \text{Lattice model} \\ \text{Band insulator} \\ \text{Non-zero Chern number} \\ \text{No magnetic field} \end{cases} \tag{1.118}
$$

Prototype: Haldane model

With this definition, the above question can be restated:

> *Are there Chern insulators?*

Before we focus on specific models, let us explore some generic properties of translation invariant models with two bands:

Lattice models with two bands

1. ⊲ Most general two-band Hamiltonian on a lattice:

$$H = \bigoplus_{\boldsymbol{k} \in T^2} \tilde{H}(\boldsymbol{k}) \quad \text{with} \quad \tilde{H}(\boldsymbol{k}) = \varepsilon(\boldsymbol{k})\,\mathbb{1} + \vec{d}(\boldsymbol{k}) \cdot \vec{\sigma} \qquad (1.119)$$

- T^2: Brillouin zone (= Torus)

- σ_i with $i = x, y, z$: Pauli matrices

- $\vec{d}(\boldsymbol{k}) : T^2 \to \mathbb{R}^3$: real, vector-valued function on BZ

2. *Spectrum:* $E_\pm(\boldsymbol{k}) = \varepsilon(\boldsymbol{k}) \pm |\vec{d}(\boldsymbol{k})|$

→ Band insulator iff

$$\min_{\boldsymbol{k} \in T^2} E_+(\boldsymbol{k}) > \max_{\boldsymbol{k} \in T^2} E_-(\boldsymbol{k}) \qquad (1.120)$$

Strictly speaking, this condition *allows* the system to be a band insulator *if* the chemical potential (= Fermi energy) is in the gap which the above condition guarantees to exist. We assume this situation in the following.

→ *Weaker* condition:

$$\forall \boldsymbol{k} \in T^2 : \quad E_+(\boldsymbol{k}) - E_-(\boldsymbol{k}) = 2|\vec{d}(\boldsymbol{k})| > 0 \qquad (1.121)$$

→ Normalization possible:

$$\hat{d}(\boldsymbol{k}) := \frac{\vec{d}(\boldsymbol{k})}{|\vec{d}(\boldsymbol{k})|} \quad \text{such that} \quad \hat{d} : T^2 \to S^2 \qquad (1.122)$$

S^2: unit sphere in $\mathbb{R}^3$

3. *Chern number of the lower band:*

$$C \overset{\circ}{=} -\frac{1}{4\pi} \int_{T^2} \underbrace{\hat{d}(\boldsymbol{k}) \cdot [\tilde{\partial}_x \hat{d}(\boldsymbol{k}) \times \tilde{\partial}_y \hat{d}(\boldsymbol{k})]}_{\substack{\text{(Oriented) Jacobian for surface integral} \\ 4\pi\,\mathbb{Z}}} \; d\boldsymbol{k} \; \in \mathbb{Z} \qquad (1.123)$$

Derivation: ➲ Problemset 4

4. *Geometric interpretation:*

The expression for the Berry curvature is just the Jacobian for the (oriented) surface integral over the sphere S^2:

$$\hat{d}(k) \cdot \left[\tilde{\partial}_y \hat{d}(k) \times \tilde{\partial}_x \hat{d}(k) \right]$$

$\rightarrow$
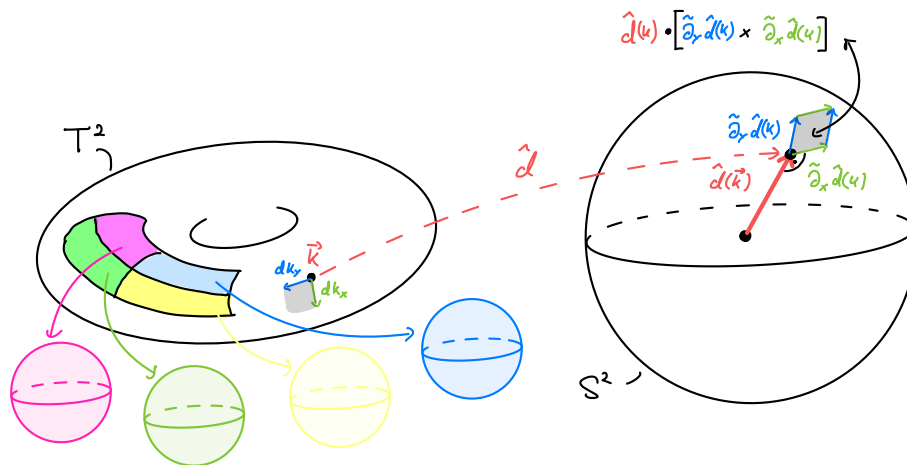
a) C counts how often $\hat{d}(\boldsymbol{k})$ covers S^2 when sweeping over the Brillouin zone T^2

b) $C = C[\hat{d}] \in \mathbb{Z}$ is a *topological invariant* (two maps $\hat{d}_a$ and $\hat{d}_b$ that can be continuously deformed into each other have the same winding number C)

c) Hamiltonian H_a can be continuously deformed into H_b without closing the gap iff $\hat{d}_a$ can be continuously deformed into $\hat{d}_b$

d) C labels different topological phases

5. *Skyrmion interpretation:*

The region on T^2 where the field $\hat{d}(\boldsymbol{k})$ wraps around the sphere can be quite localized. This creates a local "knot" in the field that can be viewed as an excitation of a specific type of non-linear field theory known as *non-linear sigma models*. In this context, these localized excitations are called *skyrmions* (after TONY SKYRME who introduced them to describe the strong force [45]); they are an example for *topological solitons*. Here an illustration of a skyrmion that represents a field $\hat{d}$ wrapping once around the sphere:
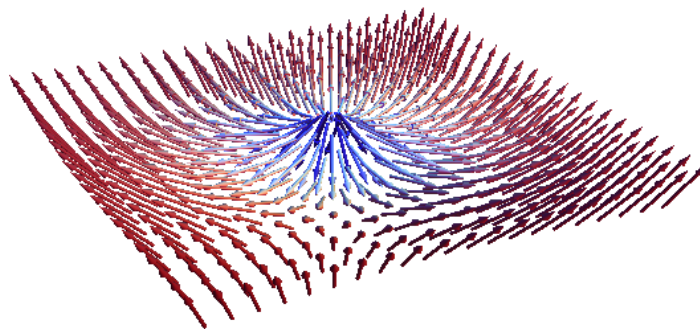
If the direction how the field sweeps over the sphere is inverted, one ends up with an *antiskyrmion*. A single skyrmion is a topologically protected field configuration and cannot be removed by continuous deformations of $\hat{d}$ (this is just our argument from above about the topological character of C restated in terms of skyrmions). However, a skyrmion and an antiskyrmion *can* be continuously removed (they "annihilate" each other):

↑ Notes
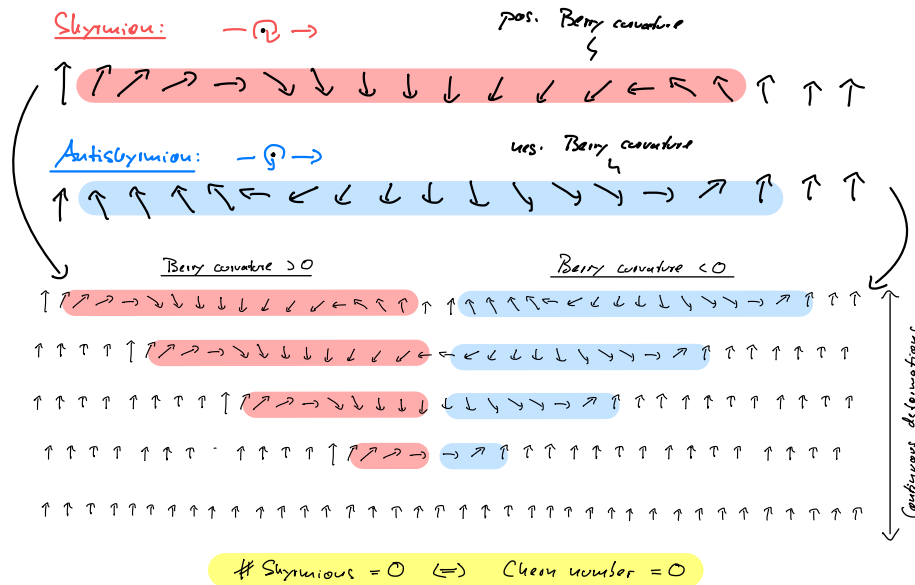
(Note that this is a 1D cut through the 2D surface on which the skyrmion-antiskyrmion pair lives.)

Summary:

- Skyrmions are "twists" of $\hat{d}$ and "live" on the BZ
- Positive (negative) Berry curvature indicates a finite (anti-)skyrmion *density*
- The Chern number is the number of skyrmions minus the number of antiskyrmions

---

† Note: Pontryagin number

The fact that $\hat{d}$ lives on a torus T^2 (the Brillouin zone) is not important in this situation. Thus it is possible to replace the torus T^2 by a sphere S^2 (which can be seen as the one-point compactified momentum space $\mathbb{R}^2$ of the continuum). Then,

$$\hat{d} \,:\, S^2 \to S^2 \tag{1.124}$$

is a continuous function that maps the sphere onto the sphere. Two Hamiltonians H_a and H_b belong then to the same phase, if the corresponding functions $\hat{d}_a$ and $\hat{d}_b$ can be smoothly transformed into each other.

In topology, this is known as *homotopy*; the set of equivalence classes under homotopy has a group structure and is known as (second) homotopy group of S^2, write $\pi_2(S^2)$; it is well-known that $\pi_2(S^2) = \mathbb{Z}$. The equivalence classes in $\pi_2(S^2)$ can be labeled by an integer known as *Pontryagin number*; it counts how often a map $\hat{d}$ traces out the (target) sphere S^2 when sweeping the (domain) sphere S^2. In the current situation, this is exactly the Chern number C.

That the torus can be replaced by a sphere is also evident in the skyrmion picture. Since the skyrmions can be localized, they do not care whether they live on a torus or a sphere:
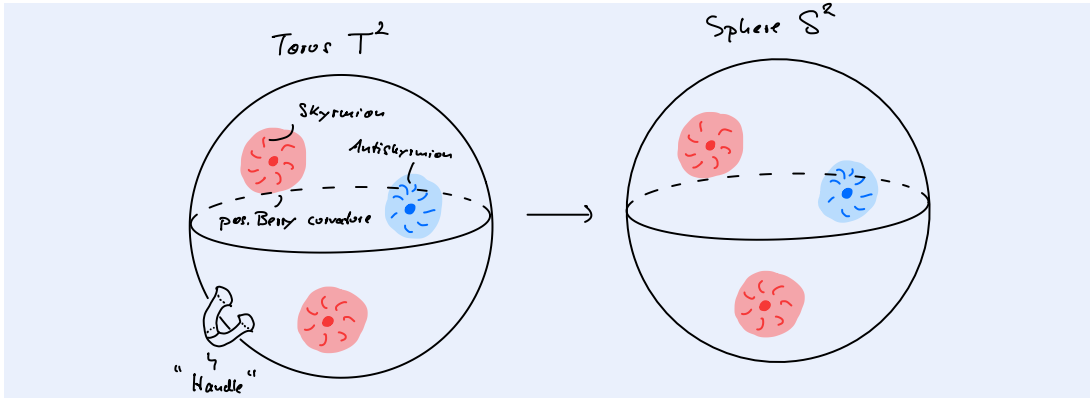
However, note that $\hat{d}$ can have "twists" around the torus that are not reflected in the Chern number (and are not related to skyrmions). These "twists" give rise to *weak topological indices* which can have physical effects on the boundary physics in specific directions [12, 46, 47]. Since these effects rely on the domain of $\hat{d}$ to be a torus (= Brillouin zone), they are protected by the translation symmetry of the lattice (this makes them "weak"). Weak topological indices are not important for the models discussed below.

Time-reversal Symmetry

Preliminary note: We will introduce here time-reversal symmetry as one of three "generic" symmetries and discuss the restrictions it imposes on the Bloch Hamiltonian $H(\boldsymbol{k})$. It play a role for the Haldane model but *not* as protecting symmetry; quite the contrary: it must be *broken* to make the model interesting (recall that the IQHE—which we would like to mimic—is not an SPT phase). However, in upcoming lectures we will use this symmetry as a *protecting symmetry* instead which then leads us to the concept of topological insulators and their classification.

Setting:

- *Single-particle (SP) Hilbert space* $\mathcal{H} = \text{span}\{|\Psi_{i\alpha}\rangle\}_{i\alpha}$ with SP Hamiltonian

$$H = \sum_{i\alpha, j\beta} H_{i\alpha, j\beta} |\Psi_{i\alpha}\rangle\langle\Psi_{j\beta}| \tag{1.125}$$

  $i = 1 \ldots N$: site index
  $\alpha = 1 \ldots M$: internal degrees of freedom (e.g., multiple sites per unit cell, spin, …)

- *Many-body (MB) Hilbert space* $\hat{\mathcal{H}} = \bigoplus_n \bigwedge^n(\mathcal{H})$ (= fermionic Fock space) with MB Hamiltonian

$$\hat{H} = \sum_{i\alpha, j\beta} c_{i\alpha}^{\dagger} H_{i\alpha, j\beta} c_{j\beta} \tag{1.126}$$

  $c_{i\alpha}/c_{i\alpha}^{\dagger}$: fermionic creation/annihilation operators for fermion in state $|\Psi_{i\alpha}\rangle$

- *Translation symmetry* $\rightarrow$

$$\hat{H} = \sum_{\boldsymbol{k};\alpha,\beta} c_{\boldsymbol{k}\alpha}^{\dagger} H_{\alpha\beta}(\boldsymbol{k}) c_{\boldsymbol{k}\beta} \tag{1.127}$$

with

$$c_{k\alpha} := \frac{1}{\sqrt{N}} \sum_i e^{i x_i k} c_{i\alpha} \tag{1.128}$$

x_i: position of site i

So the SP Hamiltonian decomposes as $H = \bigoplus_k H(k)$ with Bloch Hamiltonian $H(k)$ (a Hermitian $M \times M$-matrix). Diagonalizing the latter yields

$$H(k) = \sum_n \varepsilon_n(k) |u_{nk}\rangle\langle u_{nk}| \tag{1.129}$$

$|u_{kn}\rangle$: Bloch wavefunction
$n = 1 \dots M$: band index
$\varepsilon_n(k)$: SP spectrum

Then the SP Hilbert space can be written as $\mathcal{H} = \bigoplus_k \mathcal{H}_k$ with mode space $\mathcal{H}_k = \text{span}\{|u_{nk}\rangle\}_n$.

1. We start by considering a single particle and its SP Hilbert space $\mathcal{H}$:

   TRS $T : t \mapsto -t$ is a $\mathbb{Z}_2$-symmetry (inverting time twice should do nothing) and sould act as

   $$T x T^{-1} \overset{!}{=} x \quad \text{but} \quad T p T^{-1} \overset{!}{=} -p \tag{1.130}$$

   $\rightarrow T i \hbar T^{-1} = T[x, p]T^{-1} = -[x, p] = -i\hbar$
   $\rightarrow T$ is *antiunitary*:

   $$T_U = U \mathcal{K} \quad \text{with} \quad \mathcal{K} = \text{Complex conjugation} \tag{1.131}$$

   U: unitary operator that determines the *representation* T_U of T on the SP Hilbert space

   Wigner's theorem [48] states that a *symmetry* (i.e., an operator O that preserves all probability amplitudes, $|\langle O\Psi|O\Phi\rangle|^2 = |\langle \Psi|\Phi\rangle|^2$) acts either as a *unitary* or an *antiunitary* operator on the Hilbert space. In combination with $T i T^{-1} = -i$, this fixes T to the generic form T_U above.

   $\rightarrow$ SP Hamiltonian H is *time-reversal symmetric* iff $[H, T_U] = 0$
   for a U chosen appropriately to describe the system (see below)

2. *Consequence of antiunitarity:*

   $$T_U^2 = U U^* = U(U^T)^{-1} \tag{1.132}$$

   - $U U^*$ is unitary

   - $[H, U U^*] = 0 \rightarrow U U^*$ is a symmetry of H

   Assume H does not have any *additional* unitary symmetries
   This step is a bit tricky [37], but for now, assume that you made the total Hamiltonian block-diagonal by "using up" all its potential unitary symmetries. Then *each block* carries an irreducible representation of the unitary symmetry group and an "irreducible Hamiltonian" so that the arguments below hold. How T is represented in each block can vary, however the result for T^2 must be the same on all blocks because otherwise T is

not a (projective) representation of $\mathbb{Z}_2$ on the whole SP Hilbert space—and this would contradict our intuition that applying time-reversal twice does nothing.

= Hamiltonian irreducible $\rightarrow UU^* = \lambda\mathbb{1}$
(this is an application of *Schur's lemma* on the irreducible *Hamiltonian*)

$$\text{Eq. (1.132)} \quad \Rightarrow \quad U = \lambda U^T \quad \Leftrightarrow \quad U^T = U\lambda \tag{1.133}$$
$$\Rightarrow \quad U = \lambda^2 U \tag{1.134}$$
$$\Rightarrow \quad \lambda = \pm 1 \tag{1.135}$$

$\rightarrow$

$$\boxed{T_U^2 = \pm\mathbb{1}} \tag{1.136}$$

If $T_U^2 = -\mathbb{1}$, T_U is an *antiunitary*, *projective* representation of $\mathbb{Z}_2$.

3. *Examples:*

- Spinless particles:

$$\boxed{T_0 := \mathcal{K} \quad \Rightarrow \quad T_0^2 = +\mathbb{1}} \tag{1.137}$$

- Spin-$\frac{1}{2}$ particles:

$\vec{S} = \frac{\hbar}{2}\vec{\sigma}$: angular momentum operator $\rightarrow T_U \vec{S} T_U^{-1} \stackrel{!}{=} -\vec{S}$
So we want that $T_U \sigma^i T_U^{-1} = -\sigma^i$ for $i = x, y, z$.

$\rightarrow$ *Solution:*

$$\boxed{T_{\frac{1}{2}} := \sigma^y \mathcal{K} \quad \Rightarrow \quad T_{\frac{1}{2}}^2 = -\mathbb{1}} \tag{1.138}$$

  - Often you will find the choice $T_{\frac{1}{2}} = -i\sigma^y \mathcal{K}$. This follows if one derives $T_{\frac{1}{2}}$ as a spin rotation. Note that you can multiply $T_{\frac{1}{2}}$ with an arbitrary phase without changing its algebraic properties.

  - The statement $T_U^2 = -\mathbb{1}$ is true for all particles with *half-integer* spin (but with other choices for U that depend on the spin, of course).

4. *Consequence of $T_U^2 = -\mathbb{1}$:*

⁂ **Important: Kramers theorem [49]**

Every eigenenergy of a time-reversal invariant Hamiltonian H with $T_U^2 = -\mathbb{1}$ is at least two-fold degenerate.

Proof: ➲ Problemset 4

This theorem has far-reaching consequences. For instance, the degeneracy of atomic energy levels with half-integer total angular momentum cannot be lifted completely by electric fields alone (which preserve TRS); instead, magnetic fields are needed (which do break TRS). Later we will see that Kramers theorem restricts the band structure of time-reversal invariant systems in that it requires crossing bands at so called *time-reversal invariant momenta* (TRIMs) in the Brillouin zone.

5. Now we generalize these SP concepts to the MB Hilbert space and Hamiltonian:
   Action on Fock space:

   a) ◁ Representation $\mathcal{T}_U$ of TRS on the *fermionic Fock space* $\hat{\mathcal{H}}$:

   > ★ **Definition: Time-reversal symmetry**
   >
   > $$\mathcal{T}_U i \mathcal{T}_U^{-1} := -i \quad \text{and} \quad \mathcal{T}_U c_{i\alpha} \mathcal{T}_U^{-1} := \sum_\beta U_{\alpha\beta}^\dagger c_{i\beta}, \qquad (1.139)$$
   >
   > $$\mathcal{T}_U c_{i\alpha}^\dagger \mathcal{T}_U^{-1} := \sum_\beta \underbrace{(U_{\alpha\beta}^\dagger)^*}_{U_{\beta\alpha}} c_{i\beta}^\dagger \qquad (1.140)$$
   >
   > Note that we assume that time-reversal mixes only internal DOFs but not spatial ones. This restriction complies with our every-day experience and simplifies the following discussion. Furthermore, we assume that TR acts on every site in the same way (which is reasonable for translational invariant systems).

   b) Let us check that this definition of TRS on $\hat{\mathcal{H}}$ is consistent with our definition on $\mathcal{H}$ above:

   $$\mathcal{T}_U \hat{H} \mathcal{T}_U^{-1} = \sum_{i\alpha',j\beta'} c_{i\alpha'}^\dagger \sum_{\alpha,\beta} \left[U_{\alpha'\alpha} H_{i\alpha,j\beta}^* U_{\beta\beta'}^\dagger \right] c_{j\beta'} \qquad (1.141)$$

   $$\overset{!}{=} \sum_{i\alpha',j\beta'} c_{i\alpha'}^\dagger H_{i\alpha',j\beta'} c_{j\beta'} = \hat{H} \qquad (1.142)$$

   →

   $$\boxed{\begin{array}{ll} \left[\hat{H}, \mathcal{T}_U \right] = 0 \quad \Leftrightarrow \quad T_U H T_U^{-1} = H & (1.143) \\[2mm] \text{with} \quad T_U = \bar{U}\mathcal{K} \quad \text{where} \quad \bar{U} := \oplus_i U_i \quad \text{with} \quad U_i \equiv U & (1.144) \end{array}}$$

   This is the form of TR in the SP Hilbert space that we discussed earlier (where the role of U is now played by $\bar{U}$ since we have single-particle states on each site).

   Note that $\bar{U}$ is a unitary $NM \times NM$-matrix whereas U is a unitary $M \times M$ matrix.

   c) We want to consider *translational invariant* systems →

   $$\mathcal{T}_U c_{k\alpha} \mathcal{T}_U^{-1} = \frac{1}{\sqrt{N}} \sum_i e^{-i x_i k} \sum_\beta U_{\alpha\beta}^\dagger c_{i\beta} = \sum_\beta U_{\alpha\beta}^\dagger c_{-k\beta} \qquad (1.145)$$

   → $\mathcal{T}_U$ inverts momenta & mixes internal DOFs

   For a TRI MB Hamiltonian we find:

   $$\mathcal{T}_U \hat{H} \mathcal{T}_U^{-1} = \sum_{k;\alpha',\beta'} c_{-k\alpha'}^\dagger \sum_{\alpha,\beta} \left[U_{\alpha'\alpha} H_{\alpha\beta}^*(k) U_{\beta\beta'}^\dagger \right] c_{-k\beta'} \qquad (1.146)$$

   $$\overset{!}{=} \sum_{k;\alpha',\beta'} c_{-k\alpha'}^\dagger H_{\alpha'\beta'}(-k) c_{-k\beta'} = \hat{H} \qquad (1.147)$$

(In the last equation, we substituted $\boldsymbol{k} \to -\boldsymbol{k}$.)

$\to$ Thus we find a constraint on the Bloch Hamiltonians:

$$\left[\hat{H}, \mathcal{T}_U\right] = 0 \quad \Leftrightarrow \quad \tilde{T}_U H(\boldsymbol{k}) \tilde{T}_U^{-1} = H(-\boldsymbol{k}) \tag{1.148}$$

$$\text{with} \quad \tilde{T}_U = U\mathcal{K} \tag{1.149}$$

Note that $\tilde{T}_U$ maps between the mode spaces $\mathcal{H}(\boldsymbol{k})$ and $\mathcal{H}(-\boldsymbol{k})$ since TR inverts momenta!

In summary, time-reversal invariance means:

$$\left[\hat{H}, \mathcal{T}_U\right] = 0 \quad \Leftrightarrow \quad T_U H T_U^{-1} = H \tag{1.150}$$

$$\Leftrightarrow \quad \bar{U} H^* \bar{U}^\dagger = H \tag{1.151}$$

$$\Leftrightarrow \quad \tilde{T}_U H(\boldsymbol{k}) \tilde{T}_U^{-1} = H(-\boldsymbol{k}) \tag{1.152}$$

$$\Leftrightarrow \quad U H^*(\boldsymbol{k}) U^\dagger = H(-\boldsymbol{k}) \tag{1.153}$$

The last two lines are only defined if the system is translation invariant.

- *In words:* A (non-interacting) MB Hamiltonian $\hat{H}$ is time-reversal invariant if its SP Hamiltonian H is unitarily equivalent to its complex conjugate.

- Note that often the formal distinction between T_U and $\tilde{T}_U$ is not made in the literature (similarly for $\bar{U}$ and U) and one simply writes T_U (or even just T) for both.

- Conditions like $\bar{U} H^* \bar{U}^\dagger = H$ are sometimes referred to *reality conditions* on the Hamiltonian. We will encounter another example when we discuss particle-hole symmetry later in this course.

Furthermore:

$$T_U^2 = +\mathbb{1} \quad \Leftrightarrow \quad \tilde{T}_U^2 = +\mathbb{1} \quad \Leftrightarrow \quad \mathcal{T}_U^2 \overset{\circ}{=} +\mathbb{1} \tag{1.154}$$

$$T_U^2 = -\mathbb{1} \quad \Leftrightarrow \quad \tilde{T}_U^2 = -\mathbb{1} \quad \Leftrightarrow \quad \mathcal{T}_U^2 \overset{\circ}{=} (-1)^{\hat{N}} \tag{1.155}$$

$\hat{N} = \sum_{i\alpha} c_{i\alpha}^\dagger c_{i\alpha}$: total fermion number operator

$\mathcal{P} = (-1)^{\hat{N}}$ is the fermion *parity operator*.

6. Consequence of TRS for the *spectrum:*

$$H(\boldsymbol{k})|u_{n\boldsymbol{k}}\rangle = \varepsilon_n(\boldsymbol{k})|u_{n\boldsymbol{k}}\rangle \tag{1.156}$$

$$\Rightarrow \quad H(-\boldsymbol{k}) U |u_{n\boldsymbol{k}}\rangle^* = \varepsilon_n(\boldsymbol{k}) U |u_{n\boldsymbol{k}}\rangle^* \tag{1.157}$$

$\to$ Eigenstate $U|u_{n\boldsymbol{k}}\rangle^*$ of $H(-\boldsymbol{k})$ has *same* energy $\varepsilon_n(\boldsymbol{k})$ as eigenstate $|u_{n\boldsymbol{k}}\rangle$ of $H(\boldsymbol{k})$

$\to$ *Inversion-symmetric* band structure

This means that for TRI systems, one half of the BZ is determined by the other half via $\tilde{T}_U$. This motivates the introduction of a so called *effective Brillouin zone (EBZ)* (essentially "half" the original BZ) which has the topology of a cylinder [50].

7. Consequence of TRS for the *Chern number:*

- $\lhd$ Two bands from pseudo-spin-$\frac{1}{2}$: $\tilde{T}_0 = \mathcal{K}$

$$H^*(\boldsymbol{k}) = H(-\boldsymbol{k}) \quad \Leftrightarrow \quad \hat{d}_{x,z}(\boldsymbol{k}) = \hat{d}_{x,z}(-\boldsymbol{k}) \tag{1.158}$$
$$\hat{d}_y(\boldsymbol{k}) = -\hat{d}_y(-\boldsymbol{k})$$

- $\lhd$ Two bands from real spin-$\frac{1}{2}$: $\tilde{T}_{\frac{1}{2}} = \sigma^y \mathcal{K}$

$$\sigma^y H^*(\boldsymbol{k})\sigma^y = H(-\boldsymbol{k}) \quad \Leftrightarrow \quad \hat{d}(\boldsymbol{k}) = -\hat{d}(-\boldsymbol{k}) \tag{1.159}$$

Both cases $\rightarrow$

$$C = -\frac{1}{4\pi} \int_{-\pi}^{\pi} dk_x \int_{-\pi}^{\pi} dk_y \, \varepsilon_{ijk} \hat{d}_i(\boldsymbol{k})\tilde{\partial}_x \hat{d}_j(\boldsymbol{k})\tilde{\partial}_y \hat{d}_k(\boldsymbol{k}) = 0 \tag{1.160}$$

This follows since $\hat{d}_i(\boldsymbol{k})\tilde{\partial}_x \hat{d}_j(\boldsymbol{k})\tilde{\partial}_y \hat{d}_k(\boldsymbol{k})$ is antisymmetric for both representations if i, j, k are pairwise distinct (which is enforced by ε_{ijk}).

$\rightarrow$

⁂ **Important**

Systems with Chern bands must *break* time-reversal symmetry.

This is true in general, i.e., even for models with more than two bands.

- This also makes sense from another perspective: Conductivity transforms as $\sigma \mapsto -\sigma$ under time-reversal since $\vec{J} = \sigma\vec{E}$ and $\vec{J} \mapsto -\vec{J}$ but $\vec{E} \mapsto \vec{E}$ (⊙ Maxwell equations). Thus in a time-reversal invariant system $\sigma = \sigma_a + \sigma_s = 0$. Note that $\sigma_a \neq 0$ indeed requires a magnetic field (which breaks time-reversal symmetry) and $\sigma_s \neq 0$ requires dissipation (recall the Drude model) and breaks time-reversal symmetry because of entropy production.

- Note that this is completely consistent with the IQHE (or the Hofstadter model) where we found Chern bands and the magnetic field clearly breaks TRS.

- This is a restriction (and a hint) for the construction of a Chern insulator.

Dirac fermions

1. $\lhd$ Dirac equation in 2D:

$$H_D \Psi = \left(\beta m + \sum_{n=1}^{2} \alpha_n p_n\right) \Psi = i\partial_t \Psi \tag{1.161}$$

with

- $\alpha_1, \alpha_2, \beta$ Hermitian matrices
- $\alpha_1^2 = \alpha_2^2 = \beta^2 = \mathbb{1}$

- $\{\alpha_1, \alpha_2\} = \{\beta, \alpha_1\} = \{\beta, \alpha_2\} = 0$

$\rightarrow$ Solution: $\alpha_1 = \sigma^x$, $\alpha_2 = \sigma^y$, and $\beta = \sigma^z$
In particular, Ψ is a 2-dimensional spinor!

$\rightarrow$ Fourier transform of H_D ($\boldsymbol{k} \in \mathbb{R}^2$):

$$H_D(\boldsymbol{k}) = k_x \sigma^x + k_y \sigma^y + m \sigma^z = \vec{d}(\boldsymbol{k}) \cdot \vec{\sigma} \quad \text{with} \quad \vec{d}(\boldsymbol{k}) = \begin{pmatrix} k_x \\ k_y \\ m \end{pmatrix} \qquad (1.162)$$

Fermions in condensed matter physics that are (approximately) described by a 2-band Bloch Hamiltonian of this form are therefore known as *Dirac fermions* (this also refers to more general Hamiltonians linear in $\boldsymbol{k}$, see below).

Spectrum: $\varepsilon_\pm(\boldsymbol{k}) = \pm|\vec{d}(\boldsymbol{k})| = \pm\sqrt{k^2 + m^2} \rightarrow$ Gapped if $m \neq 0$
This is where the name "mass gap" comes from.

2. *Time-reversal symmetry:*

- $\tilde{T}_0 = \mathcal{K} \rightarrow d_x(\boldsymbol{k}) \overset{!}{=} d_x(-\boldsymbol{k}) \rightarrow H_D$ not TRI!

- $\tilde{T}_{\frac{1}{2}} = \sigma^y \mathcal{K} \rightarrow d_z(\boldsymbol{k}) \overset{!}{=} -d_z(-\boldsymbol{k}) \rightarrow H_D$ not TRI for $m \neq 0$!

$\rightarrow H_D$ is only TRI for $m = 0$ but there the gap closes anyway.
$\rightarrow$ Non-zero Chern number *possible*

3. *Berry curvature of the lower band:*

$$\mathcal{F}_{xy}(\boldsymbol{k}) \overset{\circ}{=} \frac{m}{2(\boldsymbol{k}^2 + m^2)^{3/2}} \qquad (1.163)$$

Proof: ❯ Problemset 4

4. *"Chern number":*

$$C = -\frac{1}{2\pi} \int_{\mathbb{R}^2} \mathcal{F}_{xy}(\boldsymbol{k}) \, d^2k = -\int_0^\infty \frac{mk}{2(\boldsymbol{k}^2 + m^2)^{3/2}} \, dk \overset{\circ}{=} -\frac{\text{sign}(m)}{2} \qquad (1.164)$$

Why $C \notin \mathbb{Z}$?
The quantization of C is based on Stokes' theorem which is only valid for integrations over *compact* manifolds (sphere, torus). Here, however, we integrate over the non-compact $\mathbb{R}^2$ instead, so we cannot expect C to be quantized.

$\rightarrow$ Change from $m < 0$ to $m > 0 \Rightarrow$ Change of Chern number $\Delta C = -1$

5. ◁ 2-band lattice model $H_\Gamma(\boldsymbol{k}) = \varepsilon_\Gamma(\boldsymbol{k})\mathbb{1} + \vec{d}_\Gamma(\boldsymbol{k}) \cdot \vec{\sigma}$
Γ: parameters of the model

$\rightarrow \boldsymbol{K} \in T^2$ = *Dirac point* if

$$H_\Gamma(\boldsymbol{K} + \boldsymbol{k}) = v_F \left[k_x \sigma^x + k_y \sigma^y + v_F m_\Gamma \, \sigma^z \right] + \mathcal{O}(k^2) \qquad (1.165)$$

$m_\Gamma = 0 \rightarrow$ Band structure at $\boldsymbol{K}$: $\varepsilon_\pm(\boldsymbol{K} + \boldsymbol{k}) = \pm v_F |\boldsymbol{k}|$ = *Dirac cone*
v_F: Fermi velocity (corresponds to the speed of light c in the Dirac equation)
In the following we set always $|v_F| = 1$.

Dirac points are interesting because they harbour "half a (anti-)skyrmion" (depending on the sign of m_Γ). When the sign of m_Γ changes at a gap closing (by varying Γ), this can change the (quantized) Chern number of the bands by ± 1 (as discussed above).

↑ Notes

1.2.2 The Qi-Wu-Zhang Model

Historically, the Haldane model (see below) was the first CI. However, it is not the simplest one (at least its momentum space representation is rather complex due to the honeycomb lattice). Later, Qi, Wu and Zhang introduced a simpler model on the square lattice [51] which we will discuss first. "Simpler" refers here to its representation in momentum space—the real-space representation of the QWZ model is rather unintuitive.

1. *Idea:* "Regularize" Dirac Hamiltonian on a lattice $\rightarrow H_{\text{QWZ}}(\boldsymbol{k}) = \vec{d}(\boldsymbol{k}) \cdot \vec{\sigma}$ with

$$d_x = \sin(k_x) \qquad\qquad = k_x + \mathcal{O}(k^2) \qquad (1.166)$$
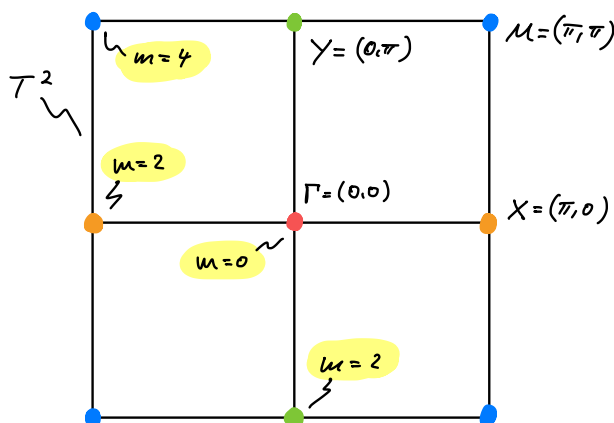$$d_y = \sin(k_y) \qquad\qquad = k_y + \mathcal{O}(k^2) \qquad (1.167)$$
$$d_z = -m + 2 - \cos(k_x) - \cos(k_y) = -m + \mathcal{O}(k^2) \qquad (1.168)$$

$m \in \mathbb{R}$: only parameter of the theory

The inverted sign of m is convention and motivated by the results (see below).

The two bands are interpreted as spin-$\frac{1}{2}$ DOFs of fermions hopping on a square lattice (see below).

2. *Spectrum:* $\varepsilon_{\pm}(\boldsymbol{k}) = \pm|\vec{d}(\boldsymbol{k})| \neq 0$ for all $\boldsymbol{k} \in T^2 \setminus \{\boldsymbol{\Gamma}, \boldsymbol{X}, \boldsymbol{Y}, \boldsymbol{M}\}$ with

In the sketch we indicate for which parameter m the gap closes at which point in the BZ. This follows directly by inspection of d_z in Eq. (1.168).

3. *Phases:*

   - $m < 0$:
     $\vartriangleleft m \rightarrow -\infty \rightarrow \vec{d}(\boldsymbol{k}) \approx -m\vec{e}_z \rightarrow C(m < 0) = 0 \rightarrow$ Trivial band insulator
     Recall that C counts the skyrmions in the BZ, i.e., how often $\vec{d}$ "wraps" around the sphere. If $\vec{d}$ is pinned to the north pole, it clearly cannot "wrap" anything.

   - $m > 4$:
     $\vartriangleleft m \rightarrow +\infty \rightarrow \vec{d}(\boldsymbol{k}) \approx -m\vec{e}_z \rightarrow C(m > 0) = 0 \rightarrow$ Trivial band insulator
     The argument is the same as for $m < 0$.

   - $0 < m < 2$:
     $\vartriangleleft$ Transition from $m < 0$ to $m > 0 \rightarrow$ Gap closing at $\boldsymbol{\Gamma}$:

$$H(\boldsymbol{\Gamma} + \boldsymbol{k}) = k_x \sigma^x + k_y \sigma^y - m\sigma^z + \mathcal{O}(k^2) \qquad (1.169)$$

$\rightarrow$

$$C(0 < m < 2) = C(m < 0) + \Delta C(m < 0 \to m > 0) \tag{1.170}$$

$$= 0 - \left[\frac{\text{sign}(-m)|_{m>0}}{2} - \frac{\text{sign}(-m)|_{m<0}}{2} \right] \tag{1.171}$$

$$= +1 \tag{1.172}$$

$\rightarrow$ Topological phase (I)

- $2 < m < 4$: $\lhd$ Transition from $m > 4$ to $m < 4 \to$ Gap closing at $\boldsymbol{M}$:

$$H(\boldsymbol{M} + \boldsymbol{k}) = -k_x \sigma^x - k_y \sigma^y + (4 - m)\sigma^z + \mathcal{O}(k^2) \tag{1.173}$$
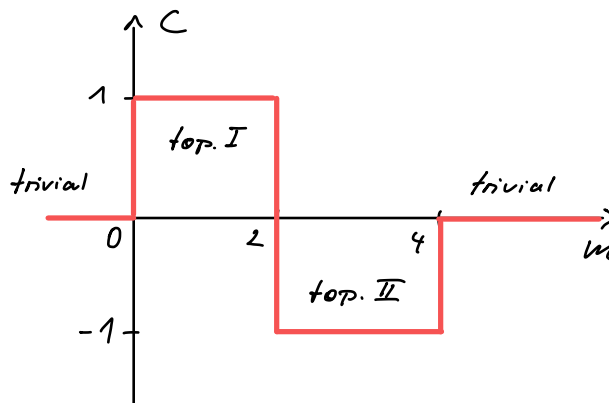
$\rightarrow$

$$C(2 < m < 4) = C(m > 4) + \Delta C(m > 4 \to m < 4) \tag{1.174}$$

$$= 0 - \left[\frac{\text{sign}(4 - m)|_{m<4}}{2} - \frac{\text{sign}(4 - m)|_{m>4}}{2} \right] \tag{1.175}$$

$$= -1 \tag{1.176}$$

$\rightarrow$ Topological phase (II)

$\rightarrow$ *Phase diagram:*

- Note that we can compute $C(2 < m < 4)$ alternatively via the transition from $m < 2$ to $m > 2$. At this transition there are *two* Dirac points ($\boldsymbol{X}$ and $\boldsymbol{Y}$), each of which contributes a change of the Chern number by -1 which explains the jump from $C(0 < m < 2) = +1$ to $C(2 < m < 4) = -1$.

- The two trivial phases for $m < 0$ and $m > 4$ are the *same* trivial quantum phase, i.e., they can be connected by continuously deforming the Hamiltonian without closing the gap. To do this, start from the limit $m \ll 0$ where $\vec{d}$ points to the north pole and then rotate this vector [more precisely: this (almost constant) function] continuously to the south pole (without changing its length). Then you end up in the phase for $m \gg 4$ while the gap on the path was always on the order of $|\vec{d}|$ (i.e., very large).

- The two topological phases I and II are *different* quantum phases that cannot be connected by smooth deformations of the Hamiltonian without closing the gap. This follows from the discreteness of the Chern number and the definition of the latter in terms of the normalized Bloch vector $\hat{d}(\boldsymbol{k})$.

- It is highly recommended to plot $\vec{d}(\boldsymbol{k})$ on the BZ as a vector field and observe the changes for $m < 0$ to $m > 4$ (in `Mathematica` you can use the `Manipulate` function to visualize the changes). Try to count the skyrmions, i.e., how often $\vec{d}(\boldsymbol{k})$ "wraps" around the sphere (and in which direction).

4. *Real-space Hamiltonian:*

   The real-space Hamiltonian of the QWZ model is defined on a square lattice with spin-$\frac{1}{2}$ fermions on the sites (the spin DOF is responsible for the two bands):

   SP Hilbert space spanned by

   $$|\Psi_{i\alpha}\rangle \rightarrow \underbrace{|x, y\rangle}_{\text{external}} \otimes \underbrace{|\sigma\rangle}_{\text{internal}} \tag{1.177}$$

   $x = 1, \ldots, N_x$: x-position
   $y = 1, \ldots, N_y$: y-position
   $\sigma = \pm 1$: spin

   Representation of Pauli algebra:

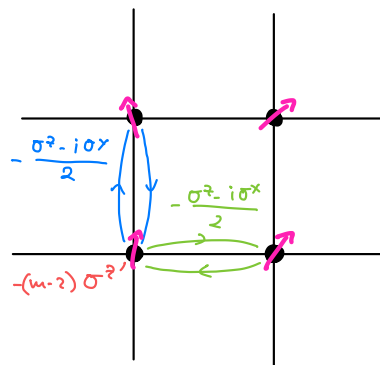 $$\sigma^x = |+1\rangle\langle-1| + |-1\rangle\langle+1| \tag{1.178}$$
   $$\sigma^y = i|-1\rangle\langle+1| - i|+1\rangle\langle-1| \tag{1.179}$$
   $$\sigma^z = |+1\rangle\langle+1| - |-1\rangle\langle-1| \tag{1.180}$$

   SP Hamiltonian:

   $$H_{\text{QWZ}} \overset{\circ}{=} -\sum_{x,y}\left[|x+1, y\rangle\langle x, y| \otimes \frac{\sigma^z - i\sigma^x}{2} + \text{h.c.}\right] \tag{1.181}$$
   $$-\sum_{x,y}\left[|x, y+1\rangle\langle x, y| \otimes \frac{\sigma^z - i\sigma^y}{2} + \text{h.c.}\right]$$
   $$-(m-2)\sum_{x,y}|x, y\rangle\langle x, y| \otimes \sigma^z$$

   Pictorially:

   Note that there is *no magnetic field* involved and therefore no magnetic unit cell necessary!

   - The kinetic terms of the Hamiltonian (hopping in x- and y-direction) couple the spatial ("orbital") motion with the internal ("spin") degrees of freedom. This is an example of *spin-orbit coupling* in a lattice model.

   - Fourier transform H_{QWZ} in both spatial directions and show that the Bloch Hamiltonian is $H_{\text{QWZ}}(\boldsymbol{k})$ as defined above.

↑ Notes

1.2.3 The Haldane Model

- Historically, the Haldane model (HM) on the honeycomb lattice was the first model that realizes the phenomenology of the IQHE without magnetic fields (and therefore without Landau levels) [52]; this phenomenon is nowadays referred to as *quantum anomalous Hall effect (QAHE)*.

- Therefore, the Haldane model is also regarded as the prototype of a *Chern insulator*. However, some also refer to the Hofstadter model as Chern insulators* [38].

- Regarding classification, the Haldane model belongs to the same invertible topological order as the IQHE: it features chiral edge modes but no anyonic excitations and is not protected by any symmetry (only quantization of the Hall response requires charge conservation).

- Haldane discussed this model in his Nobel Lecture [53].

1. *Idea:*

   a) Start with the Hamiltonian of *graphene*:
      $\rightarrow$ 2 Dirac cones in the BZ (but not gapped!)

   b) Add a staggered potential (parameter m) to break the *sublattice symmetry (SLS)* (⊘ Section 1.4):
      $\rightarrow$ Gap opens at Dirac points but Chern number is zero since TRS not broken.
      $\rightarrow$ Dead end!

   c) Add instead a complex NNN hopping (strength t and phase φ) to break *time-reversal symmetry*:
      $\rightarrow$ Gap opens at Dirac points *and* Chern number non-zero.
      $\rightarrow$ Success!

   d) Map out the phase diagram in the m/t-φ plane.

2. *Real-space MB Hamiltonian* on the honeycomb lattice:
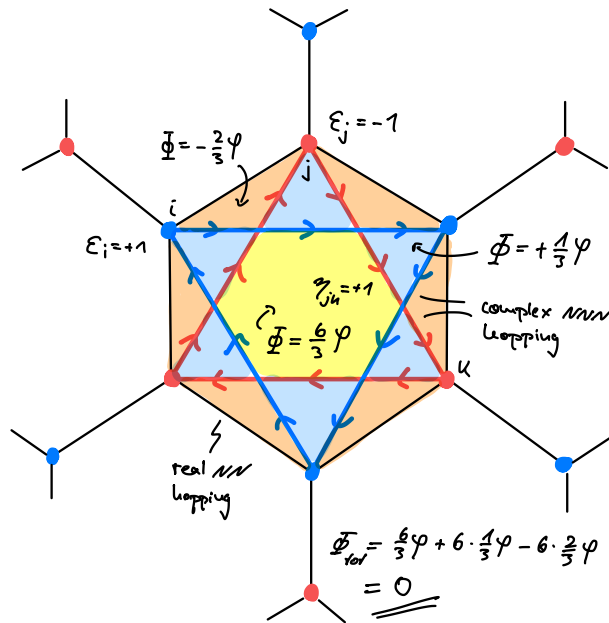
$$\hat{H}_\text{H} = \underbrace{\sum_{\langle i,j \rangle} c_i^\dagger c_j}_{\text{Graphene}} + \underbrace{m \sum_i \epsilon_i c_i^\dagger c_i}_{\text{Staggered potential}} + \underbrace{t \sum_{\langle\langle i,j \rangle\rangle} e^{\eta_{ij} i\varphi} c_i^\dagger c_j}_{\text{Complex NNN hopping}} \qquad (1.182)$$

- $\langle i, j \rangle$: Nearest-neighbours
- $\langle\langle i, j \rangle\rangle$: Next-Nearest-neighbours
- m: Strength of the staggered potential
- t: Strength of the complex hopping
- φ: Phase of the complex hopping
- $\epsilon_i = \pm 1$: Sublattice-dependent sign (see sketch above)
- $\eta_{ij} = \pm 1$ and $\eta_{ij} = -\eta_{ji}$: Direction-dependent sign (see sketch above)

Notes:

- This is a 2-band model because of the two sites in each unit cell of the honeycomb lattice (in contrast to the QWZ model where the 2 bands described internal spin DOFs).

- Despite the complex hopping, there is no *net* magnetic flux through the plaquettes of the honeycomb model; therefore no magnetic unit cell is needed. You can think of the complex hoppings arising from a *local* magnetic field "curled up" in each plaquette:
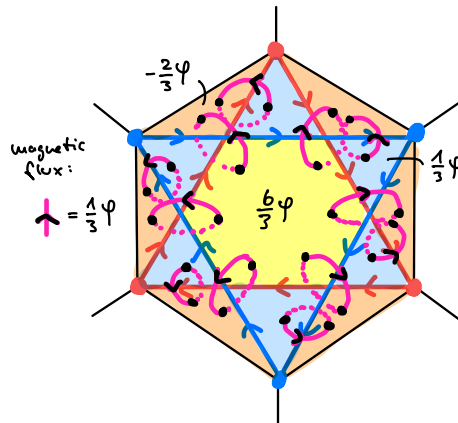
Note that other gauges are possible; for instance, one can "concentrate" the accumulated phase on the central third of the NNN hopping trajectories so that the outer (orange) triangles do not carry any flux and the blue triangles cancel the flux through the yellow hexagon.

- The staggered potential breaks SLS (⊖ Section 1.4) but not TRS, whereas the complex NNN hopping breaks SLS *and* TRS. Breaking SLS *and/or* TRS is sufficient to open a gap at the Dirac points, but only breaking of TRS can result in bands with non-zero Chern number.

3. a) *Brillouin zone:*

Honeycomb lattice = Hexagonal/Triangular lattice + 2-atom basis

- Hexagonal lattice → Brillouin zone
- 2-atom basis → 2 bands

Hexagonal lattice: $\boldsymbol{a}_1 = \frac{1}{2}(\sqrt{3}, 1)^T$, $\boldsymbol{a}_2 = \frac{1}{2}(\sqrt{3}, -1)^T$

Reciprocal lattice (= Hexagonal lattice): $\boldsymbol{b}_1 = 2\pi(1/\sqrt{3}, 1)^T$, $\boldsymbol{b}_2 = 2\pi(1/\sqrt{3}, -1)^T$
The reciprocal lattice is defined by vectors $\boldsymbol{b}$ that satisfy $\boldsymbol{b} \cdot \boldsymbol{a} \in 2\pi\mathbb{Z}$ for $\boldsymbol{a} \in \mathbb{Z}\boldsymbol{a}_1 + \mathbb{Z}\boldsymbol{a}_2$ some lattice vector of the original lattice. The vectors $\boldsymbol{b}_i$ above are a basis of this reciprocal lattice.

Brillouin zone = Wigner-Seitz cell of the reciprocal lattice:
(= rotated Honeycomb plaquette)
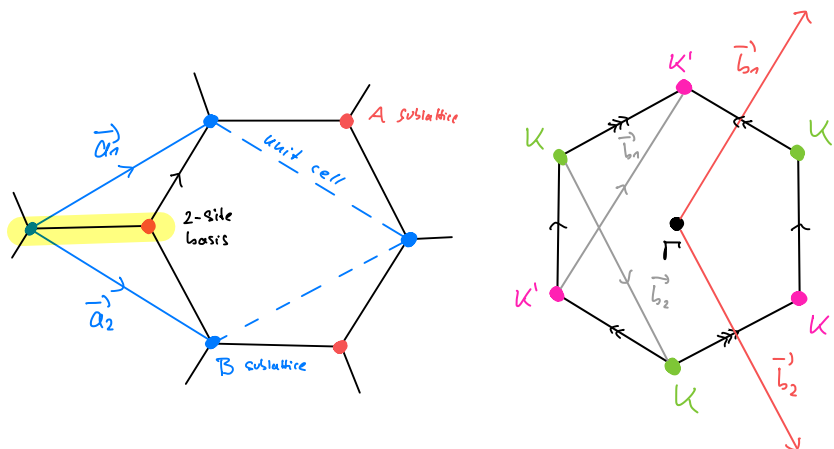
Note that the BZ obtained from the Wigner-Seitz cell is a torus T^2 even though this is not obvious from its shape (the BZ of *every* 2D periodic system is a torus as

it is just the parallelogram spanned by the reciprocal basis $\vec{b}_i$ with opposite edges identified):
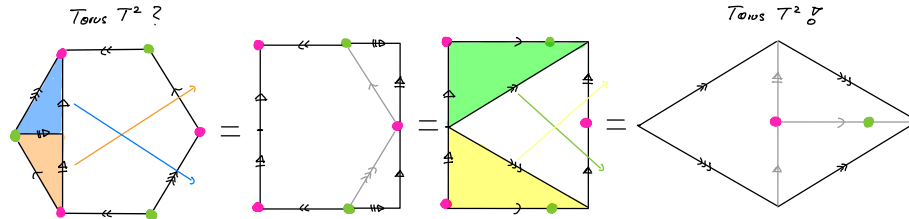
Edges with the same arrow type are identified along the direction indicated by the arrow.

The last diagram is known as *fundamental polygon* of the torus.

b) *Bloch Hamiltonian* $H_{\mathrm{H}}(\boldsymbol{k}) = \varepsilon(\boldsymbol{k})\mathbb{1} + \vec{d}(\boldsymbol{k}) \cdot \vec{\sigma}$ with

$$d_x \overset{\circ}{=} \cos(\boldsymbol{k}\boldsymbol{a}_1) + \cos(\boldsymbol{k}\boldsymbol{a}_2) + 1 \tag{1.183}$$

$$d_y \overset{\circ}{=} \sin(\boldsymbol{k}\boldsymbol{a}_1) + \sin(\boldsymbol{k}\boldsymbol{a}_2) \tag{1.184}$$

$$d_z \overset{\circ}{=} m + 2t\sin(\varphi)\left[\sin(\boldsymbol{k}\boldsymbol{a}_1) - \sin(\boldsymbol{k}\boldsymbol{a}_2) - \sin(\boldsymbol{k}(\boldsymbol{a}_1 - \boldsymbol{a}_2))\right] \tag{1.185}$$

$$\varepsilon(\boldsymbol{k}) \overset{\circ}{=} 2t\cos(\varphi)\left[\cos(\boldsymbol{k}\boldsymbol{a}_1) + \cos(\boldsymbol{k}\boldsymbol{a}_2) + \cos(\boldsymbol{k}(\boldsymbol{a}_1 - \boldsymbol{a}_2))\right] \tag{1.186}$$

As $\varepsilon(\boldsymbol{k})$ has no effect on the gap and the Chern number, we set it the following to zero.

The above Bloch Hamiltonian follows straightforwardly from the Hamiltonian Eq. (1.182) together with the sketches above (for the sign conventions) and the Fourier transform

$$c_{x,\boldsymbol{r}} = \frac{1}{\sqrt{L_1 L_2}} \sum_{\boldsymbol{k} \in T^2} e^{-i\boldsymbol{k}\boldsymbol{r}} \tilde{c}_{x,\boldsymbol{k}} \quad \text{and} \quad \tilde{c}_{x,\boldsymbol{k}} = \frac{1}{\sqrt{L_1 L_2}} \sum_{\boldsymbol{r} \in \mathcal{L}} e^{i\boldsymbol{k}\boldsymbol{r}} c_{x,\boldsymbol{r}} \tag{1.187}$$

of the fermion modes on the sublattices $x = A, B$ with $\mathcal{L} = \boldsymbol{a}_1 \mathbb{Z}_{L_1} + \boldsymbol{a}_2 \mathbb{Z}_{L_2}$ the (periodic) lattice and T^2 the Brillouin zone. It is then

$$\hat{H}_{\mathrm{H}} = \sum_{\boldsymbol{k} \in T^2} \Psi_{\boldsymbol{k}}^{\dagger} H_{\mathrm{H}}(\boldsymbol{k}) \Psi_{\boldsymbol{k}} \tag{1.188}$$

with $\Psi_{\boldsymbol{k}} = (\tilde{c}_{A,\boldsymbol{k}}, \tilde{c}_{B,\boldsymbol{k}})^T$.

$\rightarrow$ Gap can only close at the corners of the BZ (check for $m = 0$ and $t = 0$):

$$\boldsymbol{K} = \frac{2\pi}{3}\left(\sqrt{3}, 1\right) \quad \text{and} \quad \boldsymbol{K}' = \frac{2\pi}{3}\left(\sqrt{3}, -1\right) \tag{1.189}$$

For $m = 0$ and $t = 0$ the Hamiltonian Eq. (1.182) describes the semimetal *Graphene* with two Dirac cones.

$\rightarrow$ Dirac Hamiltonians:

Here i, j run only over $1, 2$, i.e., σ^x and σ^y:

$$H_{\mathrm{H}}(\boldsymbol{K} + \boldsymbol{k}) \,\hat{=}\, k_i h_{ij} \sigma^j + \overbrace{[m - 3\sqrt{3}t \sin(\varphi)]}^{h_z} \sigma^z + \mathcal{O}(k^2) \tag{1.190}$$

$$\text{with} \quad h = \frac{\sqrt{3}}{2} \begin{bmatrix} 0 & -1 \\ 1 & 0 \end{bmatrix} \tag{1.191}$$

$$H_{\mathrm{H}}(\boldsymbol{K}' + \boldsymbol{k}) \,\hat{=}\, k_i h'_{ij} \sigma^j + \overbrace{[m + 3\sqrt{3}t \sin(\varphi)]}^{h'_z} \sigma^z + \mathcal{O}(k^2) \tag{1.192}$$
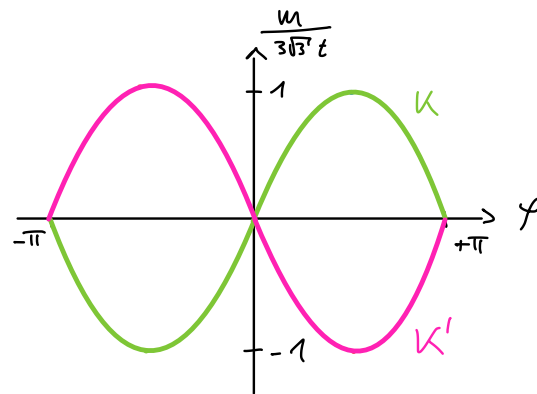
$$\text{with} \quad h' = \frac{\sqrt{3}}{2} \begin{bmatrix} 0 & -1 \\ -1 & 0 \end{bmatrix} \tag{1.193}$$

4. *Gap closings:*

$$@\boldsymbol{K}: \quad h_z \overset{!}{=} 0 \quad \Leftrightarrow \quad \frac{m}{3\sqrt{3}t} = +\sin(\varphi) \tag{1.194}$$

$$@\boldsymbol{K}': \quad h'_z \overset{!}{=} 0 \quad \Leftrightarrow \quad \frac{m}{3\sqrt{3}t} = -\sin(\varphi) \tag{1.195}$$

Phase diagram $\rightarrow$

There are 4 different parameter regimes that are separated by lines where the gap closes. To identify the phases, we have to compute the Chern number (of the lower band) in all 4 areas.

5. To do this, we need the following generalized expression for the Chern number of a Dirac Hamiltonian (cf. discussion of the QWZ model):

$$H(\boldsymbol{k}) = \sum_{i,j=1}^{2} k_i h_{ij} \sigma^j + h_z \sigma^z \quad \Rightarrow \quad C = -\frac{\mathrm{sign}(h_z)\,\mathrm{sign}(\det h)}{2} \tag{1.196}$$

Proof: ➲ Problemset 4

Thus

$$C_{\boldsymbol{K}} = -\frac{1}{2} \,\mathrm{sign}[m - 3\sqrt{3}t \sin(\varphi)], \tag{1.197}$$

$$C_{\boldsymbol{K}'} = +\frac{1}{2} \,\mathrm{sign}[m + 3\sqrt{3}t \sin(\varphi)]. \tag{1.198}$$

6. *Phase diagram:*

   a) $m \to +\infty$: $\vec{d}(\boldsymbol{k}) \approx m\vec{e}_z \to$ Trivial phase with $C = 0$

   b) $m \to -\infty$: $\vec{d}(\boldsymbol{k}) \approx m\vec{e}_z \to$ Trivial phase with $C = 0$

   c) Let $0 < \varphi < \pi$ and (1) $m > 3\sqrt{3}t\sin(\varphi)$ to (2) $m < 3\sqrt{3}t\sin(\varphi)$:
      We cross a phase boundary where the gap closes at $\boldsymbol{K}$!

   $$C = 0 + C_{\boldsymbol{K}}(2) - C_{\boldsymbol{K}}(1) = [-1/2 \cdot (-1)] - [-1/2 \cdot (+1)] = +1 \qquad (1.199)$$

   $\to$ Topological phase (I)

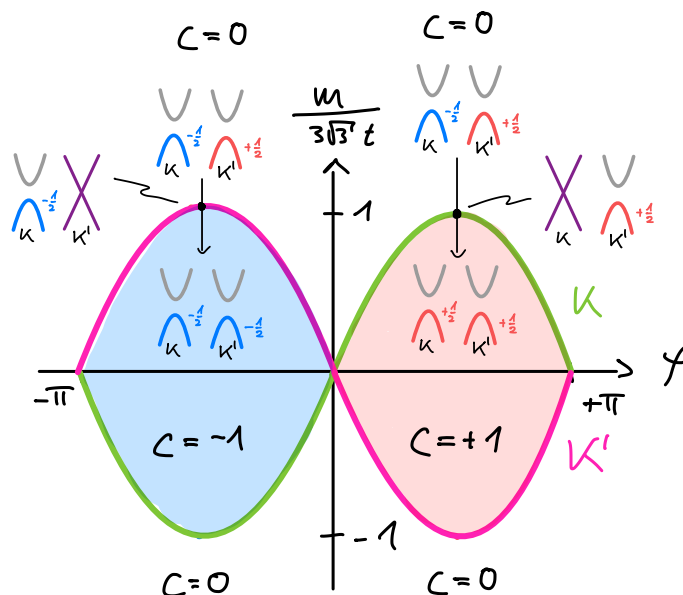   d) Let $-\pi < \varphi < 0$ and (1) $m > -3\sqrt{3}t\sin(\varphi)$ to (2) $m < -3\sqrt{3}t\sin(\varphi)$:
      We cross a phase boundary where the gap closes at $\boldsymbol{K}'$!

   $$C = 0 + C_{\boldsymbol{K}'}(2) - C_{\boldsymbol{K}'}(1) = [+1/2 \cdot (-1)] - [+1/2 \cdot (+1)] = -1 \qquad (1.200)$$

   $\to$ Topological phase (II)

Phase diagram $\to$

Thus in total ther are *three* different phases, one trivial ($C = 0$) and two topological ($C = \pm 1$). Note that just as for the QWZ model, the two trivial regions with $C = 0$ are continuously connected without closing the gap, i.e., they are the same phase.

7. *Time-reversal symmetry:* $\sphericalangle \tilde{T}_0 = \mathcal{K}$ (assume $t \neq 0$)

   $$d_x(\boldsymbol{k}) \overset{?}{=} d_x(-\boldsymbol{k}) \quad \checkmark \qquad (1.201)$$

   $$d_y(\boldsymbol{k}) \overset{?}{=} -d_y(-\boldsymbol{k}) \quad \checkmark \qquad (1.202)$$

   $$d_z(\boldsymbol{k}) \overset{?}{=} d_z(-\boldsymbol{k}) \quad \checkmark \text{ for } \varphi = 0, \pi \mod 2\pi \quad \times \text{ otherwise} \qquad (1.203)$$

Note that the spin-$\frac{1}{2}$ TRS representation $\tilde{T}_{\frac{1}{2}} = \sigma^y \mathcal{K}$ is always broken, irrespective of the parameter φ.

$\to C = 0$ for $\varphi = 0, \pi \mod 2\pi$ (i.e., for real NNN hopping)

Note that for $\varphi \neq 0, \pi \mod 2\pi$ it is only *possible* that $C \neq 0$; the phase diagram above demonstrate that it is *not* sufficient!

1.3 Topological bands with time-reversal symmetry: The quantum spin Hall effect

> **† Note**
>
> This section is based on various sources. A detailed account can be found in Bernevig's textbook [26]. However, also the original papers by Kane and Mele [54, 55] and Fu and Kane [47, 56] are accessible and worthwhile to read. The concept of vector bundles is discussed by Carpentier [57,58] from a physicists perspective; a more mathematical account is given by Wehefritz-Kaufmann [59]. The mathematical foundations underlying topological band theory (in particular the concepts of vector bundles and their characterization) are covered in the textbooks by Nash and Sen [60] and Nakahara [61].

We seek for models with the following properties:

- Lattice model
- Band insulator
- Time-reversal symmetric (!)
- Topological band structure (!)
  We do not call for *Chern bands* as we known that this is impossible without breaking time-reversal symmetry! So we need to look for another topological invariant.

Before we proceed, let us fix the nomenclature:

> **★ Definition: Topological insulator**
>
> $$\text{Topological insulator (TI)} \quad := \quad \begin{cases} \text{Lattice model} \\ \text{Band insulator} \\ \text{Topological band structure} \\ \text{Time-reversal symmetric} \end{cases} \qquad (1.204)$$
>
> *Prototype:* Kane-Mele model

With this definition, the question we want to answer reads:

> *Are there topological insulators?*

The term "topological insulator" is not used consistencly in the literature. In particular, the above definition is only one of at least three:

- Sometimes "TI" refers specifically to the Kane-Mele model. This is usually the case when people talk about *the* topological insulator.

- Sometimes "TI" is used to denote the class of gapped free fermion theories with time-reversal symmetry, particle number conservation (to distinguish them from superconductors, see below) and topological bands. This is essentially our definition above.

- Sometimes "TI" refers to arbitrary band insulators with topological bands (then including also Chern insulators). This is how the term is used when refering to the class of *topological insulators & superconductors*. I.e., there the term "insulator" distinguishes models from "superconductors" (which violate particle number conservation) without refering to time-reversal symmetry.

So be aware of this when you study other sources.

1.3.1 Construction of the Kane-Mele model

1. *Starting point:* Low-energy theory of graphene:

   Recall that this is just the Haldane model for $m = 0 = t$:

   $$H(\mathbf{K} + \mathbf{k}) = -\frac{\sqrt{3}}{2}(k_x \sigma^y - k_y \sigma^x) \tag{1.205}$$

   $$H(\mathbf{K'} + \mathbf{k}) = -\frac{\sqrt{3}}{2}(k_x \sigma^y + k_y \sigma^x) \tag{1.206}$$

   To translate into the conventions used in the original papers, we rotate in momentum space by $\pi/2$ so that $k_x \mapsto k_y$ and $k_y \mapsto -k_x$:

   $$H(\mathbf{k}) := H(\mathbf{K} + \mathbf{k}) = -\frac{\sqrt{3}}{2}(k_x \sigma^x + k_y \sigma^y) \tag{1.207}$$

   $$H'(\mathbf{k}) := H(\mathbf{K'} + \mathbf{k}) = -\frac{\sqrt{3}}{2}(-k_x \sigma^x + k_y \sigma^y) \tag{1.208}$$

   The low-energy physics is determined by momentum modes in the vicinity of $\mathbf{K}$ and $\mathbf{K'}$. We can therefore combine the two Bloch Hamiltonians by a direct sum (corresponding to the direct sum of low-energy single-particle momentum modes):

   $\rightarrow$

   $$\tilde{H}_0(\mathbf{k}) = H(\mathbf{k}) \oplus H'(\mathbf{k}) \tag{1.209}$$

   $$= v_F \begin{pmatrix} k_x \sigma^x + k_y \sigma^y & 0 \\ 0 & -k_x \sigma^x + k_y \sigma^y \end{pmatrix} \tag{1.210}$$

   $$= v_F (\sigma^x \otimes \tau^z \, k_x + \sigma^y \otimes \mathbb{1} \, k_y) \tag{1.211}$$

   $$= v_F (\sigma^x \tau^z k_x + \sigma^y k_y) \tag{1.212}$$

   σ^i: band DOF (mixes modes of upper/lower bands)
   τ^i: valley DOF (mixes modes between valleys $\mathbf{K}/\mathbf{K'}$)
   $v_F = -\sqrt{3}/2$: Fermi velocity

   Time-reversal:
   Note that under time-reversal we have $\mathbf{K} + \mathbf{k} \mapsto -\mathbf{K} - \mathbf{k} = \mathbf{K'} - \mathbf{k}$ so that in the low-energy description time-reversal flips the valley DOF; this can be achieved by τ^x.

   $$\tilde{T}_0 := \mathbb{1}_\sigma \otimes \tau^x \, \mathcal{K} \quad \text{with} \quad \tilde{T}_0^2 = +\mathbb{1} \tag{1.213}$$

   $\rightarrow \tilde{T}_0 \tilde{H}_0(\mathbf{k}) \tilde{T}_0^{-1} = \tilde{H}_0(-\mathbf{k})$

2. Add *Spin-$\frac{1}{2}$*: Pauli matrices μ^i with $i = x, y, z$

   This gives us more possibilities to add gap-opening terms to $\tilde{H}_0$. It is also physically motivated: electrons *do have* spin.

$$\tilde{H}_{\frac{1}{2}}(\boldsymbol{k}) = v_F \left(\sigma^x \otimes \mathbb{1}_\mu \otimes \tau^z \, k_x + \sigma^y \otimes \mathbb{1}_\mu \otimes \mathbb{1}_\tau \, k_y \right) \tag{1.214}$$

$$= v_F \left(\sigma^x \tau^z k_x + \sigma^y k_y \right) \tag{1.215}$$

$\rightarrow$ Bloch space $\mathcal{H}(\boldsymbol{k}) \simeq \mathbb{C}^2 \otimes \mathbb{C}^2 \otimes \mathbb{C}^2 \simeq \mathbb{C}^8$

$\rightarrow$ *Time-reversal:*

$$\tilde{T}_{\frac{1}{2}} = \mathbb{1}_\sigma \otimes \mu^y \otimes \tau^x \, \mathcal{K} \quad \text{with} \quad \tilde{T}_{\frac{1}{2}}^2 = -\mathbb{1} \tag{1.216}$$

$\rightarrow$ $\tilde{T}_{\frac{1}{2}} \tilde{H}_{\frac{1}{2}}(\boldsymbol{k}) \tilde{T}_{\frac{1}{2}}^{-1} = \tilde{H}_{\frac{1}{2}}(-\boldsymbol{k})$

3. *Goal:* Open topological gap by adding terms to $\tilde{H}_{\frac{1}{2}}(\boldsymbol{k})$:

   (We can then later reconstruct a lattice model from the low-energy (= small momentum) Hamiltonian as we did for the QWZ model.)

   a) *Observation I:* Must contain σ^z!

   Otherwise we only shift the position of the Dirac points:

$$\tilde{H}(\boldsymbol{k}) = v_F \left[\sigma^x \tau^z k_x + \sigma^y k_y \right] + v_F \left(\delta_x \sigma^x \tau^z + \delta_y \sigma^y \right) \tag{1.217}$$

$$= v_F \left[\sigma^x \tau^z (k_x + \delta_x) + \sigma^y (k_y + \delta_y) \right] \tag{1.218}$$

$$= H(\underbrace{\boldsymbol{K} + \boldsymbol{\delta} + \boldsymbol{k}}_{\boldsymbol{K}_\delta}) \oplus H(\underbrace{\boldsymbol{K}' + \boldsymbol{\delta} + \boldsymbol{k}}_{\boldsymbol{K}'_\delta}) \tag{1.219}$$

   with $\boldsymbol{\delta} = (\delta_x, \delta_y)^T$.

   b) We know already the *trivial mass term*:

$$\delta \tilde{H}_m(\boldsymbol{k}) = m \sigma^z \tag{1.220}$$

   $\rightarrow$

   - Time-reversal invariant: $\tilde{T}_{\frac{1}{2}} \delta \tilde{H}_m(\boldsymbol{k}) \tilde{T}_{\frac{1}{2}}^{-1} = \delta \tilde{H}_m(-\boldsymbol{k})$

   - Opens a gap of $2m$

   - *But:* Bands are topologically trivial!

     They are "topologically trivial" because their Chern number vanishes. However, below we will derive a new topological invariant distinct from the Chern number so that this statement seems short-sighted. The true argument is therefore that for $m \to \infty$ the system is clearly a trivial band insulator where one sublattice is empty and the other completely filled; this phase is "trivial" in the original sense of being a product state. Then, no matter which topological invariant we cook up, to comply with our physically motivated notion of "trivial", it *must* vanish in the gapped phase dominated by $\delta \tilde{H}_m$.

   So we should look for other gap opening terms …

   c) We also know the *Haldane mass term* ($\varphi = -\pi/2$):

$$\delta \tilde{H}_{\mathrm{H}}(\boldsymbol{k}) = \tau^z \sigma^z \, 3\sqrt{3} \, t \tag{1.221}$$

→ $\tilde{H}_{\mathrm{H}} := \tilde{H}_{\frac{1}{2}} + \delta\tilde{H}_m + \delta\tilde{H}_{\mathrm{H}}$ = two independent copies of the Haldane model
(one for spin up, one for spin down)

→ *Not* TRI:

$$\tilde{T}_{\frac{1}{2}}\,\delta\tilde{H}_{\mathrm{H}}(\boldsymbol{k})\,\tilde{T}_{\frac{1}{2}}^{-1} \neq \delta\tilde{H}_{\mathrm{H}}(-\boldsymbol{k}) \tag{1.222}$$

d) *Observation II:* Must contain spin-coupling that anticommutes with $\tilde{T}_{\frac{1}{2}}$!

→

$$\delta\tilde{H}_{\mathrm{KM}}(\boldsymbol{k}) := \lambda_{\mathrm{SO}}\,\sigma^z \otimes \mathbb{1}_\mu \otimes \tau^z \qquad \rightarrow \text{Not TRI} \tag{1.223}$$

$$\delta\tilde{H}_{\mathrm{KM}}(\boldsymbol{k}) := \lambda_{\mathrm{SO}}\,\sigma^z \otimes \mu^z \otimes \mathbb{1}_\tau \qquad \rightarrow \text{Not TRI} \tag{1.224}$$

$$\delta\tilde{H}_{\mathrm{KM}}(\boldsymbol{k}) := \lambda_{\mathrm{SO}}\,\sigma^z \otimes \mu^z \otimes \tau^z \qquad \rightarrow \text{TRI} \tag{1.225}$$

→ *Kane-Mele mass term*

- Couples "orbital" DOFs (τ^z) with spin DOFs (μ^z)
  → Example of *Spin-orbit coupling (SO)*

- The choice of μ^z is arbitrary since all μ^i anticommute with $\tilde{T}_{\frac{1}{2}}$. It is just conventional to think in the z-basis for spin (i.e., spin "up" and "down" now have conjugate imaginary hopping phases). Note also that on its own, μ^z is interchangeable with the other Pauli matrices by permutations (or spin rotations) without changing the spin-algebra.

- $\delta\tilde{H}_{\mathrm{KM}}(\boldsymbol{k})$ is just Haldane's TRI breaking term $\tau^z\sigma^z\,3\sqrt{3}t\,\sin(\varphi)$ augmented by spin-orbit coupling to "fix" the time-reversal symmetry.

4. *Kane-Mele model [54, 55]:*

Low-energy description:

$$\tilde{H}'_{\mathrm{KM}}(\boldsymbol{k}) := \tilde{H}_{\frac{1}{2}}(\boldsymbol{k}) + \delta\tilde{H}_m(\boldsymbol{k}) + \delta\tilde{H}_{\mathrm{KM}}(\boldsymbol{k}) \tag{1.226}$$

→ Reconstruction of the Full lattice model:

$$\hat{H}'_{\mathrm{KM}} = \overbrace{\sum_{\langle i,j\rangle,\alpha} c^\dagger_{i\alpha}c_{j\alpha}}^{\triangleq\,\tilde{H}_{\frac{1}{2}}(\boldsymbol{k})} + \overbrace{m\sum_{i,\alpha}\epsilon_i c^\dagger_{i\alpha}c_{i\alpha}}^{\triangleq\,\delta\tilde{H}_m(\boldsymbol{k})} + \overbrace{\lambda_{\mathrm{SO}}\sum_{\langle\langle i,j\rangle\rangle,\alpha,\beta} i\,\eta_{ji}\,c^\dagger_{i\alpha}\mu^z_{\alpha\beta}c_{j\beta}}^{\triangleq\,\delta\tilde{H}_{\mathrm{KM}}(\boldsymbol{k})} \tag{1.227}$$

$$\underbrace{\text{Spinful graphene}}_{} \qquad \underbrace{\text{Staggered potential}}_{} \qquad \underbrace{\text{Complex NNN hopping \textit{with SO coupling}}}_{}$$

$c^\dagger_{i\alpha}$: Creates fermion with spin $\alpha \in \{\uparrow,\downarrow\}$ on site i

Note that the phase in the Kane-Mele term is the phase $e^{i\eta_{ij}\varphi}$ of the Haldane term for $\varphi = -\pi/2$.

If you don't believe this, you can retrace our path to derive the Dirac Hamiltonian for the Haldane model again for the Kane-Mele model to derive $\tilde{H}'_{\mathrm{KM}}(\boldsymbol{k})$.

5. *Observation III:* $\hat{H}'_{\mathrm{KM}}$ does not mix spin:

$$\left[\hat{H}'_{\mathrm{KM}}, N_\alpha\right] = 0 \quad \text{with} \quad N_\alpha := \sum_i c^\dagger_{i\alpha}c_{i\alpha} \tag{1.228}$$

$\rightarrow \hat{H}'_{\mathrm{KM}}$ = two *decoupled* copies of the Haldane model with opposite complex phases

Note that this rather trivial construction already fixed the breaking of time-reversal symmetry because the two copies map onto each other under time reversal. However:

$\rightarrow$ Not generic (mixing of up and down spins can happen, e.g., by applying an electric field perpendicular to the plane)

$\rightarrow$ Add term that breaks the unitary symmetry generated by N_α (but preserves TRS)

6. *Rashba term [62]:*
   There is indeed another SO coupling term that does not break TRS known as *Rashba spin-orbit coupling*:

$$\delta \tilde{H}_{\mathrm{R}}(\boldsymbol{k}) := \lambda_R \left[\sigma^x \mu^y \tau^z - \sigma^y \mu^x \right] \tag{1.229}$$

$\rightarrow \tilde{T}_{\frac{1}{2}} \delta \tilde{H}_{\mathrm{R}}(\boldsymbol{k}) \tilde{T}_{\frac{1}{2}}^{-1} = \delta \tilde{H}_{\mathrm{R}}(-\boldsymbol{k})$

- Does not open a gap (missing σ^z) …

- … but modifies the gap generated by the Kane-Mele term

- Breaks spin conservation (the $\uparrow$ and $\downarrow$ sectors no longer decouple)

$\rightarrow$

$$\hat{H}_{\mathrm{KM}} := \hat{H}'_{\mathrm{KM}} + \overbrace{\underbrace{\lambda_R \sum_{\langle i,j \rangle, \alpha, \beta} c^\dagger_{i\alpha} R^{\alpha\beta}_{ij} c_{j\beta}}_{\text{NN hopping with Rashba SO coupling}}}^{\triangleq \delta \tilde{H}_R(\boldsymbol{k})} \tag{1.230}$$

with

$$R^{\alpha\beta}_{ij} \stackrel{\circ}{=} i \left[(\vec{\mu} \times \vec{d}_{ij}) \cdot \hat{e}_z \right]_{\alpha\beta} \tag{1.231}$$

$\vec{d}_{ij}$: vector from site i to site j (in the x-y-pane)
$\hat{e}_z$: unit vector in z-direction

- Note that $(\vec{\mu} \times \vec{d}_{ij})_z = \mu^x d^y_{ij} - \mu^y d^x_{ij}$ is a Hermitian 2×2 matrix.

- Because of the μ^x and μ^y in the Rashba term, it is now $[\hat{H}_{\mathrm{KM}}, N_\alpha] \neq 0$ so that $\hat{H}_{\mathrm{KM}}$ can no longer be interpreted as a sum of two independent Haldane models.

- The direction-dependent phase and spin-coupling of the *Kane-Mele term* can be similarly encoded (for the fixed hopping phase $\varphi = -\pi/2$)
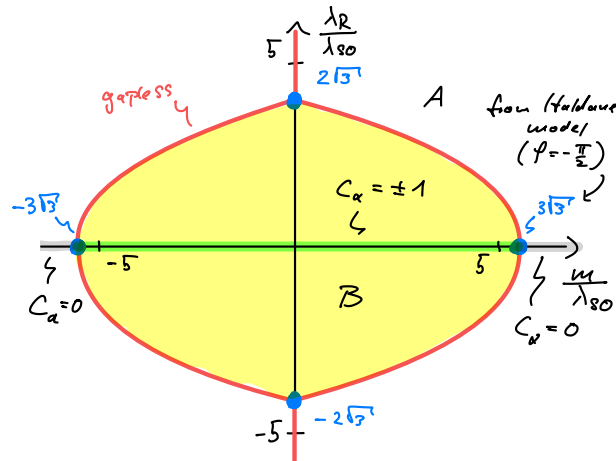
$$H^{\alpha\beta}_{ij} := e^{\eta_{ij} i \varphi} \mu^z_{\alpha\beta} = -i \eta_{ij} \mu^z_{\alpha\beta} \stackrel{\circ}{=} i \, 2\sqrt{3} \left[(\vec{d}_{ik} \times \vec{d}_{kj}) \cdot \vec{\mu} \right]_{\alpha\beta} \tag{1.232}$$

where k denotes the site that is skipped when jumping from i to the next-nearest neighbour j.

1.3.2 Phase diagram

1. *Gap closings:*

   We have three parameters (in units of the graphene hopping strength), so let us fix the Kane-Mele term at $0 < \lambda_{\mathrm{SO}} \ll 1$ and plot the gap closings in the λ_R-m-plane:

- The gapless values on the m-axis follow directly from our discussion of the Haldane model with $\varphi = -\pi/2$.

- To derive the full plot, you must Fourier transform $\hat{H}_{\mathrm{KM}}$ on a periodic lattice to derive the 4×4-Bloch Hamiltonian,

$$\tilde{H}_{\mathrm{KM}}(\boldsymbol{k}) = \sum_{i=1}^{5} d_i(\boldsymbol{k})\Gamma_i + \sum_{i<j=1}^{5} d_{ij}(\boldsymbol{k})\Gamma_{ij} \tag{1.233}$$

which is generated by (at most) 15 terms which take the place of the three-component Bloch vector $\vec{d}(\boldsymbol{k})$ for models with two bands. Recall that $n \times n$ Hamiltonians (with vanishing trace) generate unitaries in the group $\mathrm{SU}(n)$ which has $n^2 - 1$ generators, e.g., 3 Pauli matrices for $n = 2$ or 15 Γ-matrices for $n = 4$. The generators for $n = 4$ satisfy $\{\Gamma_i, \Gamma_j\} = 2\delta_{ij}$ and $\Gamma_{ij} = 1/2i\,[\Gamma_i, \Gamma_j]$ with $i, j \in \{1, \ldots, 5\}$. See [55] for the expressions for d_i and d_{ij}.

2. $\lhd\ \lambda_R = 0$ (*m-axis in the above plot*) $\rightarrow$ Spin-sectors decouple
   $\rightarrow$ Chern number C_α of spin-polarized sub-bands well-defined $\rightarrow$

$$I^* := \frac{C_\uparrow - C_\downarrow}{2} \mod 2 = \begin{cases} 1 & \text{topologial phase of Haldane model(s)} \\ 0 & \text{trivial phase of Haldane model(s)} \end{cases} \tag{1.234}$$

Note that the *sum* $C_\uparrow + C_\downarrow = 0$ of the filled bands is zero everywhere because of TRS!

$\rightarrow$ *Suggests* that Phase B is in some sense topological. (Phase A is a trivial insulator.)

$\rightarrow$ *Not* characterized by I^* since I^* requires spin-conservation whereas the phase is stable against perturbations that violate spin-conservation (like the Rashba term).

$\rightarrow$ What characterizes Phase B?

### 1.3.3 Vorticity of the Pfaffian and the $\mathbb{Z}_2$-Index

So what is the label that distinguishes the two phases of the Kane-Mele model? We need a new topological index that replaces the Chern number.

1. $\lhd$ TRI system with $\tilde{T}_U^2 = -\mathbb{1} \rightarrow$ Band crossings at TRIMs

TRIM = Time-reversal invariant momentum

$$K^* \in T^2 : \text{TRIM} \Leftrightarrow -K^* = K^* + G , \quad G : \text{reciprocal lattice vector} \qquad (1.235)$$

→ Generic bandstructure of *TRI System in 1D with* $\tilde{T}_U^2 = -1$:
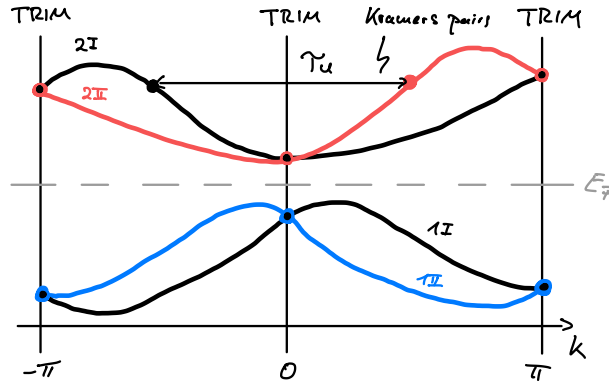
◁ Gapped system → *Even* number $2n$ of filled bands

- Note that time-reversal symmetry (irrespective of $T_U^2 = \pm 1$) implies the $k \leftrightarrow -k$ symmetry of the spectrum. However, this does *not* imply a degeneracy at the TRIMs! (Think of the free fermion on a lattice.)

- If $T_U^2 = -1 \Leftrightarrow \tilde{T}_U^2 = -1$ Kramer's theorem applies to the single-particle Hamiltonian, $T_U H T_U^{-1} = H$, and demands a two-fold degeneracy for *every* eigenenergy. At the TRIMs, this requires a crossing band; thus all bands come in pairs!

- For the Bloch Hamiltonians $H(k)$, Kramer's theorem does *not* apply in general, since TRI requires $\tilde{T}_U H(k) \tilde{T}_U^{-1} = H(-k)$ which is *not* a symmetry of $H(k)$. Only at the TRIMs we have $\tilde{T}_U H(K^*) \tilde{T}_U^{-1} = H(-K^*) = H(K^* + G) = H(K^*)$ so that Kramer's theorem implies a two-fold degeneracy *in the Bloch space* of a TRIM K^*. This is another perspective on the band crossings at the TRIMs.

- Note that the Kamers pairs of bands (I and II) *can* be degenerate everywhere in the BZ (for the Kane-Mele model they are perfectly degenerate for $\lambda_R = 0 = m$). TRI only requires this degeneracy at the TRIMs but does not exlude it anywhere else.

Four *TRIMs* of the hexagonal lattice:
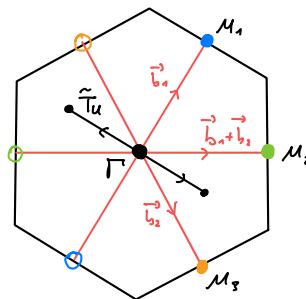
2. ◁ Matrix of $\tilde{T}_U$ on *occupied* Bloch space $\mathcal{H}_k^{\text{filled}} := \text{span} \{|u_i(k)\rangle\}_{i=1...2n}$
   I.e., i, j run over the occupied bands. For the 4-band Kane-Mele model, this means $i, j \in \{1, 2\}$ which correspond to the filled lower bands of the spin-up and -down copy of

the Haldane model (for $\lambda_R = 0$).

$$M_{ij}(\boldsymbol{k}) := \langle u_i(\boldsymbol{k})|\tilde{T}_U|u_j(\boldsymbol{k})\rangle \tag{1.236}$$

$$= \langle u_i(\boldsymbol{k})|Uu_j^*(\boldsymbol{k})\rangle \tag{1.237}$$

$$= -\langle U^*u_i(\boldsymbol{k})|u_j^*(\boldsymbol{k})\rangle \tag{1.238}$$

$$= -\langle u_j(\boldsymbol{k})|Uu_i^*(\boldsymbol{k})\rangle \tag{1.239}$$

$$= -\langle u_j(\boldsymbol{k})|\tilde{T}_U|u_i(\boldsymbol{k})\rangle \tag{1.240}$$

$$= -M_{ij}^T(\boldsymbol{k}) \tag{1.241}$$

Here we used $U^\dagger = (U^*)^T$ and $U^T = -U$ since $\tilde{T}_U^2 = \tilde{T}_{\frac{1}{2}}^2 = -\mathbb{1}$ with $\tilde{T}_{\frac{1}{2}} = \mathbb{1}_\sigma \otimes \mu^y \mathcal{K}$.

- Gauge-dependent (= depends on chosen basis of $\mathcal{H}_{\boldsymbol{k}}^{\text{filled}}$)
- For every $\boldsymbol{k} \in T^2$, $M(\boldsymbol{k})$ is a *skew-symmetric* matrix of *even* dimensions (Remember that TRI demands an even number of filled bands.)

$\rightarrow$ *Pfaffian*:

Definition: For M a skew-symmetric $2n \times 2n$-matrix, the Pfaffian is defined as

$$\text{Pf}[M] := \frac{1}{2^n n!} \sum_{\sigma \in S_{2n}} (-1)^\sigma \prod_{i=1}^n M_{\sigma(2i-1),\sigma(2i)} \tag{1.242}$$

It follows:

- $(\text{Pf}[M])^2 = \det(M)$, i.e., the Pfaffian contains the same information as the determinant (but with an additional sign that is lost when considering the determinant).
- $\text{Pf}[BAB^T] = \det(B)\,\text{Pf}[A]$ for an arbitrary $2n \times 2n$-matrix B
- For skew-symmetric matrices of even dimension, the Pfaffian is a "more natural" object than the determinant (it contains at least as much information!).

This motivates the definition of the following function:

$$P : T^2 \rightarrow \mathbb{C} \qquad P(\boldsymbol{k}) := \text{Pf}[M(\boldsymbol{k})] \tag{1.243}$$

Kane-Mele model: $P(\boldsymbol{k}) = M_{12}(\boldsymbol{k}) = \langle u_1(\boldsymbol{k})|\tilde{T}_U|u_2(\boldsymbol{k})\rangle$

$\rightarrow$ $P(\boldsymbol{k})$ is a complex-valued function on the BZ that depends (continuously) on the Hamiltonian. The idea is now to identify topologically robust properties of this function to distinguish the two phases of the Kane-Mele model.

3. *Properties of $P(\boldsymbol{k})$:*

- *Not* gauge invariant: $\lhd\ U \in \text{U}(2n)$ and $|u_i'(\boldsymbol{k})\rangle := U_{ij}|u_j(\boldsymbol{k})\rangle$

    This gauge transformation mixes the filled bands!

↑ Notes

$$U = e^{i\phi}\tilde{U} \text{ with } \tilde{U} \in \text{SU}(2n) \rightarrow$$

$$P'(\boldsymbol{k}) = \text{Pf}\left[\left(\langle u_i'(\boldsymbol{k})|\tilde{T}_U|u_j'(\boldsymbol{k})\rangle\right)_{ij}\right] \tag{1.244}$$

$$= \text{Pf}\left[\left(U_{ii'}^*\langle u_{i'}(\boldsymbol{k})|\tilde{T}_U|u_{j'}(\boldsymbol{k})\rangle U_{jj'}^*\right)_{ij}\right] \tag{1.245}$$

$$= \text{Pf}\left[U^*\left(\langle u_{i'}(\boldsymbol{k})|\tilde{T}_U|u_{j'}(\boldsymbol{k})\rangle\right)_{i'j'}(U^*)^T\right] \tag{1.246}$$

$$= \det(U^*)P(\boldsymbol{k}) \tag{1.247}$$

$$= e^{-i2n\phi}P(\boldsymbol{k}) \tag{1.248}$$

Here we used that $\det(\tilde{U}) = 1$.

$\rightarrow |P(\boldsymbol{k})|$ *is* gauge invariant

Note: We can consider even unitary transformations *between* filled bands (for a fixed $\boldsymbol{k}$) although these states are not energetically degenerate (strictly speaking, they do not even have to be energy eigenstates to begin with, see below) because such transformations do *not* alter the many-body ground state (namely the Fermi sea or the Slater determinant):

$$|\Psi_0'\rangle = \prod_{\boldsymbol{k}}\prod_i c_{\boldsymbol{k},i}'^\dagger|0\rangle = \prod_{\boldsymbol{k}}\prod_i U_{ij}c_{\boldsymbol{k},j}^\dagger|0\rangle \tag{1.249}$$

$$= \prod_{\boldsymbol{k}}\det(U)\prod_i c_{\boldsymbol{k},i}^\dagger|0\rangle = e^{i\chi}\prod_{\boldsymbol{k}}\prod_i c_{\boldsymbol{k},i}^\dagger|0\rangle = e^{i\chi}|\Psi_0\rangle. \tag{1.250}$$

Here, $c_{\boldsymbol{k},i}^\dagger$ creates a fermion in mode $|u_i(\boldsymbol{k})\rangle$ and $e^{i\chi}$ is some *global* (and therefore unphysical) phase determined by (powers of) $\det(U)$. The determinant arises due to the anticommutation relations $\{c_{\boldsymbol{k},i}^\dagger, c_{\boldsymbol{k},j}^\dagger\} = 0$; have a look at the concepts of *alternating multilinear forms* and the *exterior algebra* if so don't believe this (or prove it by hand).

- TRS
  $\rightarrow$ Chern numbers of valence bundle $\mathcal{H}_{\boldsymbol{k}}^{\text{filled}} = \text{span}\{|u_i(\boldsymbol{k})\rangle\}_{i=1\ldots2n}$ vanish

  $\rightarrow \mathcal{H}_{\boldsymbol{k}}^{\text{filled}}$ = *trivial vector bundle*

  $\rightarrow \exists$ *Continuous* basis $\{|e_i(\boldsymbol{k})\rangle\}_{i=1\ldots2n}$ of $\mathcal{H}_{\boldsymbol{k}}^{\text{filled}}$ on T^2
  It is $|e_i(\boldsymbol{k})\rangle = U_{ij}(\boldsymbol{k})|u_j(\boldsymbol{k})\rangle$ a (potentially discontinuous) gauge transformation.

  $\rightarrow P(\boldsymbol{k})$ continuous on T^2 if defined by $\{|e_i(\boldsymbol{k})\rangle\}_{i=1\ldots2n}$

This follows from the fact that the Chern number(s) of the filled Bands (mathematically speaking, the filled *Bloch bundle* or *valence bundle*) vanish. Thus there is no obstruction in choosing a globally defined, continuous basis $\{|e_i(\boldsymbol{k})\rangle\}_{i=1\ldots2n}$ of the filled band fiber $\mathcal{H}_{\boldsymbol{k}}^{\text{filled}}$ at every $\boldsymbol{k}$. Mathematically, this means that the Bloch bundle of filled bands can be *trivialized.* Because there is a continuous basis choice $\{|e_i(\boldsymbol{k})\rangle\}_{i=1\ldots2n}$ for the filled bands, the matrix of $\tilde{T}_U$ and subsequently the Pfaffian $P(\boldsymbol{k})$ are continous on T^2 as well if defined with this basis choice.

Note that in general the continuous basis $\{|e_i(\boldsymbol{k})\rangle\}_{i=1\ldots2n}$ is *not* necessarily an eigenbasis of the Bloch Hamiltonian! This is why we changed the notation from $u_i(\boldsymbol{k})$ to $e_i(\boldsymbol{k})$; in the following, $\{|e_i(\boldsymbol{k})\rangle\}_{i=1\ldots2n}$ always denotes a globally continuous basis whereas $\{|u_i(\boldsymbol{k})\rangle\}_{i=1\ldots2n}$ is a (potentially discontinuous) *eigen*basis of the Bloch Hamiltonian.

- ◁ Two subspaces of Bloch Hamiltonians:

    – $\mathcal{H}_k^{\text{filled}}$ is *even* :⇔ $\tilde{T}_U \mathcal{H}_k^{\text{filled}} = \mathcal{H}_k^{\text{filled}}$
    This means that $\tilde{T}_U |u_i(k)\rangle = M_{ij} |u_j(k)\rangle$ with a *unitary* matrix $M \neq 0$.

    $$\rightarrow |P(k)| = |\text{Pf}[M(k)]| = \sqrt{|\det M(k)|} = 1$$

    – $\mathcal{H}_k^{\text{filled}}$ is *odd* :⇔ $\tilde{T}_U \mathcal{H}_k^{\text{filled}} \perp \mathcal{H}_k^{\text{filled}}$
    This means that $\langle u_j(k)|\tilde{T}_U|u_i(k)\rangle = 0 = M_{ij}$. Remember that i runs only over *filled* bands whereas $\tilde{T}_U$ can mix the *whole* fiber $\mathcal{H}_k = \mathcal{H}_k^{\text{filled}} \oplus \mathcal{H}_k^{\text{empty}}$.

    $$\rightarrow |P(k)| = |\text{Pf}[M(k)]| = 0$$

    These are two special cases; $\mathcal{H}_k^{\text{filled}}$ can also be *neither* even *nor* odd!

- *Observation:* K^* TRIM → $\mathcal{H}_{K^*}^{\text{filled}}$ is *even* since

$$\tilde{T}_U H(K^*)\tilde{T}_U^{-1} = H(K^*) \tag{1.251}$$

This means that $\tilde{T}_U$ can only mix states with the same eigenenergy. In particular, a mixing between valence and conduction bands cannot occur. Note that this argument breaks down at a gapless point!

$\rightarrow |P(K^*)| = 1$ at all TRIMs K^*

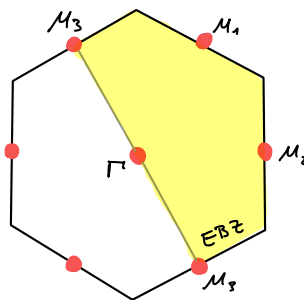- *Effective Brillouin Zones (EBZ)* [50, 57]:

$$\tilde{T}_U H(k)\tilde{T}_U^{-1} = H(-k) \tag{1.252}$$

$\rightarrow$ Defining $H(k)$ on *half* the BZ is sufficient
(TRS then determines the other half)

$\rightarrow$ EBZ = Subset of T^2 that never contains both k and $-k$ except for the boundaries which connect pairs of TRIMs

Example:

    – The EBZ has the topology of a cylinder

    – The EBZ is not unique [57]

$\rightarrow$ Consequences for $P(k)$:
(Remember the TRI band structure with Kramers pairs above!)

$$\tilde{T}_U H(k)\tilde{T}_U^{-1} = H(-k) \quad \Rightarrow \quad \tilde{T}_U \mathcal{H}_k^{\text{filled}} = \mathcal{H}_{-k}^{\text{filled}} \tag{1.253}$$

$$\Rightarrow \quad |e_i(-k)\rangle = w_{ij}^*(k)\tilde{T}_U|e_j(k)\rangle \tag{1.254}$$

$w_{ij}(k) = \langle e_i(-k)|\tilde{T}_U|e_j(k)\rangle$: unitary *sewing matrix* [56]

$\rightarrow$

$$P(-\boldsymbol{k}) = \mathrm{Pf}[M(-\boldsymbol{k})] \tag{1.255}$$

$$= \mathrm{Pf}\left[\left(\langle e_i(-\boldsymbol{k})|\tilde{T}_U|e_j(-\boldsymbol{k})\rangle\right)_{ij}\right] \tag{1.256}$$

$$= \mathrm{Pf}\left[\left(w_{ii'}(\boldsymbol{k})\,\langle \tilde{T}_U e_{i'}(\boldsymbol{k})|\tilde{T}_U|\tilde{T}_U e_{j'}(\boldsymbol{k})\rangle\,w_{jj'}(\boldsymbol{k})\right)_{ij}\right] \tag{1.257}$$

$$= (-1)^n\,\mathrm{Pf}\left[\left(w_{jj'}(\boldsymbol{k})\,\langle e_{j'}(\boldsymbol{k})|\tilde{T}_U|e_{i'}(\boldsymbol{k})\rangle^*\,w_{ii'}(\boldsymbol{k})\right)_{ij}\right] \tag{1.258}$$

$$= (-1)^n\,\mathrm{Pf}\left[w(\boldsymbol{k})\,M^*(\boldsymbol{k})\,w^T(\boldsymbol{k})\right] \tag{1.259}$$

$$= (-1)^n\,\det[w(\boldsymbol{k})]\,[P(\boldsymbol{k})]^* \tag{1.260}$$

Here we used $\tilde{T}_U^2 = -1$, $\mathrm{Pf}[\lambda A] = \lambda^n\,\mathrm{Pf}[A]$ and that $\tilde{T}_U$ is antiunitary.

$\rightarrow$ Two conclusions:

- $P(\boldsymbol{k}') = 0 \Leftrightarrow P(-\boldsymbol{k}') = 0$

  Note that $w^\dagger(\boldsymbol{k})w(\boldsymbol{k}) = \mathbb{1}$ so that $\det[w(\boldsymbol{k})] \neq 0$ for all $\boldsymbol{k} \in T^2$.

- The *vorticities* v around $\boldsymbol{k}'$ and $-\boldsymbol{k}'$ have opposite signs:

$$v[\boldsymbol{k}'] = \frac{1}{2\pi i} \oint_{\partial \boldsymbol{k}'} \nabla \log[P(\boldsymbol{k})] \cdot d\boldsymbol{k} = -v[-\boldsymbol{k}'] \quad \in \mathbb{Z} \tag{1.261}$$

$\partial\boldsymbol{k}'$: loop around $\boldsymbol{k}'$

$v[\boldsymbol{k}']$ measures the complex phase accumulated when travelling around the zero of $P(\boldsymbol{k})$ at $\boldsymbol{k}'$. Since $P(\boldsymbol{k})$ is chosen continuous, this can only be integer multiples of 2π.

Since $w(\boldsymbol{k})$ is continuous, this forces the vorticity of $\det[w(\boldsymbol{k})]$ to vanish everywhere so that the vorticity of the expression in Eq. (1.260) is completely determined by $[P(\boldsymbol{k})]^*$.

$\rightarrow$ Vortices come in pairs of opposite vorticity

- *Observation:* Zeros of $P(\boldsymbol{k})$ with $v[\boldsymbol{k}'] \neq 0$ are *topologically stable*.
  This is intuitively clear: If one makes the function non-zero at the vortex, it becomes discontinuous at this point due to the winding phase. Furthermore, the winding phase cannot be smoothly removed without discontinuous deformations of the function as well.

If we combine all the above facts, we end up with the
$\rightarrow$ *Generic picture:*
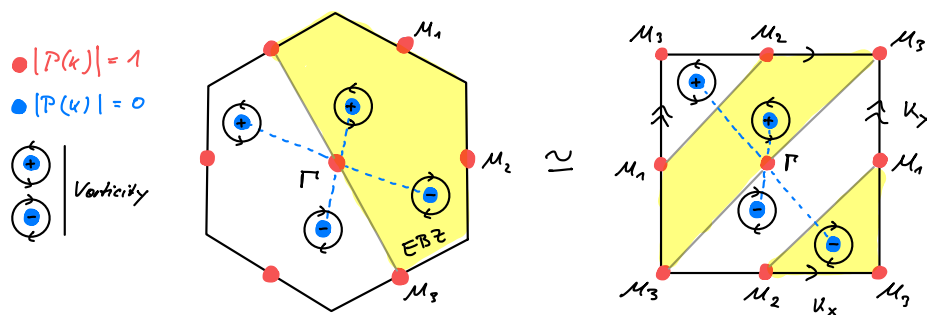
- Without additional symmetries, the zeros of $|P(\boldsymbol{k})|$ occur at *points* in the BZ (this is true for the Kane-Mele model if $m \neq 0$).

- With additional symmetries, the zeros can form *lines* that avoid the TRIMs (this happens for $m = 0$, ➥ Ref. [55] and below).

- Zeros with vanishing vorticity are not stable and therefore not "generic" but "fine-tuned."

- In the following, we focus on the least symmetric (and therefore most generic) case with point-like zeros. Without loss of generality, we assume a vorticity of ± 1 per vortex (a vortex with vorticity $|\nu| > 1$ can be continuously split into $|\nu|$ vortices of vorticity ± 1). Furthermore, we assume that all vortices in the EBZ have the same vorticity (vortices of opposite vorticity in the EBZ can be pairwise annihilated).

4. *Two situations:*

   - *Even* number of vortices in EBZ
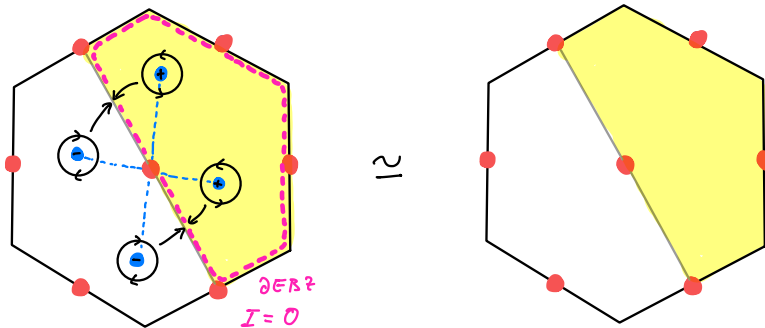
   - *Odd* number of vortices in EBZ
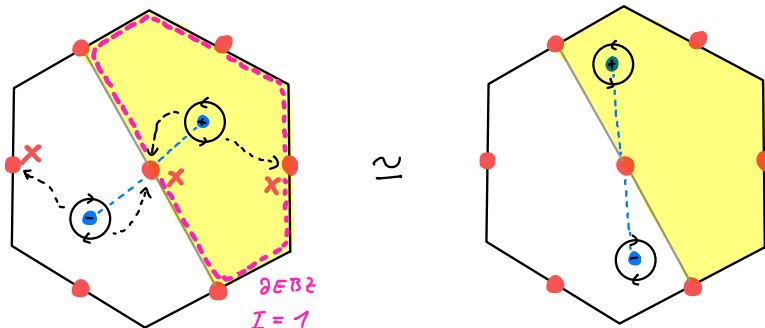
     – To remove the last vortex pair, the partners must meet at one of the TRIMs.

     – However, this is impossible because of TRS which demands $P|(\boldsymbol{K}^*)| = 1$.

   → The two situations are topologically distinct (as long as TRS is not broken)

   → *Odd* number of vortices = Topological phase protected by time-reversal symmetry (This is our first example of a SPT phase.)

5. This distinction is quantified by the *Topological $\mathbb{Z}_2$ index*

$$I = \frac{1}{2\pi i} \oint_{\partial \text{EBZ}} d \log\left[P(\boldsymbol{k})\right] \quad \text{mod } 2 \tag{1.262}$$

$$= \frac{1}{2\pi i} \oint_{\partial \text{EBZ}} \nabla \log[P(\boldsymbol{k})] \cdot d\boldsymbol{k} \quad \text{mod } 2 \tag{1.263}$$

∂EBZ: Closed path that encircles an EBZ

which measures the parity of the total vorticity in half the Brillouin zone.

- The choice of a EZB is constrained by the vortices. It should be chosen such that the vortices stay away from the boundary ∂EBZ. E.g. ➲ Fig. 2 in Ref. [55].

- $I \in \mathbb{Z}_2$ is gauge invariant because a gauge transformation that is continuous everywhere cannot change the vorticity of $P(\boldsymbol{k})$.

6. *Example:* Kane-Mele model:
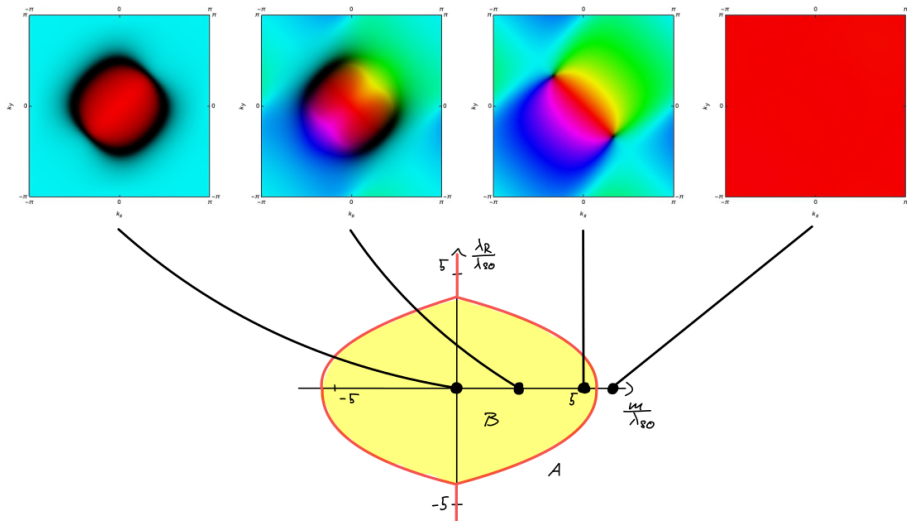
- In the color plots, the BZ is deformed to a square. The color denotes the phase (red = $+1$, turquoise = -1) and the lightness the absolute value (black = 0) of the Pfaffian computed from a family of global sections of the valence bundle.

- Note that in the topological phase (for $m \neq 0$) there is a single vortex in each EBZ and the phase winds once around each vortex so that $I = 1$. For this result, it is crucial that the Pfaffian is computed from a *globally continuous basis* (= a family of global sections of the valence bundle that form a basis at every point), otherwise the vorticity can be changed by integers (even if the Pfaffian is continuous!) and I cannot distinguish the phases. Note that these global sections are typically not eigenstates of the Bloch Hamiltonian; their existence, however, is guaranteed by time-reversal symmetry (because then all Chern numbers of the rank-2 valence bundle vanish).

- The enhanced symmetry for $m = 0$ make the zeros form a line that circles the central TRIM (and therefore cannot be contracted without breaking TRS). In this situation, the Pfaffian can be gauged real (as already mentioned by Kane an Mele [55]). Continuously breaking the "ring of zeros" is only possible if a pair of vortices is introduced that makes the phase wind around the two islands of zeros that result from such a procedure.

Details: ➲ Problemset 5

1.3.4 Edge modes

1. ◁ $\hat{H}_{\mathrm{KM}}$ on cylinder:
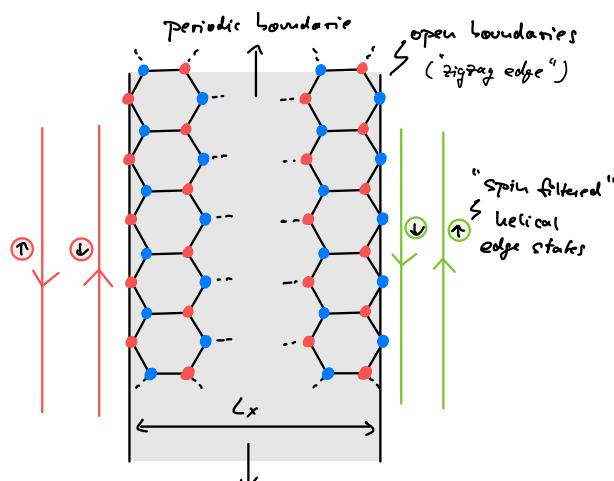
The type of boundary ("zigzag" vs. "armchair") has no effect on the existence of the edge states but the spectrum below looks different for armchair boundaries.

→ Interprete strip as 1D system with L_x-dependent unit cell
→ Fourier transform $\hat{H}_{\mathrm{KM}}$ in y-direction
→ 1D spectrum with $\mathcal{O}(L_x)$ bands labeled by y-momentum k_y

2. *Edge modes:*
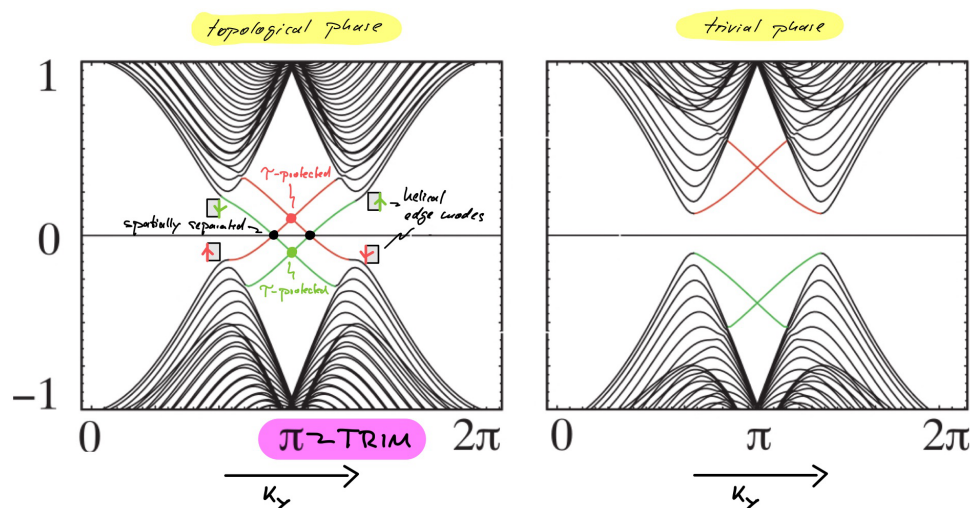
This figure is taken from Kane and Mele's original work [55].

- *Topological*: Gapless edge modes

  – Robust (= no backscattering / gap opening) to TRS perturbations

  – The four band crossings of the edge modes are protected for two reasons:

    ∗ Black crossings: The crossing modes are localized on *opposite* edges of the samples. Gapping them out is exponentially supressed with the width L_x of the strip (gapped bulk!).

    ∗ Colored crossings: The crossing modes live on the *same* edge of the sample. Gapping them out is forbidden by time-reversal symmetry as these crossings happen at a TRIM and are enforced by Kramers degeneracy. This is why the Kane-Mele topological insulator is an SPT phase.

- – On each edge there is a right propagating mode for one spin polarization and a left propagating mode for the opposite spin polarization (for $\lambda_R = 0$, i.e., if spin is conserved).
    - – The edge modes are *helical* (not *chiral*) since the product of spin and momentum is constant on each edge.
  - *Trivial*: No gapless edge modes

Details: ➲ Problemset 5

  - The two "stalactite-stalagmite" pairs in the above spectrum correspond to the 1D projections of the two (gapped) Dirac cones around K and K'. The tips of these bulk bands are connected by the edge modes.

  - For $\lambda_R = 0$ you can extract the edge modes of the Haldane Chern insulator by just looking at one of the two spin sectors (up or down, which determines the sign of the complex NNN hopping phase). Thus in the topological phase, the Haldane model supports *one* (then *chiral* [since spin does not exist]) edge mode on each boundary.

  - Just as the phenomenology of the Chern insulator is known as "quantum *anomalous* Hall effect" ("anomalous" because there is no magnetic field and consequently there are no Landau levels), the Kane-Mele topological insulator gives rise to the "quantum *spin* Hall effect" (because its crucial ingredient is spin to preserve time-reversal symmetry).

Final note:
We have now discussed two topological indices ("labels for topological phases"):

- The (first) *Chern number* classifies chiral topological phases in *two dimensions* (IQHE, QWZ model, Haldane model). It *cannot* be generalized to three dimensions! (There are generalizations in *even* dimensions, though [63].) Furthermore, for non-zero Chern numbers, time-reversal symmetry must be *broken*.

- The $\mathbb{Z}_2$ *Pfaffian index* classifies SPT phases in two dimensions (Kane-Mele topological insulator). It *can* be generalized to three dimensions and allows for the characterization of three-dimensional topological insulators [46, 50, 64]. For the Pfaffian index to be well-defined, time-reversal symmetry must be *preserved*.

↑ Notes

1.4 Topological insulators in 1D: The Su-Schrieffer-Heeger Chain

1.4.1 Preliminaries: Sublattice symmetry

1. *Symmetries we already know:*

   In the following, $\hat{H}$ denotes a non-interacting many-body Hamiltonian on (fermionic) Fock space and H its single-particle counterpart.

   - *Unitary symmetry $\mathcal{U}$:*

   $$\mathcal{U}i\,\mathcal{U}^{-1} = +i \quad \text{and} \quad \mathcal{U}c_i\,\mathcal{U}^{-1} = \sum_j U_{ij}^\dagger c_j \tag{1.264}$$

   $$\left[\hat{H},\mathcal{U}\right] = 0 \quad \Leftrightarrow \quad U H U^\dagger = H \quad \Leftrightarrow \quad [H,U] = 0 \tag{1.265}$$

   - *Time-reversal symmetry $\mathcal{T}_U$:*

   $$\mathcal{T}_U\,i\,\mathcal{T}_U^{-1} = -i \quad \text{and} \quad \mathcal{T}_U c_i \mathcal{T}_U^{-1} = \sum_j U_{ij}^\dagger c_j \tag{1.266}$$

   $$\left[\hat{H},\mathcal{T}_U\right] = 0 \quad \Leftrightarrow \quad U H^* U^\dagger \stackrel{\circ}{=} H \quad \Leftrightarrow \quad [H,\underbrace{U\mathcal{K}}_{T_U}] = 0 \tag{1.267}$$

   Note that both U and $U\mathcal{K}$ are valid *symmetries* (i.e., they commute with the Hamiltonian) on the single-particle Hilbert space in accordance with *Wigner's theorem.*

2. *What about:*

   - Unitary like $\mathcal{U}$ but with $c_i \leftrightarrow c_i^\dagger$:

   $$\mathcal{C}_U\,i\,\mathcal{C}_U^{-1} = +i \quad \text{and} \quad \mathcal{C}_U c_i \mathcal{C}_U^{-1} = \sum_j U_{ij}^{*\dagger} c_j^\dagger \tag{1.268}$$

   $$\left[\hat{H},\mathcal{C}_U\right] = 0 \quad \Leftrightarrow \quad U H^* U^\dagger \stackrel{\circ}{=} -H \quad \Leftrightarrow \quad \{H,\underbrace{U\mathcal{K}}_{C_U}\} = 0 \tag{1.269}$$

   (The complex conjugate at the U is convention but not crucial.)

   $\rightarrow$ *Particle-hole symmetry $\mathcal{C}_U$*

   � Next lecture on topological superconductors

   - Antiunitary like $\mathcal{T}_U$ but with $c_i \leftrightarrow c_i^\dagger$:

   $$\mathcal{S}_U\,i\,\mathcal{S}_U^{-1} = -i \quad \text{and} \quad \mathcal{S}_U c_i \mathcal{S}_U^{-1} = \sum_j U_{ij}^{*\dagger} c_j^\dagger \tag{1.270}$$

   $$\left[\hat{H},\mathcal{S}_U\right] = 0 \quad \Leftrightarrow \quad U H U^\dagger \stackrel{\circ}{=} -H \quad \Leftrightarrow \quad \{H,\underbrace{U}_{S_U}\} = 0 \tag{1.271}$$

   (The complex conjugate at the U is convention but not crucial.)

   $\rightarrow$ *Chiral- or Sublattice symmetry $\mathcal{S}_U$*

   Here we will stick to the term "sublattice symmetry" (SLS).
   But why should we call $\mathcal{S}_U$ "sublattice symmetry" in the first place?
   ➲ Next point below

Note: The same arguments used for time-reversal symmetry lead to

$$\{H, U\} = 0 \quad \Rightarrow \quad [H, U^2] = 0 \quad \Rightarrow \quad U^2 = e^{i\varphi} \mathbb{1} \qquad (1.272)$$

$\rightarrow$ Redefine $\tilde{U} = e^{-i\varphi/2} U \rightarrow \tilde{U}^2 = +\mathbb{1} \rightarrow$ w.l.o.g. $U^2 = +\mathbb{1}$
$\rightarrow$ In contrast to time-reversal, there are not two "types" of sublattice symmetry!
(This follows from the missing antiunitarity on the single-particle level.)

Whereas $\mathcal{U}$ and $\mathcal{T}_U$ can be interpreted as symmetries both on the Fock space and on the single-particle Hilbert space, particle-hole symmetry $\mathcal{C}_U$ and sublattice symmetry $\mathcal{S}_U$ are only symmetries on the Fock space; on the single-particle Hilbert space they act as unitary and antiunitary *pseudo*symmetries, respectively (i.e., they *anti*commute with the single-particle Hamiltonian). This should be not surprising since both include an exchange of particles with holes so that they mix sectors of different particle numbers. Such an operation is intrinsic to the many-particle description in Fock space and cannot be sensibly defined (or interpreted) as a symmetry in a (first quantized) single-particle description.

3. Why "sublattice symmetry"?

   a) $\lhd$ SP Hamiltonian H with $UHU^\dagger = -H$
      $\rightarrow$ Spectrum $\sigma(H) = \sigma(-H)$
      $\rightarrow$ Spectrum symmetric about $E = 0$
      By contrast, time-reversal implied a symmetric spectrum about the energy axis:
      $E(k) = E(-k)$.

   b) Assume H is $2L \times 2L$-matrix $\rightarrow$

   $$\exists \text{ Unitary } M : \quad MHM^\dagger = \begin{pmatrix} D & 0 \\ 0 & -D \end{pmatrix} \qquad (1.273)$$

   D: diagonal matrix

   $\rightarrow$

   $$(QM)H(QM)^\dagger = \begin{pmatrix} 0 & D \\ D & 0 \end{pmatrix} \quad \text{with} \quad Q = \frac{1}{\sqrt{2}} \begin{pmatrix} \mathbb{1} & \mathbb{1} \\ \mathbb{1} & -\mathbb{1} \end{pmatrix} \qquad (1.274)$$

   Note that QM is just a unitary basis transformation of the SP Hamiltonian.

   c) This means that for a sublattice symmetric system, there exists a unitary transformation of modes $\tilde{c}_i = \sum_j \tilde{U}_{ij} c_j$ such that
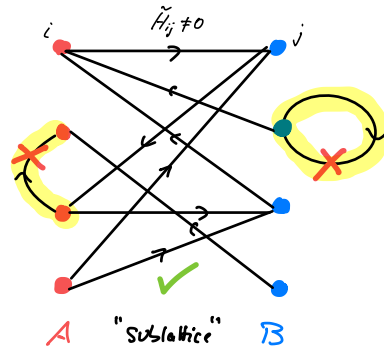
   $$\hat{H} = \sum_{i,j} c_i^\dagger H_{ij} c_j \overset{[\hat{H}, \mathcal{S}_U] = 0}{=} \sum_{i,j} \tilde{c}_i^\dagger \tilde{H}_{ij} \tilde{c}_j \qquad (1.275)$$

   with block-off-diagonal Hamiltonian

   $$\tilde{H} = \begin{pmatrix} 0 & h & \text{Hopping } A \mapsto B \\ h^\dagger & 0 & \text{Hopping } B \mapsto A \end{pmatrix} \qquad (1.276)$$

   The two subsets of modes A and B are referred to as "sublattices" even if a spatial lattice structure is missing.

   d) $\tilde{H}$ couples only modes *between* the two "sublattices" A and B:

Often this sublattice structure is already visible in the real-space basis, i.e., a transformation to $\tilde{H}$ is not even necessary (➡ SSH chain below).

If one interprets $\tilde{H}$ as a (complex valued) adjacency matrix of a graph, the "sublattice symmetry" would be called *bipartiteness*. And indeed, it is well-known that a graph is bipartite if and only if the spectrum of its adjacency matrix is symmetric.

e) *Example:* Graphene
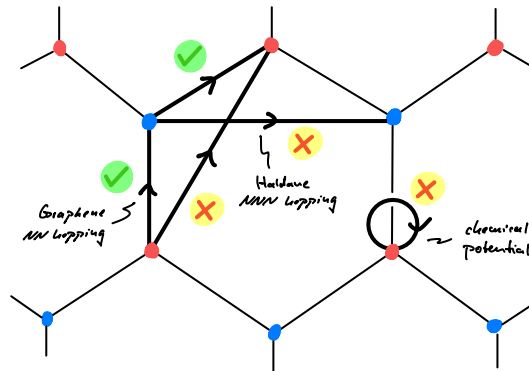
Note that a chemical potential $\mu \sum_i c_i^\dagger c_i$ can be read as a hopping from site i to the same site; therefore it violates SLS.

1.4.2 The Su-Schrieffer-Heeger chain

> **† Note**
>
> A detailed exposition of the SSH chain is given in the textbook by Asboth [65] but may also be found in almost any other textbook on topological insulators. There is also an introduction in my PhD thesis [66] (on which this section is based) with a quite detailed discussion of edge states in the appendices of Chapter 3.

- The *Su–Schrieffer–Heeger (SSH) chain* is a model of non-interacting, spinless fermions in one dimension that has been introduced by Su, Schrieffer and Heeger in 1979 to describe soliton formation in polyacetylene [67].

- In the context of topological phases, the model has become the example of choice to illustrate topological invariants and the emergence of robust edge modes [65].

1. ◁ 1D lattice with $2L$ sites grouped into L unit cells:
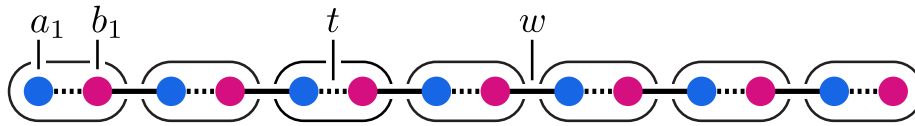
a_i, b_i $(1 \leq i \leq L)$: spinless fermion modes

$\rightarrow$ *SSH chain Hamiltonian:*

$$\hat{H}_{\text{SSH}} = t \sum_{i=1}^{L}(a_i^\dagger b_i + b_i^\dagger a_i) + w \sum_{i=1}^{L'}(b_i^\dagger a_{i+1} + a_{i+1}^\dagger b_i), \qquad (1.277)$$

- $t, w \in \mathbb{R}$: alternating hopping amplitudes
- $L' = L - 1$ for OBC and $L' = L$ for PBC

2. *Symmetries:*

- Particle-number symmetry (PNS)
  This is an intrinsic symmetry of the class of quadratic fermion models without superconductivity; we cannot break it without leaving this formalism.

- Translation symmetry (TS)
  Translation symmetry is typically broken in real samples due to disorder.

- Time-reversal symmetry (TRS):

$$\mathcal{T} i \mathcal{T}^{-1} := -i \quad \text{and} \quad \mathcal{T} a_i \mathcal{T}^{-1} := a_i \quad \text{and} \quad \mathcal{T} b_i \mathcal{T}^{-1} := b_i \qquad (1.278)$$

  $\rightarrow [\hat{H}_{\text{SSH}}, \mathcal{T}] \overset{\circ}{=} 0$

- Particle-hole symmetry (PHS):

$$\mathcal{C} i \mathcal{C}^{-1} := i \quad \text{and} \quad \mathcal{C} a_i \mathcal{C}^{-1} := a_i^\dagger \quad \text{and} \quad \mathcal{C} b_i \mathcal{C}^{-1} := -b_i^\dagger \qquad (1.279)$$

  $\rightarrow [\hat{H}_{\text{SSH}}, \mathcal{C}] \overset{\circ}{=} 0$

- Sublattice symmetry (SLS):

$$\mathcal{S} i \mathcal{S}^{-1} := -i \quad \text{and} \quad \mathcal{S} a_i \mathcal{S}^{-1} := a_i^\dagger \quad \text{and} \quad \mathcal{S} b_i \mathcal{S}^{-1} := -b_i^\dagger \qquad (1.280)$$

  $\rightarrow [\hat{H}_{\text{SSH}}, \mathcal{S}] \overset{\circ}{=} 0$

  Note that the minus sign is crucial for the commutation with the Hamiltonian!

  The above definition is realized by the operator

$$\mathcal{S} = \prod_i (a_i^\dagger - a_i)(b_i^\dagger + b_i) \circ \mathcal{K} \qquad (1.281)$$

Are all these symmetries of the same "value" for the SSH chain?

3. $\lhd$ *"Generic" SSH chain:*

$$\hat{H}'_{\text{SSH}} = \sum_{i=1}^{L}(t_i \, a_i^\dagger b_i + t_i^* \, b_i^\dagger a_i) + \sum_{i=1}^{L'}(w_i \, b_i^\dagger a_{i+1} + w_i^* \, a_{i+1}^\dagger b_i), \qquad (1.282)$$

$t_i, w_i \in \mathbb{C}$: site-dependent & complex hopping amplitudes

$\overset{\circ}{\to}$ *Symmetries left:* PN & SLS
(Check that the complex hoppings destroy both TRS and PHS!)

> → *The natural symmetry of the SSH chain is SLS.*

For the analytical analysis below, we will still assume translation invariance so that we can Fourier transform the Hamiltonian.

However, if one studies the model numerically, one can easily add translation-symmetry breaking perturbations to the Hamiltonian to verify that the features of the SSH chain are robust to SLS-symmetric disorder (➲ discussion of edge modes below).

1.4.3 Diagonalization

1. $\lhd \hat{H}_{\text{SSH}}$ with PBC and Fourier transform

$$\tilde{x}_k = \frac{1}{\sqrt{L}} \sum_{n=1}^{L} e^{-ikn} x_n, \quad x = a, b \tag{1.283}$$

$\overset{\circ}{\to}$

$$\hat{H}_{\text{SSH}} = \sum_{k \in \text{BZ}} \begin{pmatrix} \tilde{a}_k^\dagger & \tilde{b}_k^\dagger \end{pmatrix} \cdot \underbrace{\begin{pmatrix} 0 & t + we^{-ik} \\ t + we^{ik} & 0 \end{pmatrix}}_{H(k)} \cdot \begin{pmatrix} \tilde{a}_k \\ \tilde{b}_k \end{pmatrix} \tag{1.284}$$

BZ: Brillouin zone = Circle S^1

2. *Bloch Hamiltonian:*

$$H(k) = (t + w \cos k)\, \sigma^x + w \sin k\, \sigma^y = \vec{d}(k) \cdot \vec{\sigma} \tag{1.285}$$

with Bloch vector

$$\vec{d}(k) = \begin{pmatrix} t + w \cos k \\ w \sin k \\ 0 \end{pmatrix} \tag{1.286}$$

3. *Band structure:*

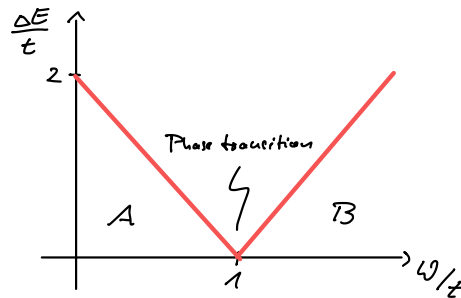$$E_\pm(k) = \pm|\vec{d}(k)| = \pm\sqrt{t^2 + w^2 + 2tw \cos k} \tag{1.287}$$

We have two bands because of the two-atom unit cell.
The $\pm$ is enforced by SLS as discussed above.

4. *Phase diagram:*

Bandgap: $\Delta E \overset{\circ}{=} 2||t| - |w||$

Let $t, w > 0 \to$ Gapless point for $w = t$, gapped insulator for $w \lessgtr t$: (The restriction $t, w > 0$ is not important as chains with different signs are unitarily equivalent.)

$\rightarrow$ Unique ground state in A and B ($\rightarrow$ no symmetry breaking)

> *Can we use SLS to define a topological invariant to distinguish the two phases?*

Just like we used TRS to define the Pfaffian invariant to characterize the phases of the Kane-Mele model …

1.4.4 A new topological invariant

1. *Observation:* PNS does not constrain $H(k)$

2. $\lhd$ SLS:

$$\left[\hat{H}_{\text{SSH}}, \mathcal{S}\right] = 0 \quad \Leftrightarrow \quad U^\dagger H U = -H \quad \Leftrightarrow \quad \sigma^z H(k)\sigma^z \overset{\circ}{=} -H(k) \tag{1.288}$$

   The last condition follows along the same lines as for time-reversal symmetry ($\bullet$ Eq. (1.147)) with the unitary U defined by Eq. (1.280).

3. Constrained Bloch vector:

$$d_z(k) \overset{!}{=} 0 \qquad \forall\, k \in \text{BZ} \tag{1.289}$$

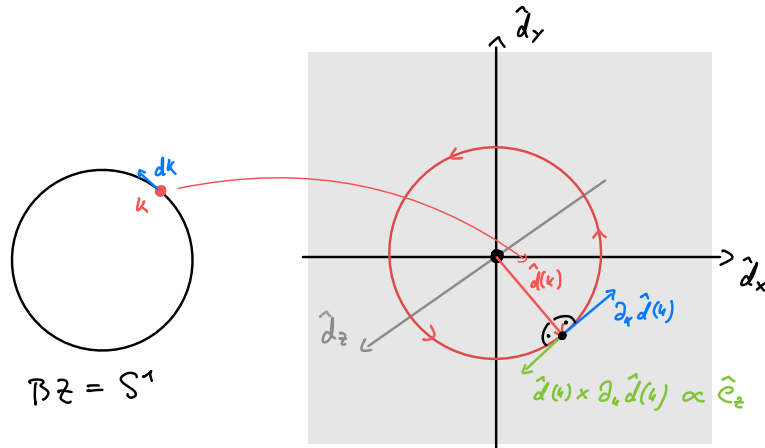 $\rightarrow \vec{d}(k)$ cannot leave the x-y-plane

4. $\lhd$ Gapped phase $\rightarrow$ Normalization possible:

$$\hat{d}(k) = \frac{\vec{d}(k)}{|\vec{d}(k)|} \tag{1.290}$$

5. *Winding number* around the origin in the x-y-plane is well defined:
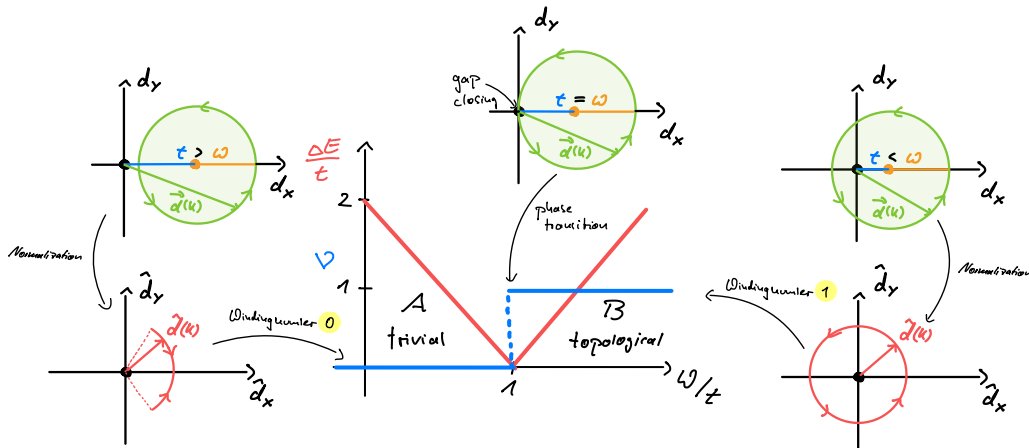
$$\nu[\hat{d}] := \frac{1}{2\pi} \int_{S^1} \hat{e}_z \cdot \left[\hat{d}(k) \times \partial_k \hat{d}(k)\right] dk \quad \in \mathbb{Z} \tag{1.291}$$

It is crucial that $\hat{d}$ is pinned to the x-y-plane by SLS for this to be an integer!

$$BZ = S^1$$

6. Two phases:

$$v = \begin{cases} 0 & \text{for} \quad t > w \text{ (Phase A)} \\ 1 & \text{for} \quad t < w \text{ (Phase B)} \end{cases} \tag{1.292}$$


This follows directly from the form of the Bloch vector Eq. (1.286).

7. *Mathematical side note:*

We can embed this new topological invariant and the Chern number into a bigger picture if we invoke the concept of *homotopy groups* from topology. Simply speaking, the homotopy group $\pi_p(X)$ for $p = 0, 1, 2, \ldots$ and a topological space X consists of equivalence classes of continuous maps from the p-dimensional sphere S^p into X where two maps are considered equivalent if they can be transformed into each other continuously (if the space X has a dedicated "base point" one can glue two such maps together and obtains a group structure on these equivalence classes).

The maps we are interested in are the Bloch vectors $\hat{d}(k)$ that map the Brillouin zone onto the sphere $X = S^2$. In 1D, the BZ is S^1 so that we are interested in the homotopy group $\pi_1(S^2) = 0$ which is trivial because every circle (S^1) that you draw onto the sphere ($X = S^2$) can be continuously contracted to a point (which represents the constant map):
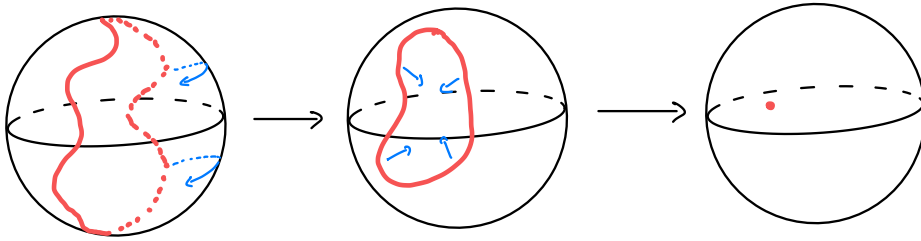
This is why there is *no* analog of the Chern number in 1D. By contrast, in 2D the BZ is a torus T^2 which we can simplify to the sphere S^2 in the continuum limit (thereby ignoring weak topological indices) so that we are interested in the homotopy group $\pi_2(S^2) = \mathbb{Z}$. Now there are different homotopy classes (corresponding to different topological phases) that are labeled by an integer—the Chern number—and distinguished by how often they wrap the target sphere when tracing over the domain sphere (which is hard to visualize).

However, if we are in 1D *and* a symmetry like SLS restricts the Bloch vector to a 2D cut of S^2, namely a circle S^1, then we are interested in the homotopy group $\pi_1(S^1) = \mathbb{Z}$. The different homotopy classes consist of maps from the circle onto the circle that have different winding numbers and therefore cannot be continuously deformed into each other:
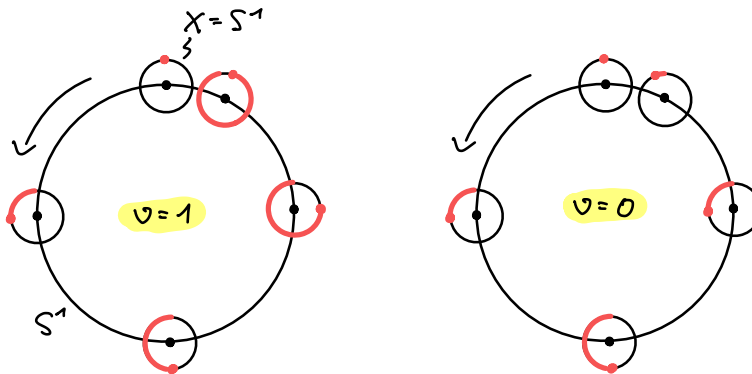
The label in this situation is the topological index ν defined above.

8. *Zak phase [68]:*

We introduced the topological index ν as a winding number of the Bloch vector. When we discussed the Chern number, we arrived at it via the Berry curvature and only later showed that in systems with two bands it can be interpreted as a winding number of the Bloch vector. This begs the question whether there is a similar expression in terms of Bloch *states* (instead of the Bloch vector) to distinguish the two phases. The answer is "yes" and known as the *Zak phase* [68]:

$$\varphi_{\text{Zak}} = \int_{S^1} i \langle u(k)|\partial_k u(k)\rangle \, dk \tag{1.293}$$

where $|u(k)\rangle$ describes the lower band.

The Zak phase is the Berry *phase* collected when traversing the 1D BZ (note that there is no Berry *curvature* in 1D).

Remember that the Berry phase is a gauge dependent quantity and can change by multiples of 2π under continuous gauge transformations. The two phases of the SSH chain are distinguished by the *difference* of their Zak phases:

$$\Delta\varphi_{\text{Zak}} = (\varphi_{\text{Zak}}^{\text{topological}} - \varphi_{\text{Zak}}^{\text{trivial}}) \mod 2\pi = \pi \tag{1.294}$$

This quantity has already been measured in experiments with cold atoms in optical lattices [69].

Proof: ➔ Problemset 6

1.4.5 Breaking the symmetry

1. The topological phase of the SSH chain with $\nu = 1$ is symmetry-protected by SLS.
   $\rightarrow$ Connect phases A and B *without* closing the gap but *with* breaking SLS?

2. Add staggered chemical potential:

$$\hat{H}'_{\mathrm{SSH}} = \hat{H}_{\mathrm{SSH}} + \mu \underbrace{\sum_{i=1}^{L}(a_i^\dagger a_i - b_i^\dagger b_i)}_{\hat{H}_\mu} \tag{1.295}$$

Important: $[\hat{H}_\mu, \mathcal{S}] \neq 0$
(Remember the interpretation of SLS as bipartiteness of the coupling graph!)

3. *Bloch vector:*

$$\vec{d}(k) = \begin{pmatrix} t + w\,\cos k \\ w\,\sin k \\ \mu \end{pmatrix} \tag{1.296}$$

$\rightarrow$ *Spectrum:*

$$\pm E_\pm(k) = |\vec{d}(k)| = \sqrt{\mu^2 + t^2 + w^2 + 2tw\,\cos k} \quad \geq \quad |\mu| \tag{1.297}$$

$\rightarrow$ Gapped for all w, t (in particular $w = t$) if $\mu \neq 0$

Note that the spectrum becomes flat for $t \cdot w = 0$ and the many-body ground state of $\hat{H}_{\mathrm{SSH}}$ for $t > 0$ and $w = 0$ is a simple product state at half-filling with one delocalized fermion per unit cell; we label this state as "trivial." For $t = 0$ and $w > 0$ the bands are again flat and the many-body ground state can be read off the Hamiltonian: now the fermions are delocalized between two modes of *adjacent* unit cells. The family of Hamiltonians $\hat{H}'_{\mathrm{SSH}}$ connects these two representatives adiabatically, i.e., without crossing a phase transition (➔ next point).

↑ Notes

4. Connect phases without closing the gap:
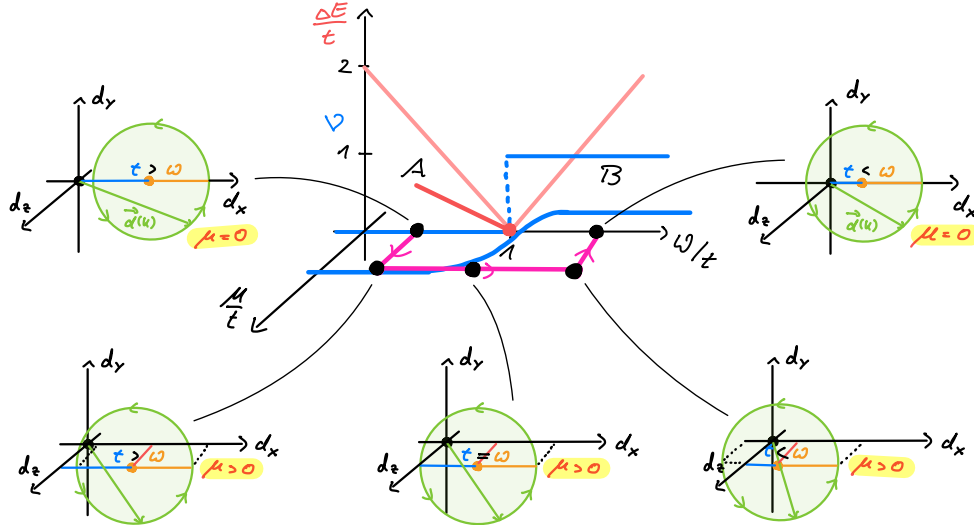
Note that the winding number is ill-defined for $\mu \neq 0$ (= no longer an integer).

This situation is typical for SPT phases!

This also demonstrates that the topological phase of the SSH chain is *not* topologically ordered (= long-range entangled).

1.4.6 Edge modes

1. ◁ *Open* chain of length L:

   • *Trivial phase* for $t > 0$ and $w = 0$:
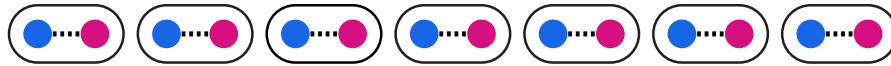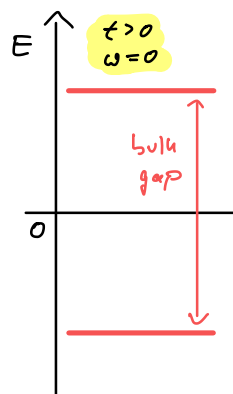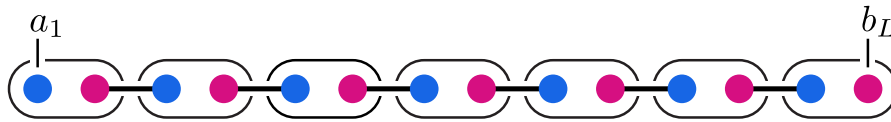

   → SP Spectrum:

   Note that due to the OBC momentum is no longer a good quantum number, the x-axis is therefore of no relevance.

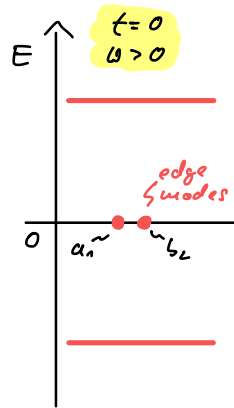   • *Topological phase* for $t = 0$ and $w > 0$:

$\rightarrow$ *Edge modes $\tilde{a}_l = a_1$ and $\tilde{b}_r = b_L$ commute with $\hat{H}_{\text{SSH}}$*
Note that a_1 and b_L no longer show up in $\hat{H}_{\text{SSH}}$.

$\rightarrow$ 4-fold degenerate ground state
The four ground states $|n_l, n_r\rangle$ are labeled by the occupancy $n_l = 0, 1$ and $n_r = 0, 1$ of the edge modes $\tilde{a}_l$ and $\tilde{b}_r$, i.e., $\tilde{a}_l^\dagger \tilde{a}_l |n_l, n_r\rangle = n_l |n_l, n_r\rangle$ etc.

$\rightarrow$ SP Spectrum:

These two choices where either t or w vanish are the *renormalization group fixed points* of the two phases with vanishing correlation length.

2. Edge modes persist for $t > 0$ as long as $t < w$:

$$\tilde{a}_l \approx \mathcal{N} \sum_{i=1}^{L} \left(-\frac{t}{w}\right)^{i-1} a_i \quad \text{and} \quad \tilde{b}_r \approx \mathcal{N} \sum_{i=1}^{L} \left(-\frac{t}{w}\right)^{i-1} b_{L-i+1} \qquad (1.298)$$

(The normalization $\mathcal{N}$ depends on t, w and L.)

$\rightarrow$ Exponentially localized on edges

To show that these are fermionic edge modes in the thermodynamic limit, you must first verify that they indeed describe two fermions,

$$\{\tilde{a}_l, \tilde{a}_l\} = 0, \quad \left\{\tilde{a}_l, \tilde{a}_l^\dagger\right\} = 1, \quad \left\{\tilde{a}_l^{(\dagger)}, \tilde{b}_r^{(\dagger)}\right\} = 0 \qquad (1.299)$$

$$\left\{\tilde{b}_r, \tilde{b}_r\right\} = 0, \quad \left\{\tilde{b}_r, \tilde{b}_r^\dagger\right\} = 1 \qquad (1.300)$$

and then that they commute with the Hamiltonian (up to corrections that vanish exponentially in the system size):

$$\left[\tilde{a}_l, \hat{H}_{\text{SSH}}\right] = \mathcal{O}\left((t/w)^L\right) \quad \text{and} \quad \left[\tilde{b}_r, \hat{H}_{\text{SSH}}\right] = \mathcal{O}\left((t/w)^L\right). \qquad (1.301)$$

This proves the four-fold degeneracy of the ground state space for $L \rightarrow \infty$ in the topological phase $t < w$ even away from the fixed point $t = 0$. Note that this argument fails in the trivial phase for $t > w$!

Details: ➔ Problemset 6

→ Finite-size scaling of SP spectrum:
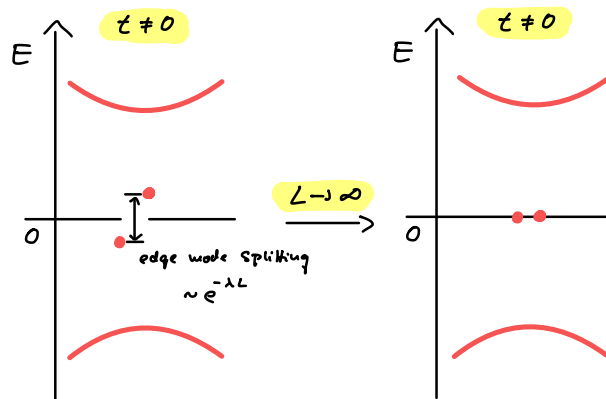
Because of the finite extend of the edge modes, there is an exponentially supressed amplitude for a fermion located on one edge to tunnel across the chain to the other edge. The true eigenstates are therefore non-degenerate symmetric and antisymmetric superpositions of exponentially localized modes on the two boundaries. This splitting vanishes exponentially fast with the system size L. The *edge mode splitting* away from the fixed point with $t = 0$ is therefore a finite-size effect.

3. Degeneracy of edge modes is robust against SLS-preserving disorder:

   a) *Clean system:*
   Plot SP spectrum of Eq. (1.277) for $w = 1 - t$ and $t \in [0, 1]$ (chain length $L = 40$).

   → Degenerate zero-energy edge modes appear for $t < 0.5$ in the topological phase.

   b) *SLS-preserving disorder:*
   Plot SP spectrum with $t \mapsto t_i$ and $w \mapsto w_i$ site dependent; choose normal distributed couplings with $\langle t_i \rangle = t$, $\langle w_i \rangle = w$ and $w = 1 - t$ for $t \in [0, 1]$ with variance of 20% of the mean. Every spectrum is computed from a *different* random configuration of couplings for a prescribed mean.

   → Bulk spectrum is scrambled but edge modes remain degenerate and are not influenced by the disorder in the topological phase.
   The behaviour of the bulk spectrum is generic; the behaviour of the edge modes is highly atypical and a consequence of the topological nature of the phase (and of course SLS). It is this remarkable behaviour of edge modes that is referred to as "topologically robust ground state degeneracy" in the context of SPT phases.

   c) *SLS-breaking disorder:*
   Let t and w be homogeneous but add a site-dependent chemical potential $\mu_i^a a_i^\dagger a_i + \mu_i^b b_i^\dagger b_i$ to the Hamiltonian Eq. (1.277); this breaks SLS. We choose μ_i^x normal distributed around zero with variance of 0.1 (remember that $w + t = 1$). Now the whole spectrum—including the edge modes—behaves generically, i.e., all degeneracies are lifted. This demonstrates the symmetry-protection of the ground-/edge-state degneracy.

Clean system

SLS–preserving disorder

SLS–breaking disorder

↑ Notes
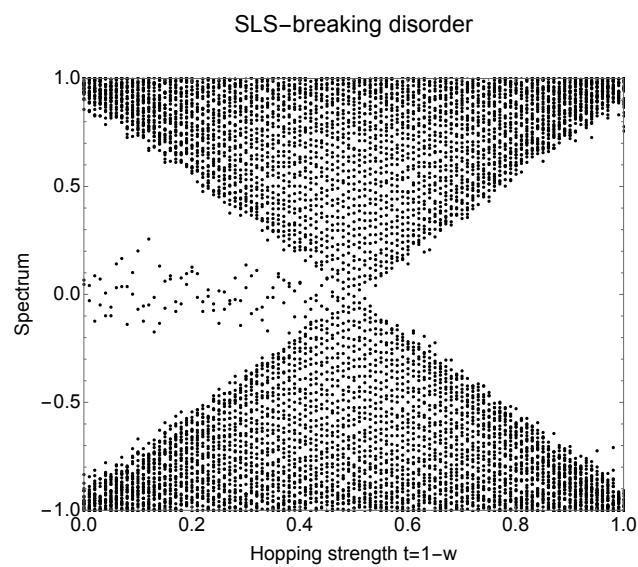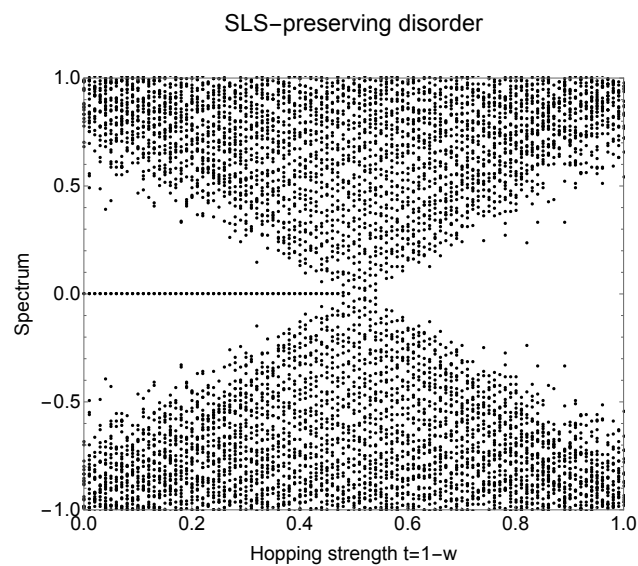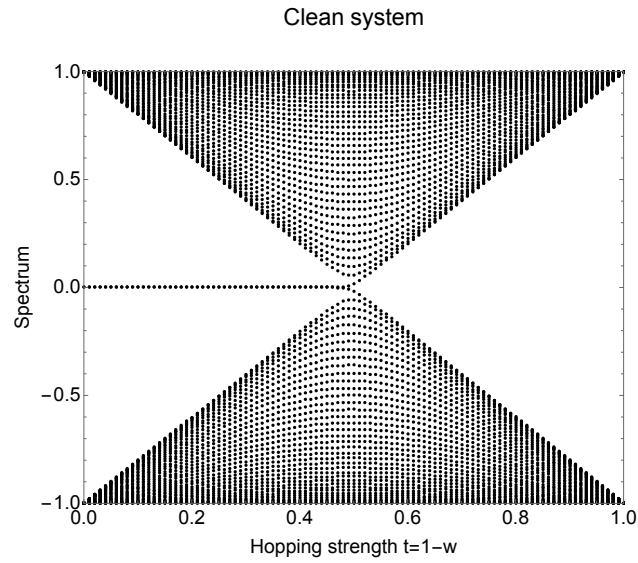
Final note: The single-particle physics of the SSH chain has already been studied in quantum simulations on various platforms (➜ [70] and references therein). The topological edge physics of the SSH chain can also be used to solve for applied problems such as state transfer in quantum chains (➜ [71] and references therein).

1.5 Topological superconductors in 1D: The Majorana chain

1.5.1 Preliminaries: Particle-hole symmetry and mean-field superconductors

- Remember (◉ last lecture): Particle-hole symmetry (PHS) $\mathcal{C}_U$:

$$\mathcal{C}_U i \mathcal{C}_U^{-1} = +i \quad \text{and} \quad \mathcal{C}_U c_i \mathcal{C}_U^{-1} = \sum_j U_{ij}^{*\dagger} c_j^\dagger \tag{1.302}$$

$$\left[\hat{H}, \mathcal{C}_U\right] = 0 \quad \Leftrightarrow \quad U H^* U^\dagger = -H \quad \Leftrightarrow \quad \{H, \underbrace{U\mathcal{K}}_{C_U}\} = 0 \tag{1.303}$$

(The complex conjugate at the U is convention but not crucial.)

→ *Unitary symmetry* on MB Hamiltonian, *antiunitary pseudosymmetry* on SP Hamiltonian

The naming should be evident: $\mathcal{C}_U$ exchanges particles with holes ($c_i \leftrightarrow c_i^\dagger$ up to a unitary transformation).

- Remember (◉ your lecture on solid state physics): BCS theory of superconductivity:

  1. *BCS Hamiltonian:* (BCS = Bardeen-Cooper-Schrieffer)

$$\hat{H}_{\text{BCS}} = \underbrace{\sum_{\boldsymbol{k},\sigma} (\varepsilon_{\boldsymbol{k}} - \mu)\, c_{\boldsymbol{k}\sigma}^\dagger c_{\boldsymbol{k}\sigma}}_{\text{Free fermions}} + \underbrace{\sum_{\boldsymbol{k},\boldsymbol{k}'} V_{\boldsymbol{k}\boldsymbol{k}'}\, c_{\boldsymbol{k}\uparrow}^\dagger c_{-\boldsymbol{k}\downarrow}^\dagger c_{-\boldsymbol{k}'\downarrow} c_{\boldsymbol{k}'\uparrow}}_{\text{Pairing term (interaction)}} \tag{1.304}$$

     $\sigma \in \{\uparrow, \downarrow\}$: fermion spin
     μ: chemical potential
     $\varepsilon_{\boldsymbol{k}}$: free fermion dispersion
     $V_{\boldsymbol{k}\boldsymbol{k}'}$: pairing potential

     Idea: Superconductivity is a condensation mechanism that is triggered by attractive interactions $V_{\boldsymbol{k}\boldsymbol{k}'}$ (mediated by phonons) between fermions. Then, the formation of bosonic Cooper pairs lowers the energy, the Cooper pairs condense and form the superconducting condensate.

  2. The BCS Hamiltonian is interacting (= not quadratic) and therefore hard to study.
     → *Mean-field theory:*

$$c_{\boldsymbol{k}\uparrow}^\dagger c_{-\boldsymbol{k}\downarrow}^\dagger = X_{\boldsymbol{k}}^* + (c_{\boldsymbol{k}\uparrow}^\dagger c_{-\boldsymbol{k}\downarrow}^\dagger - X_{\boldsymbol{k}}^*) \qquad \text{with} \quad X_{\boldsymbol{k}}^* = \langle c_{\boldsymbol{k}\uparrow}^\dagger c_{-\boldsymbol{k}\downarrow}^\dagger \rangle \tag{1.305}$$

$$c_{-\boldsymbol{k}'\downarrow} c_{\boldsymbol{k}'\uparrow} = \underbrace{X_{\boldsymbol{k}'}}_{\text{Mean}} + \underbrace{(c_{-\boldsymbol{k}'\downarrow} c_{\boldsymbol{k}'\uparrow} - X_{\boldsymbol{k}'})}_{\text{Small fluctuations } \delta X_{\boldsymbol{k}'}} \qquad \text{with} \quad X_{\boldsymbol{k}} = \langle c_{-\boldsymbol{k}'\downarrow} c_{\boldsymbol{k}'\uparrow} \rangle \tag{1.306}$$

     Cooper pair condensation $\Leftrightarrow X_{\boldsymbol{k}'} \neq 0$ and $\delta X_{\boldsymbol{k}'}$ small

     → Drop terms of order $\mathcal{O}(\delta X_{\boldsymbol{k}'}^2)$ (and a constant offset):

$$\hat{H}_{\text{BCS}}^{\text{mf}} = \underbrace{\sum_{\boldsymbol{k},\sigma} (\varepsilon_{\boldsymbol{k}} - \mu)\, c_{\boldsymbol{k}\sigma}^\dagger c_{\boldsymbol{k}\sigma}}_{\text{Free fermions}} + \sum_{\boldsymbol{k}} \underbrace{\left[\Delta_{\boldsymbol{k}}\, c_{\boldsymbol{k}\uparrow}^\dagger c_{-\boldsymbol{k}\downarrow}^\dagger + \Delta_{\boldsymbol{k}}^*\, c_{-\boldsymbol{k}\downarrow} c_{\boldsymbol{k}\uparrow}\right]}_{\text{Quadratic pairing terms}} \tag{1.307}$$

     with order parameter

$$\Delta_{\boldsymbol{k}} = \sum_{\boldsymbol{k}'} V_{\boldsymbol{k}\boldsymbol{k}'} X_{\boldsymbol{k}'} \quad \in \mathbb{C} \tag{1.308}$$

Since here Cooper pairs are formed by fermions with total spin zero, $X_{\boldsymbol{k}} = \langle c_{-\boldsymbol{k}'\downarrow} c_{\boldsymbol{k}'\uparrow} \rangle$, this is called *s-wave superconductivity*.

Important: $\hat{H}_{\mathrm{BCS}}^{\mathrm{mf}}$ is no longer charge/particle-number conserving; only the fermion parity is conserved. Such a Hamiltonian makes only sense as an effective mean-field description that excludes the superconducting condensate from/into which pairs of electrons can be transfered.

The benefit of the mean-field description of superconductivity is that the Hamiltonian is quadratic in fermions and therefore fits into our current class of models ("non-interacting fermions").

1.5.2 The Majorana chain

> **† Note**
>
> A detailed exposition of the Majorana chain is given in the textbook by Bernevig [26] but may also be found in almost any other textbook that covers topological superconductors. Furthermore, the original paper by Alexei Kitaev is worthwile to read [72]. There is also an introduction in my PhD thesis [66] (on which this section is based) and a more detailed account in my Master thesis [73].

1. ◁ 1D superconductor of *spinless* fermions c_i (= *p*-wave pairing):

$$\hat{H}_{\mathrm{MC}} = -\sum_{i=1}^{L'} \left(w\, c_i^\dagger c_{i+1} - \Delta\, c_i c_{i+1} + \mathrm{h.c.} \right) - \sum_{i=1}^{L} \mu \left(c_i^\dagger c_i - \frac{1}{2} \right), \qquad (1.309)$$

$w \in \mathbb{R}$: tunneling amplitude
$\Delta = e^{i\theta}|\Delta| \in \mathbb{C}$: superconducting gap ($\theta$ is the phase of the condensate)
$\mu \in \mathbb{R}$: chemical potential
$L' = L$ (PBC) or $L' = L - 1$ (OBC)

- This is the mean-field theory (in real space) of a "triplet superconductor" with *p*-wave pairing, i.e., Cooper pairs consist of spin-polarized (and therefore effectively spinless) electrons with total angular momentum of one.

- We are interested in topological phase transitions *between* different superconducting phases and not in the superconducting phase transition itself (which is described by spontaneous symmetry breaking, at least in the absence of a dynamical gauge field). Therefore we do not determine the gap Δ self-consistently (as done in BCS theory) but simply take it as a non-zero, translational invariant parameter of the theory.

- With a gauge transformation $c_i = e^{-i\theta/2} c_i'$ one can remove the superconducting phase so that w.l.o.g. $\Delta = |\Delta|$ is real. Note that because the system is one-dimensional, there cannot be vortices in the superconducting condensate (= flux tubes).

Note: In one dimension, the *Mermin-Wagner theorem* forbids the spontaneous breaking of the global $U(1)$ symmetry (electric charge conservation) that is responsible for the superconducting phase (instead you get a disordered phase known as *Luttinger liquid* with correlations that decay algebraically). Thus one should think of the superconducting

terms in $\hat{H}_{MC}$ as being induced by the proximity effect of an attached three dimensional bulk superconductor:
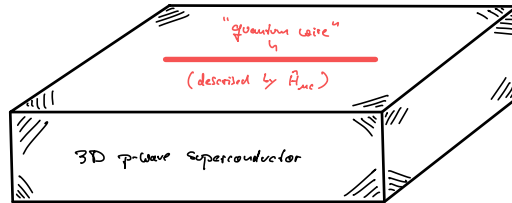
This is also (roughly) the setting used to study the Majorana chain in experiments [74], although there have been setbacks lately [75].

2. ◁ PBC → *Fourier transform:*

$$\tilde{c}_k = \frac{1}{\sqrt{L}} \sum_{n=1}^{L} e^{-ikn} c_n \quad \Leftrightarrow \quad c_n = \frac{1}{\sqrt{L}} \sum_{k \in BZ} e^{ikn} \tilde{c}_k \qquad (1.310)$$

with $k = \frac{2\pi}{L} m$ for $m = 0, \dots, L-1$.

→ (up to a constant)

$$\hat{H}_{MC} = -\sum_{k \in BZ} \left[(2w \cos k + \mu) \tilde{c}_k^\dagger \tilde{c}_k + i\Delta \sin(k) \tilde{c}_k \tilde{c}_{-k} - i\Delta \sin(k) \tilde{c}_{-k}^\dagger \tilde{c}_k^\dagger \right] \quad (1.311)$$

Note that because of the pairing terms this Hamiltonian is not yet diagonal (although there is only a single mode per unit cell and no spin involved). To diagonalize it, we can use a trick:

3. *Bogoliubov-de Gennes Hamiltonian:*

We expand the cosine term artificially (using an index substitution $k \mapsto -k$ in the sum):

$$(2w \cos k + \mu) \tilde{c}_k^\dagger \tilde{c}_k \qquad (1.312)$$

$$\mapsto \quad \frac{1}{2} [(2w \cos k + \mu) \tilde{c}_k^\dagger \tilde{c}_k + (2w \cos k + \mu) \tilde{c}_{-k}^\dagger \tilde{c}_{-k}] \qquad (1.313)$$

→

$$\hat{H}_{MC} = -\frac{1}{2} \sum_{k \in BZ} \left[\begin{array}{l} (2w \cos k + \mu) \tilde{c}_k^\dagger \tilde{c}_k + (2w \cos k + \mu) \tilde{c}_{-k}^\dagger \tilde{c}_{-k} \\ + i2\Delta \sin(k) \tilde{c}_k \tilde{c}_{-k} - i2\Delta \sin(k) \tilde{c}_{-k}^\dagger \tilde{c}_k^\dagger \end{array} \right] \qquad (1.314)$$

→ Introduce *Nambu spinors*

$$\Psi_k = \begin{pmatrix} \tilde{c}_k \\ \tilde{c}_{-k}^\dagger \end{pmatrix} \qquad (1.315)$$

Note that the degrees of freedom described by the components of the Nambu spinor are not independent but related by particle-hole symmetry. This is different from the introduction of other pseudo-spinors in the situation of multiple DOFs per unit cell (like sublattices or internal DOFs).

↑ Notes

DRAFT

and rewrite the Hamiltonian (up to a constant)

$$\hat{H}_{\mathrm{MC}} = \frac{1}{2} \sum_{k \in \mathrm{BZ}} \begin{pmatrix} \tilde{c}_k^\dagger & \tilde{c}_{-k} \end{pmatrix} \cdot \underbrace{\begin{pmatrix} -2w \cos k - \mu & -2\Delta i \sin k \\ 2\Delta i \sin k & 2w \cos k + \mu \end{pmatrix}}_{H_{\mathrm{BdG}}(k)} \cdot \begin{pmatrix} \tilde{c}_k \\ \tilde{c}_{-k}^\dagger \end{pmatrix} \tag{1.316}$$

$$= \frac{1}{2} \sum_{k \in \mathrm{BZ}} \mathbf{\Psi}_k^\dagger H_{\mathrm{BdG}}(k) \mathbf{\Psi}_k \tag{1.317}$$

with *Bogoliubov-de Gennes Hamiltonian*

$$H_{\mathrm{BdG}}(k) = -(2w \cos k + \mu)\,\sigma^z + 2\Delta \, \sin k \, \sigma^y = \vec{d}(k) \cdot \vec{\sigma} \tag{1.318}$$

and

$$\vec{d}(k) = \begin{pmatrix} 0 \\ 2\Delta \, \sin k \\ -2w \, \cos k - \mu \end{pmatrix} \tag{1.319}$$

The BdG Hamiltonian is a *redundant* matrix encoding of the MB Hamiltonian $\hat{H}_{\mathrm{MC}}$. It exists for all quadratic fermionic Hamiltonians but is non-trivial (= not diagonal), and therefore useful, only for Hamiltonians with superconducting pairing terms. As the above construction demonstrates, its existence is rooted in the algebra of the fermion operators.

4. *Bogoliubov transformation:*

$$U_k \, H_{\mathrm{BdG}}(k) \, U_k^\dagger = \begin{pmatrix} E(k) & 0 \\ 0 & -E(k) \end{pmatrix} \tag{1.320}$$

U_k: unitary rotation in Nambu space
The symmetry of the spectrum follows from PHS of the BdG Hamiltonian (➲ below).

Define new modes → *Bogoliubov quasiparticles:*

$$\tilde{\mathbf{\Psi}}_k := \begin{pmatrix} \tilde{a}_k \\ \tilde{a}_{-k}^\dagger \end{pmatrix} := U_k \mathbf{\Psi}_k = \begin{pmatrix} u_k \tilde{c}_k + v_k \tilde{c}_{-k}^\dagger \\ v_{-k}^* \tilde{c}_k + u_{-k}^* \tilde{c}_{-k}^\dagger \end{pmatrix} \tag{1.321}$$

The coefficients satisfy $|u_k|^2 + |v_k|^2 = 1$, $v_{-k} = v_k$ and $u_{-k} = -u_k$ to ensure that the new modes $\tilde{a}_k$ obey fermionic anticommutation relations. That this structure for U_k is possible is again a consequence of the PHS of the BdG Hamiltonian (➲ below). Note that this additional structure is necessary because the Bogoliubov transformation mixes particles and holes. By contrast, for the diagonalization of a non-superconducting Bloch Hamiltonian, the *unitarity* of U_k would be sufficient for the transformation to be canonical.

5. *Spectrum:*

$$E(k) = |\vec{d}(k)| = \sqrt{(2w \cos k + \mu)^2 + 4\Delta^2 \, \sin^2 k} \tag{1.322}$$

Because of the redundancy of the BdG Hamiltonian, the second band (and therefore the

↑ Notes

second eigenenergy $-|\vec{d}(k)|$ of H_{BdG}) is "fake" because

$$\hat{H}_{\text{MC}} = \frac{1}{2} \sum_{k \in \text{BZ}} \begin{pmatrix} \tilde{a}_k^\dagger & \tilde{a}_{-k} \end{pmatrix} \cdot \begin{pmatrix} +E(k) & 0 \\ 0 & -E(k) \end{pmatrix} \cdot \begin{pmatrix} \tilde{a}_k \\ \tilde{a}_{-k}^\dagger \end{pmatrix} \tag{1.323}$$

$$= \frac{1}{2} \sum_{k \in \text{BZ}} \left[E(k)\, \tilde{a}_k^\dagger \tilde{a}_k - E(k)\, \tilde{a}_{-k} \tilde{a}_{-k}^\dagger \right] \tag{1.324}$$

$$= \sum_{k \in \text{BZ}} E(k)\, \tilde{a}_k^\dagger \tilde{a}_k + \text{const} \tag{1.325}$$

where we used $E(k) = E(-k)$ and $\{\tilde{a}_k, \tilde{a}_k^\dagger\} = 1$; i.e., for every k there is only *one* mode $\tilde{a}_k$ with energy $+E(k)$.

6. *Phase diagram*: Let $\Delta \neq 0 \rightarrow E(k) = 0$ only possible for $k = 0, \pi \rightarrow$

$$E(0/\pi) = |\pm 2w + \mu| \stackrel{!}{=} 0 \quad \Rightarrow \quad 2|w| = |\mu| \tag{1.326}$$

$\rightarrow$ Two phases:

> Phase A: $2|w| > |\mu|$ and   Phase B: $2|w| < |\mu|$

7. *Ground state* $|\Omega\rangle$ with

$$\tilde{a}_k |\Omega\rangle \stackrel{!}{=} 0 \quad \forall k \in \text{BZ} \tag{1.327}$$

$\rightarrow$ Unique BCS ground state (unique in *both* phases, i.e., no symmetry breaking!)

$$|\Omega\rangle \propto \prod_{k\,:\,\tilde{a}_k|0\rangle \neq 0} \tilde{a}_k |0\rangle \tag{1.328}$$

$$\stackrel{\substack{w=\Delta \\ \mu=0}}{\propto} \prod_{k \in (-\pi,\pi)} \tilde{a}_k |0\rangle \propto \tilde{a}_0 \prod_{k \in (0,\pi)} \left(u_k + v_k \tilde{c}_k^\dagger \tilde{c}_{-k}^\dagger \right) |0\rangle \tag{1.329}$$

This ground state is called *quasi*particle vacuum ($\tilde{a}_k|\Omega\rangle = 0$) and is different from the *physical* vacuum ($\tilde{c}_k|\Omega\rangle \neq 0$), i.e., $|\Omega\rangle$ contains superpositions of states with different particle numbers of c_i-fermions (this is true as long as $\Delta \neq 0$, i.e., in the presence of a superconducting condensate).

Furthermore, notice that in phase A (for $w = \Delta$ and $\mu = 0$) $|\Omega\rangle$ has *negative* fermion parity because of the zero-mode $\tilde{a}_0$ (the other TRIM mode $\tilde{a}_\pi$ annihilates $|0\rangle$ and must not be applied). This can be shown by deriving u_k and v_k explicitly for this case.

1.5.3 Symmetries and topological indices

Our goal is now to characterize (and distinguish) the phases A and B by topological features of the BdG Hamiltonian.

1. *Time-reversal symmetry:*

a) W.l.o.g. Δ real $\to \mathcal{T} = \mathcal{K}$ TRS: $[\hat{H}_{\text{MC}}, \mathcal{T}] = 0$
More precisely: $\mathcal{T} i \mathcal{T}^{-1} = -i$ and $\mathcal{T} c_i^{(\dagger)} \mathcal{T}^{-1} = c_i^{(\dagger)}$.

$\overset{\circ}{\to}$ After a Fourier transform, TRS is represented as (acting on "Nambu space")

$$\mathbb{1}\, H_{\text{BdG}}^*(k)\, \mathbb{1} = H_{\text{BdG}}(-k) \tag{1.330}$$

$\to \tilde{T} = \mathbb{1}\mathcal{K}$: TRS with $\tilde{T}^2 = +\mathbb{1}$

Systems with a TRS that squares to $+\mathbb{1}$ are combined into the …
$\to$ Symmetry class **AI**
The label has historical/mathematical meaning but is of no importance to us.
➔ *Cartan's classification of symmetric spaces*

b) *Constraints* on the BdG vector:

$$d_x(-k) = d_x(k) \tag{1.331}$$
$$d_y(-k) = -d_y(k) \tag{1.332}$$
$$d_z(-k) = d_z(k) \tag{1.333}$$

$\to \vec{d}(k)$ on EBZ $[0, \pi]$ determines $H_{\text{BdG}}(k)$ completely

c) $\triangleleft K \in \{0, \pi\}$ TRIM $\to d_y(K) = 0$
$\to$ Image $\hat{d}$(EBZ) $(\hat{d}(k) = \vec{d}(k)/|\vec{d}(k)|)$ on S^2 must *start & end* on great circle:
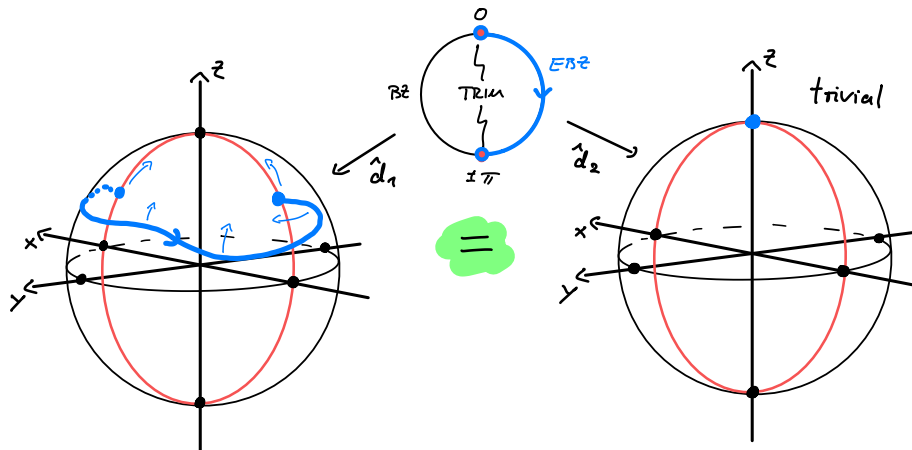
$\to$ All paths (= gapped & symmetric Hamiltonians) can be continuously contracted
$\to$ No topological phases

d) Boldly generalizing these findings, we could hypothesize:

> In 1D, systems of class **AI** do not allow for TPs.

This is true in general; ➔ next lecture on the classification of topological insulators & superconductors.

e) *Conclusion for the Majorana chain:*
TRS alone cannot make the Majorana chain topological. We need something else.

2. *Particle-hole "symmetry":*

a) The BdG Hamiltonian (matrix) has an *intrinsic* PHS:

$$\sigma^x \, H_{\text{BdG}}^*(k) \, \sigma^x = -H_{\text{BdG}}(-k) \tag{1.334}$$

In real space this would read $U H_{\text{BdG}}^* U^\dagger = -H$ where U acts as σ^x on the Nambu subspace spanned by c_i and $c_i^\dagger$. Here we had no need to explicitly define H_{BdG} in real space, though.

→ $\tilde{C} = \sigma^x \mathcal{K}$: PHS with $\tilde{C}^2 = +\mathbb{1}$

→ Symmetry class **D**

This "symmetry" is tautological in the sense that it derives solely from the fermion algebra. It does *not* correspond to a physical many body symmetry $\mathcal{C}$ of $\hat{H}_{\text{MC}}$ so that some authors do not call it a "symmetry" altogether. However, it is a valid antiunitary *pseudo*symmetry of the BdG Hamiltonian and this is all that matters for the discussion that follows. Whether the algebraic constraint Eq. (1.334) on $H_{\text{BdG}}(k)$ derives from a *physical symmetry* or from the *algebraic structure* of the fermion algebra is irrelevant for the topological classification of $H_{\text{BdG}}(k)$.

If this all seems a bit cryptic: ➔ Problemset 6

This teaches us something important: The "symmetry classes" we started to introduce (like **AI** and **D**) should be thought of as classes/ensembles of *matrices* with certain constraints. If these matrices derive from a many-body Hamiltonian (like a Bloch- oder BdG Hamiltonian), these constraints *can* descend from real symmetries of the many-body Hamiltonian. However, this is not always the case (as for the PHS of superconductors). This explains the somewhat opaque statement that **D** describes the family of superconductors *without* symmetries—where "symmetries" refers to *physical* symmetries of the many-body Hamiltonian.

Note that the proper concept of "particle-hole symmetry" has not yet been fully settled in the community [76], partially due to the tautological nature of the PHS above (which is then refered to as *charge conjugation* instead of *particle-hole transformation*).

b) *Constraints* on the BdG vector:

$$d_x(-k) = -d_x(k) \tag{1.335}$$
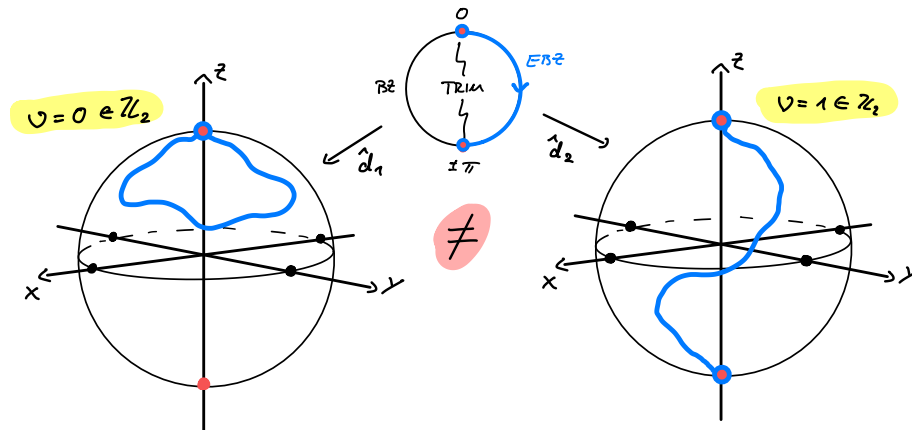$$d_y(-k) = -d_y(k) \tag{1.336}$$
$$d_z(-k) = d_z(k) \tag{1.337}$$

→ Again $\vec{d}(k)$ on EBZ $[0, \pi]$ determines $H_{\text{BdG}}(k)$ completely

c) ⊲ $K \in \{0, \pi\}$ TRIM → $d_x(K) = 0 = d_y(K)$
Note that these are now *two* constraints as compared to TRS!
→ Image $\hat{d}(\text{EBZ})$ on S^2 must *start & end* either on north or south pole:

→ Two topologicall distinct classes of paths
(Only one of which can be continuously contracted to a point.)
→ One topological phase possible → $\mathbb{Z}_2$-index

Note that the orientation of the Bloch sphere (and therefore the position of the poles) has no physical meaning as it can be changed continuously by SU(2) rotations in Nambu space (as we did for the Bogoliubov transformation). Consequently, a path attached to the *south* pole is unitarily equivalent to the shown path attached to the north pole.

d) Boldly generalizing these findings, we could hypothesize:

In 1D, systems of class **D** allow for a single TP labeled by a $\mathbb{Z}_2$-index.

Again, this is true in general; ➲ next lecture on the classification of topological insulators & superconductors.

e) *Conclusion for the Majorana chain:*

The $\mathbb{Z}_2$-index classifies the phase for $2|w| < |\mu|$ as *trivial* and $2|w| > |\mu|$ as *topological*:

$$d = \begin{bmatrix} 0 \\ 2\omega \sin k \\ -(2\omega \cos k + \mu) \end{bmatrix}$$

→
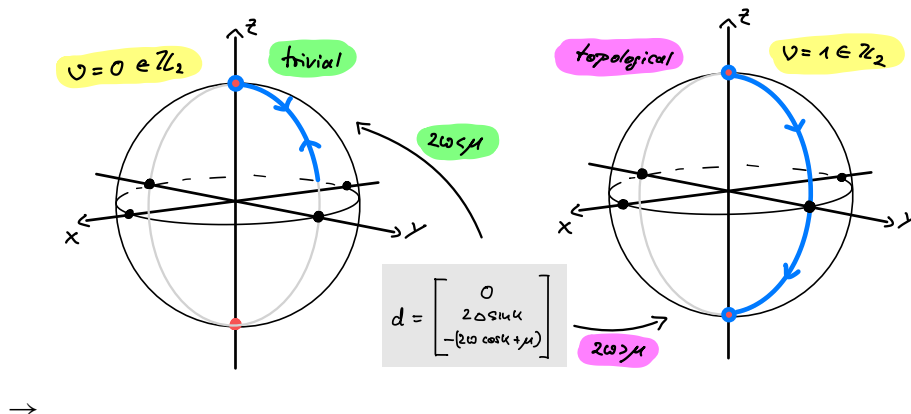
Phase A: $2|w| > |\mu|$ → topological   (1.338)
Phase B: $2|w| < |\mu|$ → trivial

In his original paper [72], Kitaev classified the two phases very differently (using the Pfaffian to distinguish two classes of quadratic fermion Hamiltonians). The classification

presented here, based on the BdG Hamiltonian, is conceptually very different. However, it can be shown [77] that the two approaches lead to the same notion of trivial and topological phases.

We could be satisfied at this point, but there is actually more to be learned if we *combine* both PHS and TRS:

3. *PHS & TRS:*

   a) As argued above, PHS is intrinsic to the form of the BdG Hamiltonian (it cannot be broken). Furthermore, for an open chain we can always find a TRS representation by gauging away complex phases. Hence it is reasonable to consider the situation where both symmetries are preserved.

     $\rightarrow$ TRS with $\tilde{T}^2 = +\mathbb{1}$ and PHS with $\tilde{C}^2 = +\mathbb{1}$

     $\rightarrow$ Symmetry class **BDI**

   b) *Constraint* on the BdG vector:

$$d_x(-k) = 0 \tag{1.339}$$
$$d_y(-k) = -d_y(k) \tag{1.340}$$
$$d_z(-k) = d_z(k) \tag{1.341}$$

     $\rightarrow$ Again $\vec{d}(k)$ on EBZ $[0, \pi]$ determines $H_{\text{BdG}}(k)$ completely

   c) Image $\hat{d}$(EBZ) on S^2 is constrained to the great circle with $d_x = 0$ *and* must *start & end* either on north or south pole:

     $\rightarrow$ Infinitely many topologically distinct classes of paths (distinguished by their winding number)
     $\rightarrow$ Infinitely many topological phases possible $\rightarrow$ $\mathbb{Z}$-index
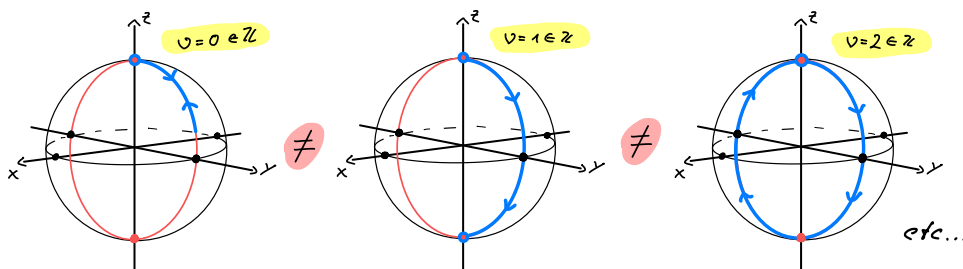
   d) Boldly generalizing these findings, we could hypothesize:

> In 1D, systems of class **BDI** allow for many TPs labeled by a $\mathbb{Z}$-index.

Again, this is true in general; $\circlearrowright$ next lecture on the classification of topological insulators & superconductors.

   e) *Conclusion for the Majorana chain:*
Although TRS is not useful on its own, in combination with PHS it boosts the $\mathbb{Z}_2$-index of **D** to a $\mathbb{Z}$-index of **BDI**. For a single Majorana chain, this has the only benefit that we can user either the topological index of **D** or the winding number of **BDI** to characterize the topological phase; in this situation, they are equivalent. This is different if one considers *stacks* of multiple parallel Majorana chains, though,

where one can create infinitely many different SPT phases when TRS is present (**BDI**) but only one if it is broken (**D**).

f) *Final note:* For the SP Hamiltonian having PHS *and* TRS means:

$$\text{PHS:} \quad U_C H^* U_C^\dagger = -H \tag{1.342}$$

$$\text{TRS:} \quad U_T H^* U_T^\dagger = +H \tag{1.343}$$

$\rightarrow$

$$U_S H U_S^\dagger = -H \quad \text{with} \quad U_S = U_T U_C^* \tag{1.344}$$

$\rightarrow$ Sublattice symmetry (SLS)

This is true in general and will be important in the next lecture.

1.5.4 Majorana fermions

Why do we call the Majorana chain "Majorana chain"? To answer this, we need a bit of algebra:

1. $\vartriangleleft$ Set of fermion operators $\{c_i\}$ and define *Majorana operators*

$$\boxed{\gamma_{2i-1} = c_i + c_i^\dagger \quad \text{and} \quad \gamma_{2i} = i(c_i^\dagger - c_i)} \tag{1.345}$$

I.e., there are *two* Majorana operators per fermion mode.

2. $\overset{\circ}{\rightarrow}$ *Properties:*

$$\boxed{\gamma_n^\dagger = \gamma_n \quad \text{and} \quad \{\gamma_n, \gamma_m\} = 2\delta_{nm}} \tag{1.346}$$

$\rightarrow$ Up to a normalization, Majorana fermions behave like *self-adjoint* or *real* fermions. The name originates from a similar concept in high-energy physics due to Ettore Majorana (namely, real-valued solutions of the Dirac equation in Majorana representation); in condensed matter physics, however, the properties Eq. (1.346) should be seen as the defining relations of *Majorana operators*. While the γ_n describe "real" (Majorana) fermions, the c_i describe "complex" (Dirac) fermions. Eq. (1.345) demonstrates that the two Majoranas γ_{2i-1} and γ_{2i} can be thought of as the "real" and "imaginary part" of the complex fermion c_i. We stress that Majorana fermions are *not* anyons, they are fermionic quasiparticles (as the name clearly states); only *Majorana zero modes* can make their hosts (like vortices in 2D $p_x + i p_y$-superconductors) behave like anyons.

3. Pairs of Majoranas can be recombined to form a complex fermion:

$$\boxed{c_i = \frac{\gamma_{2i-1} + i\gamma_{2i}}{2} \quad \text{and} \quad c_i^\dagger = \frac{\gamma_{2i-1} - i\gamma_{2i}}{2}} \tag{1.347}$$

Observation: We do not have to combine the original pairs of Majoranas. Actually it is possible to combine just *any* pair of Majoranas to form a new fermion mode ($\Rightarrow$ below).

4. Using Eq. (1.347) we rewrite the Majorana chain Hamiltonian in terms of Majorana operators:
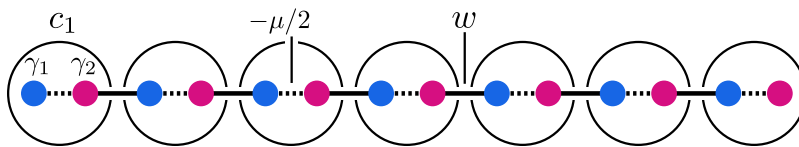
$$\hat{H}_{\mathrm{MC}} \doteq \frac{i}{2} \sum_{i=1}^{L'} \left[(\Delta + w)\, \gamma_{2i}\gamma_{2i+1} + (\Delta - w)\, \gamma_{2i-1}\gamma_{2i+2} \right] \qquad (1.348)$$

$$-\frac{i}{2} \sum_{i=1}^{L} \mu\, \gamma_{2i-1}\gamma_{2i}$$

Note that the factors of i are needed for Hermiticity.

5. To simplify $\hat{H}_{\mathrm{MC}}$ let $\Delta = w \rightarrow$

$$\hat{H}_{\mathrm{MC}} = -\frac{\mu}{2} \sum_{i=1}^{L} (i\,\gamma_{2i-1}\gamma_{2i}) + w \sum_{i=1}^{L'} (i\,\gamma_{2i}\gamma_{2i+1}) \qquad (1.349)$$

$\rightarrow$ SSH-like dimerization:

6. *Comparison to the SSH chain:*
   The connection to the SSH chain is more than superficial. If one identifies $-\mu/2 \leftrightarrow t$ and $w \leftrightarrow w$ (where t and w are the alternating hopping amplitudes of the SSH chain), then the gapless points coincide: $|\mu| = 2|w|$ for the Majorana chain and $|t| = |w|$ for the SSH chain.

   One can consider a hybrid model of Majorana and SSH chain and study their competing phases on the same footing [78]. This approach is also didactically valuable as it contrasts the different symmetries of the two models quite nicely.

1.5.5 Edge modes

Like for the SSH chain, it is most instructive to focus on the fixed points of the two phases with zero correlation length:

1. *Trivial phase (Phase B):* Let $w = \Delta = 0$ and $\mu > 0 \rightarrow$

$$\hat{H}_{\mathrm{MC}} = -\frac{\mu}{2} \sum_{i=1}^{L} (i\,\gamma_{2i-1}\gamma_{2i}) \doteq -\mu \sum_{i=1}^{L} \left(c_i^\dagger c_i - \frac{1}{2} \right). \qquad (1.350)$$

   $\rightarrow$ Pairing of Majorana modes *on* each site
   $\rightarrow$ *Unique* ground state (with all physical fermion modes c_i filled)

2. *Topological phase (Phase A):* Let $w = \Delta > 0$ and $\mu = 0 \rightarrow$

$$\hat{H}_{\mathrm{MC}} = w \sum_{i=1}^{L'} (i\,\gamma_{2i}\gamma_{2i+1}) \overset{\mathrm{OBC}}{=} w \sum_{i=1}^{L-1} (i\,\gamma_{2i}\gamma_{2i+1}) \qquad (1.351)$$

   $\rightarrow$ Pairing of Majorana modes *between* adjacent sites
   $\rightarrow$ *Unique* ground state for PBC but *2-fold degenerate* ground space for OBC

↑ Notes

a) Define new fermion modes ($i = 1, \ldots, L - 1$):

$$a_i := \frac{1}{2}(\gamma_{2i} + i\gamma_{2i+1}) \qquad \text{and} \qquad a_i^\dagger = \frac{1}{2}(\gamma_{2i} - i\gamma_{2i+1}) \tag{1.352}$$

Check that these are indeed fermions: $\{a_i, a_j^\dagger\} = \delta_{ij}$.

$\overset{\circ}{\to}$

$$\hat{H}_{\text{MC}} = 2w \sum_{i=1}^{L-1} \left(a_i^\dagger a_i - \frac{1}{2}\right) \tag{1.353}$$

b) There is one fermion mode missing:
Note that γ_1 and γ_{2L} do not show up in Eq. (1.351), so we can use them to construct a new fermion mode:

$$e := \frac{1}{2}(\gamma_{2L} + i\gamma_1) \qquad \text{and} \qquad e^\dagger = \frac{1}{2}(\gamma_{2L} - i\gamma_1) \tag{1.354}$$

→ *One* fermionic *edge* mode

Indeed, e describes a single fermion *delocalized* between the two endpoints of the chain:

$$e \overset{\circ}{=} \frac{i}{2}\left(c_L^\dagger - c_L + c_1^\dagger + c_1\right) \tag{1.355}$$

c) Ground states for OBC:

$$|\Omega_n\rangle \;\; \text{GS of } \hat{H}_{\text{MC}} \quad \Leftrightarrow \quad a_i|\Omega_n\rangle \overset{!}{=} 0 \quad \forall\, i = 1 \ldots L - 1 \tag{1.356}$$

$[\hat{H}_{\text{MC}}, e] = 0 \to$ *Two* ground states:

$$e^\dagger e\,|\Omega_0\rangle = 0\,|\Omega_0\rangle \quad \text{and} \quad e^\dagger e\,|\Omega_1\rangle = 1\,|\Omega_1\rangle \tag{1.357}$$

with $|\Omega_1\rangle = e^\dagger|\Omega_0\rangle$

d) *Comparison to the SSH chain:*
Remember that the SSH chain also has edge modes. However, these are *fermionic*, i.e., the SSH chain in the topological phase has one independent (complex) fermion on *each edge*. Consequently, the ground state degeneracy for an open chain is *four-fold*. By contrast, the Majorana chain as a *Majorana* fermion per edge (and a Majorana fermion can be thought of as "half" a fermion because it is the real/imaginary part of a complex fermion). Both edges *combined* form a single (complex) fermion so that the ground state degeneracy is only *two-fold*.

e) As for the SSH chain, the two-fold degeneracy survives beyond the fixed point for $\mu = 0$ as long as $|\mu| < 2|w|$ (up to finite-size effects). However, at the fixed point, the two states $|\Omega_0\rangle$ and $|\Omega_1\rangle$ have a particularly simple description that makes their condensate nature clear and also explains the robustness of their degeneracy (➲ [66] for details):

$$|\Omega_0\rangle \propto \sum_{n:\,|n|\,\text{odd}} |n\rangle \quad \text{and} \quad |\Omega_1\rangle \propto \sum_{n:\,|n|\,\text{even}} |n\rangle \tag{1.358}$$

with

$$|n\rangle \equiv (c_1^\dagger)^{n_1}(c_2^\dagger)^{n_2} \ldots (c_L^\dagger)^{n_L} |0\rangle \tag{1.359}$$

and $|n|$ the number of fermions in configuration n.

↑ Notes

- The ground states are the equal-weight superposition of all possible fermion configurations with a fixed parity, in particular, of fermion configurations with different particle number. This is the man-body manifestation of the superconducting condensate (note that $\langle c_i c_{i+1} \rangle \neq 0$ for $|\Omega_n\rangle$).

- Locally, the states $|\Omega_0\rangle$ and $|\Omega_1\rangle$ "look" the same. They can only be distinguished by a *global* measurement of the total fermion parity. So to lift the degeneracy, one has to add the term $e^\dagger e$ to the Hamiltonian $\hat{H}_{\mathrm{MC}}$. But for an open chain, this operator is highly non local (as can be seen from Eq. (1.355)).

- There is actually another way to lift the degeneracy. Note that $\gamma_1 e = -e^\dagger \gamma_1$ so that $|\Omega_1\rangle = \gamma_1 |\Omega_0\rangle$, i.e., $\langle \Omega_1 | \gamma_1 | \Omega_0 \rangle \neq 0$ so that the Hamiltonian $\hat{H}_{\mathrm{MC}} + \gamma_1$ lifts the degeneracy (recall that $\gamma_1^\dagger = \gamma_1$). Note that in contrast to $e^\dagger e$, γ_1 is localized on the left endpoint of the chain. However, γ_1 violates fermion parity and it is believed that in nature only Hamiltonians that commute with the parity operator are realizable (this is known as *parity superselection*), so this modification is mathematically legitimate but physically impossible (➡ Comment below).

f) *Sidenote:*

The above arguments have shown that the degeneracy of $|\Omega_0\rangle$ and $|\Omega_1\rangle$ is actually very robust and does not rely on any symmetry (note that this does not contradict the topological classification of $\hat{H}_{\mathrm{MC}}$ as part of symmetry class **D** because of the discussed tautological nature of the PHS). Consequently, the topological phase of the Majorana chain is *not* an SPT phase but a topologically ordered phase [38]. This is in stark contrast to the SSH chain which *is* an SPT phase protected by sublattice symmetry. (Remember that we had no

trouble connecting the two phases of the SSH chain with a chemical potential that breaks SLS; you cannot do the same thing with the Majorana chain.)

However, the statement that the Majorana chain does not require any symmetry is subtle. To see this, one can check that the Majorana edge modes $\gamma_l = \gamma_1$ and $\gamma_r = \gamma_{2L}$ act on the ground states as follows:

$$\gamma_l |\Omega_0\rangle = |\Omega_1\rangle \qquad \text{and} \qquad \gamma_r |\Omega_0\rangle = -i\,|\Omega_1\rangle. \qquad (1.360)$$

Since these operators are Hermitian and can be constructed from local fermion modes, we could add them to the Hamiltonian as a perturbation, e.g., $\tilde{H}_{\mathrm{MC}} = \hat{H}_{\mathrm{MC}} + \gamma_l$. This perturbation lifts the degeneracy such that the ground state of $\tilde{H}_{\mathrm{MC}}$ is unique, namely $|\Omega_1\rangle - |\Omega_0\rangle$. This is not surprising as γ_l *violates* the fermion parity symmetry $\mathbb{Z}_2^f = \{\mathbb{1}, \mathcal{P}\}$. So the Majorana chain *is* protected by a symmetry after all: fermion parity. In the literature, however, this symmetry is often not counted as a real symmetry but as an implicit feature of fermionic Hamiltonians (for instance, quadratic Hamiltonians automatically commute with $\mathcal{P}$). This makes sense for the following reason:

Assume that the Hermitian (and unitary) operators γ_l and γ_r were admissible observables of the theory. Make the length L of the chain large and assume that Alice can measure $\gamma_l = c_1 + c_1^\dagger$ on the left endpoint while Bob can apply the unitary gate $\gamma_r = i(c_L^\dagger - c_L)$ on the right endpoint. Define the basis $|x\rangle \equiv |\Omega_1\rangle + (-1)^x |\Omega_0\rangle$ and let the system be initialized in the symmetric state

$|x = 0\rangle$ so that Alice measures $+1$ with certainty. Now Bob can send Alice a classical bit $x \in \mathbb{Z}_2$ of information by flipping or not flipping this state with γ_r:

$$(\gamma_r)^x \, |0\rangle \propto \begin{cases} |0\rangle & \text{for} \quad x = 0 \\ |1\rangle & \text{for} \quad x = 1 \,. \end{cases} \tag{1.361}$$

This clearly violates causality since the bit x can be transmitted instantaneously over arbitrary distances L; this is really a "spooky action at a distance" and should not be possible with *local* measurements and operations. Therefore γ_l and γ_r are actually *non-local* operators, despite their local appearance in terms of fermion modes! The reason is that fermions are intrinsically non-local objects due to their statistics, and this non-locality becomes relevant for operators that violate fermion parity. The upshot is that the parity symmetry required for the Majorana chain (or any other fermion Hamiltonian) is a logical consequence of *locality*—and not an additional symmetry constraint.

Final note:

Here we focused on the "condensed-matter side" of the Majorana chain. However, the topological robustness of the ground state degeneracy suggests the use of this system for quantum information processing. In particular:

- The degenerate ground state space can be used to encode a qubit that is, in principle, decoupled from the environment. This make the Majorana chain a possible candidate for a *topological quantum memory* [79].

- If one extends the Majorana chain into networks of interconnected wires, the Majorana zero modes at the endpoints behave as "particles" with non-abelian statistics [80]. This establishes "Majorana wire networks" as possible building blocks of a *topological quantum computer* [81].

1.6 Classification of non-interacting fermionic topological phases

> **† Note**
>
> A good introduction to the classification of topological insulators and superconductors is given by Ludwig [37] (this lecture is partly based on his paper). A more technical description of the scheme with examples is given by Ryu et.al. [63] (their detailed introduction is quite useful). A completely different angle on the classification is provided by Kitaev [12] (this paper looks "simple" as it is extremely high-level but the underlying mathematical framework is very deep).

Goal: By now we have seen various models of non-interacting fermions in one and two dimensions that are classified by different topological indices and protected by different symmetries. Since all of these models are described by band structures, the question arises whether one can find a unifying approach to classify the topological phases of non-interacting fermions. The description of such an approach is the goal of this lecture.

1.6.1 Generic symmetries and the tenfold way

1. *Goal:* Classify TPs of non-interacting fermions

   Approach: Use SP Hamiltonian H to describe & classify MB Hamiltonian $\hat{H}$
   (H can either be a "standard" SP Hamiltonian or a Bogoliubov-de Gennes Hamiltonian if superconductivity is present.)

   $\rightarrow$ We are interested in constraints on the matrix H that arise from symmetries of $\hat{H}$.

2. *Which symmetries of $\hat{H}$ to use?*

   Remember: $\mathcal{X}$ symmetry of $\hat{H}$:$\Leftrightarrow [\mathcal{X}, \hat{H}] = 0$

   Wigner's theorem $\rightarrow \mathcal{X}$ unitary or antiunitary

   $\rightarrow$ Four possibilities on Fock space:

$$
\begin{array}{rll}
\textbf{Unitary:} & \mathcal{U}i\,\mathcal{U}^{-1} = +i\,, & \mathcal{U}c_i\,\mathcal{U}^{-1} = U_{ij}c_j \qquad (1.362a) \\
\text{(unitary MB sym.)} & \left[\mathcal{U}, \hat{H}\right] = 0 \quad \Leftrightarrow & [U, H] = 0 \quad \text{(unitary SP sym.)} \\[4pt]
\textbf{TRS:} & \mathcal{T}i\,\mathcal{T}^{-1} = -i\,, & \mathcal{T}c_i\,\mathcal{T}^{-1} = U_{ij}c_j \qquad (1.362b) \\
\text{(antiunitary MB sym.)} & \left[\mathcal{T}, \hat{H}\right] = 0 \quad \Leftrightarrow & [U\mathcal{K}, H] = 0 \quad \text{(antiunitary SP sym.)} \\[4pt]
\textbf{PHS:} & \mathcal{C}i\,\mathcal{C}^{-1} = +i\,, & \mathcal{C}c_i\,\mathcal{C}^{-1} = U_{ij}c_j^{\dagger} \qquad (1.362c) \\
\text{(unitary MB sym.)} & \left[\mathcal{C}, \hat{H}\right] = 0 \quad \Leftrightarrow & \{U\mathcal{K}, H\} = 0 \quad \text{(antiunitary SP pseudosym.)} \\[4pt]
\textbf{SLS:} & \mathcal{S}i\,\mathcal{S}^{-1} = -i\,, & \mathcal{S}c_i\,\mathcal{S}^{-1} = U_{ij}c_j^{\dagger} \qquad (1.362d) \\
\text{(antiunitary MB sym.)} & \left[\mathcal{S}, \hat{H}\right] = 0 \quad \Leftrightarrow & \{U, H\} = 0 \quad \text{(unitary SP pseudosym.)}
\end{array}
$$

   Note that the unitary *mixing* of particles ($c_i^{\dagger}$) and holes (c_i) is not necessarily canonical, i.e., does not preserve the fermionic anticommutation relations in general (remember the Bogoliubov transformation).

Using *unitary* symmetries of $\hat{H}$ (H) is possible but not universal!
(In the sense that the classification would be "infinite" because there are infinitely many unitarily realized symmetries and the classification depends on the specific symmetry (representation); see also the extended note below.)

$\rightarrow \lhd$ TRS, PHS and SLS ...

This is a conceptually important but subtle point: The decision to "factor out" all unitary symmetries is not so much physically motivated but more a decision based on systematics. One *can* classify fermionic SPTs with unitary symmetries but this is a question that cannot really be conclusively answered because there are infinitely many possible symmetry groups. Thus the most systematic approach asks whether there is anything below that sprawling complexity that is simpler and more systematic. After all, one should first understand these basics before plunging into the never ending story that lies beyond. To put this into context: There *are* classifications for certain unitary symmetry groups for free fermions [82–85] (but only "certain" not "all"). Also for *bosonic* SPTs one considers unitary symmetries [8]. So there is nothing inherently "bad" about them. The difference becomes clear when one compares the classification table below (the "periodic table") with similar tables for bosonic SPTs [8]: The latter always have an exemplary character in that one must hope that the unitary symmetry one is interested in is listed; these lists are not exhaustive (they cannot be). However, once one throws all unitary symmetries away, what is left is, quite unexpectedly, (1) *non-trivial* and (2) *finite* so that the classification introduced in the following *is* exhaustive (although in a more restricted sense).

...and only SP Hamiltonians *without* unitary symmetries:

$$H \text{ irreducible} \quad :\Leftrightarrow \quad \left([U, H] = 0 \;\Rightarrow\; U = e^{i\lambda}\mathbb{1} \right) \tag{1.363}$$

Hamiltonians without unitary symmetries can be understood as the "atomic building blocks" of all Hamiltonians. To see this, consider an arbitrary Hamiltonian H with symmetry group G_0 that is unitarily realized on the SP Hilbert space $\mathcal{H}$. As always, we can decompose the Hilbert space into irreducible representations λ of G_0 (with possible multiplicities):

$$\mathcal{H} = \bigoplus_{\lambda} \mathcal{H}_\lambda \tag{1.364}$$

Each subspace $\mathcal{H}_\lambda$ is composed of equivalent copies of the same irrep λ ("equivalent" in the sense of "isomorphic"):

$$\mathcal{H}_\lambda = \bigoplus_{\alpha=1}^{m_\lambda} \mathcal{H}_\lambda^{(\alpha)} \simeq \tilde{\mathcal{H}}_\lambda \otimes \mathcal{V}_\lambda \tag{1.365}$$

where $\mathcal{H}_\lambda^{(\alpha)} \simeq \mathcal{V}_\lambda$ for all α with the irrep $\mathcal{V}_\lambda$ and $\tilde{\mathcal{H}}_\lambda = \mathbb{C}^{m_\lambda}$. It is $d_\lambda = \dim \mathcal{V}_\lambda$ the dimension of the irrep λ and m_λ the multiplicity of the irrep λ in $\mathcal{H}$. The $\mathcal{H}_\lambda$ are known as G_0-*isotypic components* of $\mathcal{H}$ [86].

Since $[H, U_g] = 0$ for all $g \in G_0$ (with unitary representation U_g) and $\mathcal{V}_\lambda$ is irreducible, it is

$$H = \bigoplus_{\lambda} H_\lambda \otimes \mathbb{1}_{d_\lambda} \quad \text{and} \quad U_g = \bigoplus_{\lambda} \mathbb{1}_{m_\lambda} \otimes U_g^{(\lambda)}. \tag{1.366}$$

↑ Notes

The Hamiltonian blocks H_λ act on $\tilde{\mathcal{H}}_\lambda$ and have no longer any unitary symmetry left, they are the "irreducible building blocks" of all Hamiltonians, just as the $U_g^{(\lambda)}$ are the irreducible building blocks of all representations of the symmetry group G_0. It is these irreducible Hamiltonians that we will focus on below.

3. For a given irreducible SP Hamiltonian H check (henceforth we forget about $\hat{H}$):

$$\exists\, U_T \;?\; : \; [U_T \mathcal{K}, H] = 0 \quad \text{and if so:} \quad U_T U_T^* \overset{?}{=} \pm\mathbb{1} \tag{1.367a}$$

$$\exists\, U_C \;?\; : \; \{U_C \mathcal{K}, H\} = 0 \quad \text{and if so:} \quad U_C U_C^* \overset{?}{=} \pm\mathbb{1} \tag{1.367b}$$

$$\exists\, U_S \;?\; : \quad \{U_S, H\} = 0 \tag{1.367c}$$

$\rightarrow$ Define:

$$\text{TRS:} \quad T = U_T \mathcal{K} \quad \text{(antiunitary symmetry)} \tag{1.368a}$$

$$\text{PHS:} \quad C = U_C \mathcal{K} \quad \text{(antiunitary pseudosymmetry)} \tag{1.368b}$$

$$\text{SLS:} \quad S = U_S \quad \text{(unitary pseudosymmetry)} \tag{1.368c}$$

Note: Here we switch from the notation $T_U = U \mathcal{K}$ to $T \equiv T_{U_T} = U_T \mathcal{K}$ (similarly for $C = C_U$ and $S = S_U$) because we will mix T, C and S below and then it is important to distinguish the unitaries U_T, U_C and U_S.

$\rightarrow$ *Labeling scheme:*

$$
\begin{aligned}
&&[T, H] \neq 0 &\;\Rightarrow\; & T &= 0 & \tag{1.369a}\\
[T, H] = 0 \;\; \text{with} \quad T^2 &= +\mathbb{1} &\;\Rightarrow\; & T &= +1 & \tag{1.369b}\\
[T, H] = 0 \;\; \text{with} \quad T^2 &= -\mathbb{1} &\;\Rightarrow\; & T &= -1 & \tag{1.369c}\\[6pt]
&&\{C, H\} \neq 0 &\;\Rightarrow\; & C &= 0 & \tag{1.369d}\\
\{C, H\} = 0 \;\; \text{with} \quad C^2 &= +\mathbb{1} &\;\Rightarrow\; & C &= +1 & \tag{1.369e}\\
\{C, H\} = 0 \;\; \text{with} \quad C^2 &= -\mathbb{1} &\;\Rightarrow\; & C &= -1 & \tag{1.369f}\\[6pt]
&&\{S, H\} \neq 0 &\;\Rightarrow\; & S &= 0 & \tag{1.369g}\\
&&\{S, H\} = 0 &\;\Rightarrow\; & S &= 1 & \tag{1.369h}
\end{aligned}
$$

Note that this is an abuse of notation: In the left column, $T/C/S$ denote the *operators* of Eq. (1.368) whereas in the right column they are simply *variables* used to label the situation on the left. From the context it is always clear which use is intended.

$\rightarrow$ Triple (T, C, S) encodes answers to classification in Eq. (1.367)

Note: These constraints on the SP level can also be constructed quite systematically without deriving them from MB symmetries:

Imagine you are given a gapped SP Hamiltonian (= Hermitian matrix) H and a unitary U and your job is to formulate a linear/antilinear constraint on H using only U and complex conjugation. The constraint can be written in the form

$$f(H, U) \overset{!}{=} H\,. \tag{1.370}$$

We want f to be linear/antilinear in H and its result must be Hermitian because H is; hence it should be $f(H, U) = \alpha U H^{(*)} U^\dagger$ with $\alpha \in \mathbb{R}$. Now note that $\det(H) = \det(\alpha U H^{(*)} U^\dagger) = \alpha^N \det(H)$; since H is gapped we can w.l.o.g. shift the Fermi energy (= zero energy) into the gap so that $\det(H) \neq 0$ and we have $\alpha^N = 1$.

In general, this leaves only four possibilities:

$$f(H, U) = \begin{cases} +1 \cdot U H U^\dagger & \text{(unitary symmetry)} \\ -1 \cdot U H U^\dagger & \text{(unitary pseudosymmetry} \rightarrow \text{SLS)} \\ +1 \cdot U H^* U^\dagger & \text{(antiunitary symmetry} \rightarrow \text{TRS)} \\ -1 \cdot U H^* U^\dagger & \text{(antiunitary pseudosymmetry} \rightarrow \text{PHS)} \end{cases} \tag{1.371}$$

Since for an irreducible Hamiltonian (by construction) there is no unitary symmetry (except the trivial one), we are left with the latter three constraints that are nothing but the three symmetries (on the MB level) we have discussed before.

4. *Important:* For a given irreducible Hamiltonian, TRS T_U, PHS C_U and SLS S_U are *unique* (if present)

Assume T_{U_1} and T_{U_2} were two *different* time-reversal symmetries:

$$[T_{U_1}, H] = 0 \quad \text{and} \quad [T_{U_2}, H] = 0 \tag{1.372}$$

Then $\tilde{U} := T_{U_1} T_{U_2} = U_1 U_2^*$ is a *unitary* symmetry of H:

$$[\tilde{U}, H] = 0 \quad \xRightarrow{H \text{ irreducible}} \quad \tilde{U} = e^{i\lambda} \mathbb{1} \tag{1.373}$$

and therefore $T_{U_1} = U_1 \mathcal{K} = e^{i\lambda} U_2^{*\dagger} \mathcal{K} \propto T_{U_2}^{-1}$

So we can replace T_{U_1} by T_{U_2} or vice versa.

The same argument applies to PHS and similarly to SLS.

5. *Sublattice symmetry:* As already mentioned in the last lecture:

$$S = T \circ C = U_T U_C^* \quad \textit{unitary} \text{ operator} \tag{1.374}$$

$$\text{w.l.o.g.} \quad S^2 = +\mathbb{1} \tag{1.375}$$

One the many-body level: $\mathcal{S} = \mathcal{T} \circ \mathcal{C}$.

In particular:

$$\boxed{\begin{array}{ll} \text{TRS: } [T, H] = 0 \\ \text{PHS: } \{C, H\} = 0 \end{array} \left.\begin{array}{c} \Rightarrow \\ \nRightarrow \end{array}\right\} \{S, H\} = 0} \tag{1.376}$$

$\rightarrow$ C *cannot* be eliminated in favour of T since S is not a unitary *symmetry* (but a *pseudo*symmetry)

I.e., by "factoring out" all unitary symmetries of the SP Hamiltonian H, there can still be a *unitary* PHS symmetry $\mathcal{C}$ of the MB Hamiltonian $\hat{H}$ left because (1) C is *anti*unitary on the SP level and (2) $\mathcal{S} = \mathcal{T} \circ \mathcal{C}$ is a *pseudo*symmetry on the SP level.

$\rightarrow$ Keep T, C, and S

↑ Notes

6. *The "tenfold way":*

Important consequence of Eq. (1.376):

$(T \neq 0 \lor C \neq 0) \Rightarrow S = |TC|$ but if $T = 0 = C$ it can be either $S = 0$ or $S = 1$

This is easy to understand: If T and/or C are present, the relation $S = T \circ C$ determines the absence/presence of S automatically. Only if both T *and* C are *absent*, the absence/presence of S is not determined. (Note that $\mathcal{T} \circ \mathcal{C}$ can be a symmetry even if $\mathcal{T}$ and $\mathcal{C}$ are not symmetries separately!)

$\rightarrow 3 \times 3 + 1 = 10$ symmetry classes:

Class	T	C	S
A	0	0	0
AIII	0	0	1
AI	+1	0	0
BDI	+1	+1	1
D	0	+1	0
DIII	−1	+1	1
AII	−1	0	0
CII	−1	−1	1
C	0	−1	0
CI	+1	−1	1

Remember: We encountered the classes **AI**, **D** and **BDI** before; the Kane-Mele model belonged to **AII** and the Chern insulator to **A**.

As mentioned before, the names of the classes go back to the mathematician ÉLIE CARTAN who assigned them to so called *(large) symmetric spaces (of compact type)*; in the present context the labels are typically taken "as is" without assigning any deeper meaning to them. The order in the above table seems arbitrary but is actually not—this will become clear later.

1.6.2 The periodic table of topological insulators and superconductors

1. ◁ Gapped Hamiltonians H of class **X** in dimension d

Question: How to label the topological phases that can be realized by these systems?

Note that a *specific* system H in **X** may have *additional* symmetries (both unitary and antiunitary). However, the classification below does not rely on these symmetries so that they can be broken by perturbations without leaving the phase.

↑ Notes

2. *Answer:* Periodic table of topological insulators & superconductors [11, 12, 63]:

	Class	T	C	S	0D	1D	2D	3D	...	8D	...
Complex (w/o T&C)	A	0	0	0	$\mathbb{Z}$	0	$\mathbb{Z}$	0	*2-periodic* →	$\mathbb{Z}$	...
	AIII	0	0	1	0	$\mathbb{Z}$	0	$\mathbb{Z}$	complex K-groups	0	...
Real (w/ T or C)	AI	+1	0	0	$\mathbb{Z}$	0	0	0		$\mathbb{Z}$	...
	BDI	+1	+1	1	$\mathbb{Z}_2$	$\mathbb{Z}$	0	0		$\mathbb{Z}_2$	...
	D	0	+1	0	$\mathbb{Z}_2$	$\mathbb{Z}_2$	$\mathbb{Z}$	0	*"Bott periodicity"*	$\mathbb{Z}_2$	...
	DIII	−1	+1	1	0	$\mathbb{Z}_2$	$\mathbb{Z}_2$	$\mathbb{Z}$	real K-groups	0	...
	AII	−1	0	0	$2\mathbb{Z}$	0	$\mathbb{Z}_2$	$\mathbb{Z}_2$		$2\mathbb{Z}$	...
	CII	−1	−1	1	0	$2\mathbb{Z}$	0	$\mathbb{Z}_2$	*8-periodic* →	0	...
	C	0	−1	0	0	0	$2\mathbb{Z}$	0		0	...
	CI	+1	−1	1	0	0	0	$2\mathbb{Z}$		0	...

This course:

Remember, remember...

- Chern number
  - IQHE
  - QWZ
  - Haldane

- Pfaffian Index
  - Kane–Mele model

- No Kramers pairs? (Kane–Mele model)

- Winding number
  - SSH-chain

- All paths contractible? (Majorana chain)

- Endpoints = Poles
  - Majorana chain

- Winding number
  - Majorana chain

The classification is referred to as "periodic table" because of its periodic structure for $d = 0, 1, \ldots$ where the period for the "complex" classes is 2 and for the "real" classes 8.

→ In every dimension, 5 out of 10 symmetry classes support TPs

There are several equivalent ways to derive this table (and its periodicity), none of which is trivial. We will *sketch* one of the approaches below.

In case you wonder about the column for $d = 0$: One should think of these systems as "blobs" without spatial structure. Mathematically, this column follows naturally and is not really special (actually, it is simpler because the constraints on the Hamiltonians are easier to implement). The Brillouin zone is simply T^0 (which is a point).

3. *Recipe:*

If one studies a specific model (specified by a SP Hamiltonian H) and wants to find out whether any of its phases are topological, the standard procedure goes as follows:

a) Check whether the SP Hamiltonian H features TRS, PHS, and/or SLS and (if so) whether TRS/PHS square to $\pm 1 \to$ (T,C,S) → Class **X**

b) Use the periodic table above to check whether **X** supports topological phases in the spatial dimension d of your given system.

c) Look up the associated topological invariant I for (**X**, d) in Ref. [63].

d) Compute $I = I[H]$ as a function of the control parameters of your system and check whether it non-zero in (some of) the phases.

Without knowing about the periodic table and the systematic approach of Ref. [63] to construct topological invariants, we nevertheless succeeded for the Chern insulator (Class **A**) with the Chern number, the Kane-Mele model (Class **AII**) with the Pfaffian index, the SSH chain (Class **AIII**) with the winding number, and the Majorana chain (Class **D**) with the $\mathbb{Z}_2$-index constructed from the BdG-Hamiltonian.

Note: The symmetry classes are not exclusive. E.g., every system in class **BDI** can also be considered a member of the classes **AI**, **D**, or **AIII**. We encountered this ambiguity for the Majorana chain which generically is considered a representative of **D** even if the "clean" Majorana chain Hamiltonian does not break TRS. In this situation, TRS is considered an "accidental" symmetry that one does not want to rely on. If, however, one considers the Majorana chain a representative of **BDI**, TRS becomes a crucial symmetry that must not be broken. This may seem arbitrary but is perfectly valid as the choice of a protecting symmetry essentially specifies which perturbations we consider allowed and which forbidden. This situation is typical for all SPT phases as they do not have intrinsic topological order. Below we discuss stacks of Majorana chains where this concept should become clear.

1.6.3 Frameworks for classification

There are different frameworks that can be used to derive the periodic table above. However, none of them is straightforward and all of them make heavy use of highly non-trivial physical and/or mathematical facts. A deep study of any of these approaches would easily fill its own course, so we keep it simple and sketch only one of the approaches exemplarily.

- *Anderson localization on the boundary* ➡ [11, 63]

  Rationale: Study field theories (nonlinear sigma models) that describe the *boundary* of the system and determine when they retain delocalized states in the presence of disorder (i.e., when they avoid *Anderson localization*). Mathematically, this happens if certain topological terms can be added to the action; the existence (and properties) of these terms depends on **X** and d and provides the periodic table.

- *Quantum anomalies on the boundary* ➡ [87]

  Rationale: Study *anomalous* field theories that can emerge as effective descriptions on the *boundaries* of the system (this approach relates to the one based on Anderson localization above). To cite Ludwig [37]:

  "[The approach] relies on the notion that the boundary of a topological insulator (superconductor) cannot exist as an isolated system in its own dimensionality. Rather it must always be attached to a higher dimensional bulk."

  We encountered such an anomaly before when we discussed the IQHE and realized that its chiral edge modes are in conflict with the Nielsen-Ninomiya theorem. These edge modes can only be consistently formulated on the boundary of a two-dimensional bulk.

- *K-Theory:* ➡ [12]

  In contrast to the other two frameworks which (1) do not require translational invariance and (2) focus on the boundary of the system, the K-theory approach pioneered by Kitaev assumes translational invariance and describes the bulk of the system.

  (Topological) K-theory is a very general mathematical framework that is used to study vector bundles over topological spaces. In its application to classify topological phases, the base space is essentially the Brillouin torus and the system/Hamiltonian is described by a (potentially non-trivial) vector bundle over this space. Before its application to topological phases, it had already found applications in string theory.

  1. ◁ Gapped system with n filled (m empty) bands described by Bloch Hamiltonian $H(\boldsymbol{k})$

2. *Spectral flattening:*

$$H(\boldsymbol{k}) \xrightarrow{\text{Continuous deformation}} \mathfrak{H}(\boldsymbol{k}) \tag{1.377}$$

$$\text{with} \quad \sigma(\mathfrak{H}(\boldsymbol{k})) = (\underbrace{-1, \ldots, -1}_{n}, \underbrace{+1, \ldots, +1}_{m}) \tag{1.378}$$

3. $\lhd$ Simplest case: Class **A** $\rightarrow$
   (Hence we do not have to implement any symmetry constraint in the following.)

$$\mathfrak{H}(\boldsymbol{k}) = \mathcal{U}(\boldsymbol{k}) \underbrace{\begin{pmatrix} \mathbb{1}_m & 0 \\ 0 & -\mathbb{1}_n \end{pmatrix}}_{\mathbb{X}} \mathcal{U}^{\dagger}(\boldsymbol{k}) \quad \text{with} \quad \mathcal{U}(\boldsymbol{k}) \in U(m+n) \tag{1.379}$$

   $U(m+n)$ is the matrix group of unitary $(m+n) \times (m+n)$-matrices.

4. *"Gauge symmetry":*

$$\mathcal{U} \sim \mathcal{U}' \quad :\Leftrightarrow \quad \mathcal{U} = \mathcal{U}' \cdot \begin{pmatrix} \mathcal{U}_1 & 0 \\ 0 & \mathcal{U}_2 \end{pmatrix} \quad \text{for} \quad \mathcal{U}_1 \in U(m), \ \mathcal{U}_2 \in U(n) \tag{1.380}$$

   since

$$\mathfrak{H}(\boldsymbol{k}) = \mathcal{U}(\boldsymbol{k}) \, \mathbb{X} \, \mathcal{U}^{\dagger}(\boldsymbol{k}) = \mathcal{U}'(\boldsymbol{k}) \, \mathbb{X} \, \mathcal{U}'^{\dagger}(\boldsymbol{k}) \tag{1.381}$$

   That is, the $\mathfrak{H}$-encoding unitary $\mathcal{U}$ is only defined up to unitaries from $U(m) \times U(n)$.

   $\rightarrow$

$$\mathfrak{H} : T^d \ni \boldsymbol{k} \mapsto \mathfrak{H}(\boldsymbol{k}) \triangleq [\mathcal{U}(\boldsymbol{k})]_{\sim} \in \frac{U(m+n)}{U(m) \times U(n)} = G_{m,n+m}(\mathbb{C}) \tag{1.382}$$

   $G_{m,n+m}(\mathbb{C})$: complex Grassmannian

   $\rightarrow G_{m,n+m}(\mathbb{C})$ is the *classifying space* C_0 for symmetry class **A**
   (and one of Cartan's *symmetric spaces*)

   This statement is not completely correct, actually it is

$$C_0 = \bigcup_{k \in \mathbb{Z}} \lim_{s \to \infty} \frac{U(2s)}{U(s+k) \times U(s-k)} \simeq \lim_{n,m \to \infty} \frac{U(m+n)}{U(m) \times U(n)} \times \mathbb{Z} \,. \tag{1.383}$$

   The idea behind this is that SP Hamiltonians of different sizes should be comparable (and the classification should not depend on system-specific parameters like m and n). In particular, for systems with $d > 0$ it should not matter whether one adds additional trivial bands to the system (like those from closed atomic shells). This leads to the concept of *stable equivalence* which has its counterpart in K-theory where one considers vector bundles *modulo trivial bundles*.

Complex classes
$UHU^\dagger = -H$
$UH^*U^t = H$

Real classes

Class	T	C	S	Classifying Space	Name
A	0	0	0	$U(m+n)/U(n)\times U(m)$	C_0
$A\mathrm{III}$	0	0	1	$U(n)\times U(n)/U(n)$	C_1
AI	$+1$	0	0	$O(n+m)/O(n)\times O(m)$	R_0
BDI	$+1$	$+1$	1	$O(n)\times O(n)/O(n)$	R_1
D	0	$+1$	0	$O(2n)/U(n)$	R_2
$D\mathrm{III}$	-1	$+1$	1	$U(2n)/Sp(2n)$	R_3
$A\mathrm{II}$	-1	0	0	$Sp(n+m)/Sp(n)\times Sp(m)$	R_4
$C\mathrm{II}$	-1	-1	1	$Sp(n)\times Sp(n)/Sp(n)$	R_5
C	0	-1	0	$Sp(2n)/U(n)$	R_6
$C\mathrm{I}$	$+1$	-1	1	$U(n)/O(n)$	R_7

$Sp(n)$ denotes the *compact symplectic group* which is the analog of the unitary group $U(n)$ if one replaces the field $\mathbb{C}$ by quaternions $\mathbb{H}$.

The distinction between the two *complex* classes **A** and **AIII** and the remaining eight *real* classes follows from the reality constraints (that is, the constraint on the SP Hamiltonian includes a complex conjugate) on the Hamiltonians for real classes, and the missing of such for complex classes. On the mathematical level, this leads to the distinction between complex and real vector bundles and henceforth complex and real K-theory with classifying spaces C_q (q mod 2) and R_q (q mod 8), respectively.

5. Simplification: $T^d \to S^d$ (we did this before when we discussed Skyrmions) $\to$

$$\{\text{Topological phases}\} = \pi_d(C_0) \tag{1.384}$$

$\pi_d(X)$: dth homotopy group of X

Example for $d = 2$: $\pi_2(C_0) \stackrel{*}{=} \mathbb{Z} \to$ Chern number

6. Undo simplification $S^d \to T^d$ & Include symmetry constraints for real classes **X$\neq$A,AIII**:

Kitaev [12] $\stackrel{*}{\to}$

$$\{\text{Topological phases of } (\mathbf{X},d)\} = \tag{1.385}$$

$$\underbrace{\pi\left(\bar{T}^d, R_q\right)}_{K_{\mathbb{R}}^{-q}(\bar{T}^d)} \stackrel{K\text{-theory}}{=} \underbrace{\pi_0(R_{q-d})}_{\text{Strong topological index}} \oplus \underbrace{\bigoplus_{s=0}^{d-1}\binom{d}{s}\pi_0(R_{q-s})}_{\text{Weak topological indices}} \tag{1.386}$$

– $\pi\left(\bar{T}^d, R_q\right)$: equivalence classes of all maps $\mathfrak{H}(\boldsymbol{k})$ from the BZ T^d into an appropriately restricted matrix space (which depends on the symmetry class **X**, ➦ Table 1 in Ref. [37]; for $d = 0$ the target space is the classifying space R_q that belongs to **X**, for $d > 0$ this is only true at the TRIMs) that, in addition, satisfy the symmetry constraints on momenta demanded by the symmetry class **X** (the latter constraint is indicated by the bar of $\bar{T}^d$); this object is known in K-theory as the "real K-group $K_{\mathbb{R}}^{-q}(\bar{T}^d)$ of $\bar{T}^d$".

↑ Notes

- $\pi_0(X)$ is the 0th homotopy group of X; its elements label the *connected components* of X. Since the connectivity of the symmetric spaces R_q is known, the right-hand side of Eq. (1.386) can be looked up in the literature.

$\rightarrow$ Computing $\pi_0(R_{q-d})$ (= strong topological indices) for $q = 0, \ldots, 7$ and $d = 0, 1, \ldots$ yields the periodic table.

Note:

- There is an analog expression for the two complex classes **A** and **AIII**.

- The contributions labeled "weak topological indices" are not part of the periodic table.

- The indices of the classifying spaces $R_{q-d/s}$ are defined modulo 8 (this is a result known as *Bott periodicity*); for the complex classes, the periodicity is 2. This leads to the periodicity of the *periodic* table.

Example for $q = 4$ (**AII**) and $d = 2$ (e.g. Kane-Mele model):

$$\pi\left(\bar{T}^2, R_4\right) = \pi_0(R_2) \oplus 1 \times \pi_0(R_4) \oplus 2 \times \pi_0(R_3) \tag{1.387}$$

$$= \underbrace{\mathbb{Z}_2}_{\text{Pfaffian index}} \oplus \underbrace{\mathbb{Z}}_{\# \text{ Valence bands}} \oplus \underbrace{2 \times 0}_{\text{No weak indices}} \tag{1.388}$$

The values for $\pi_0(R_q)$ are provided in Table 2 of Ref. [12] but can also be read off from the $d = 0$ column of the periodic table (replacing $2\mathbb{Z}$ by $\mathbb{Z}$).

1.6.4 Consequences of interactions

This course focused on *non-interacting* fermions. The crucial feature of these kind of theories is that their MB Hamiltonian $\hat{H}$ can be encoded by a SP Hamiltonian H so that their MB spectrum can be built from the SP spectrum; this makes them exactly (or efficiently) solvable. The periodic table is built on the SP Hamiltonians and is therefore only valid for systems that can be reasonably described by such theories. The natural question is then of course:

Question: What happens to the periodic table if interactions are included?

It is clear that interactions allow for more "paths" to connect gapped Hamiltonians so that the classification must become "coarser" (i.e., phases that are separated without interactions may no longer be if interactions are allowed).

Quick answer: Known for *quartic* interactions [88]; No complete classification known for arbitrary interactions (as far as I know); Current topic of research ($\bullet$ e.g. [89, 90]) (An exception is 1D where fermions can be mapped to bosons [91–93]).

However, there is an example that demonstrates that (and how) the periodic table is modified by interactions for a specific (**X**,d) [94]:

1. $\triangleleft$ Majorana chain for $w = \Delta > 0$ and $\mu = 0$:
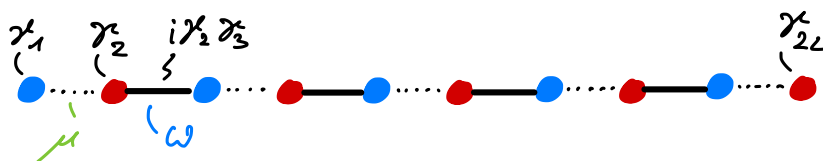
TRS & PHS $\rightarrow$ Symmetry class **BDI** in $d = 1 \rightarrow \mathbb{Z}$-index
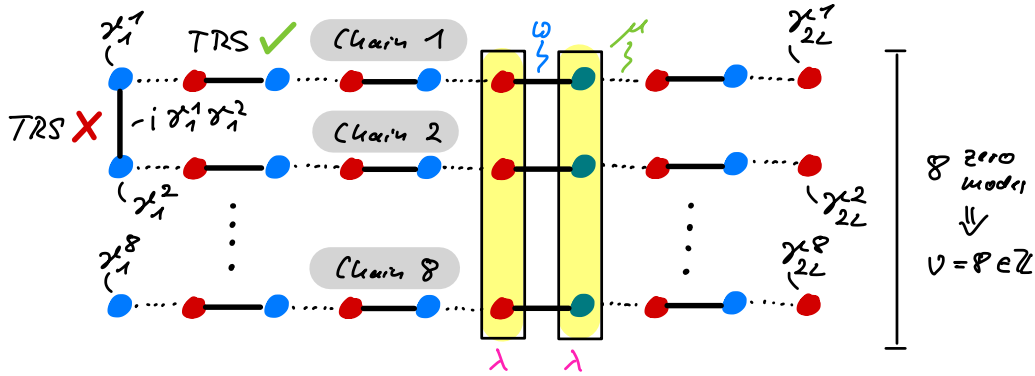
2. *Time-reversal symmetry:*

$$\mathcal{T} i \mathcal{T}^{-1} = -i \quad \text{and} \quad \mathcal{T} \gamma_{2i-1} \mathcal{T}^{-1} = +\gamma_{2i-1}, \quad \mathcal{T} \gamma_{2i} \mathcal{T}^{-1} = -\gamma_{2i} \qquad (1.389)$$

This follows from the "standard" TRS for *spinless* fermions: $\mathcal{T} c_i \mathcal{T}^{-1} = c_i$.

$\rightarrow$ Only couplings between *even* (red) and *odd* (blue) Majorana modes allowed

3. *Stack* 8 Majorana chains in the topological phase:

Note that one could gap out the edge modes with $i \gamma_1^\alpha \gamma_1^{\alpha+1}$ but these terms *break* TRS (the coupled modes are both are even or odd)!

$\rightarrow$ $\mathbb{Z}$-index = # dangling Majorana modes γ_1^α (on one end of the stack)

The chains are *oriented* in that they start with an odd and end with an even mode (which transform differently under TRS). Reversing the orientation of a chain therefore gives a negative index and indeed, a pair of chains with opposite orientation can be gapped out without breaking TRS because the two Majorana modes on one end are even and odd.

$\lhd$ 8 topological chains $\rightarrow$ **BDI**-index $\nu = 8$

Note that if there is an *odd* number of dangling Majorana modes on one end, you cannot gap them out completely even when breaking TRS because after gapping out all pairs a single mode will be left. This distinguishes the situations with an even and an odd number of Majorana zero modes and corresponds to the $\mathbb{Z}_2$-index of class **D** that does not require TRS.

4. Connect topological to trivial phase via *quartic interaction*:
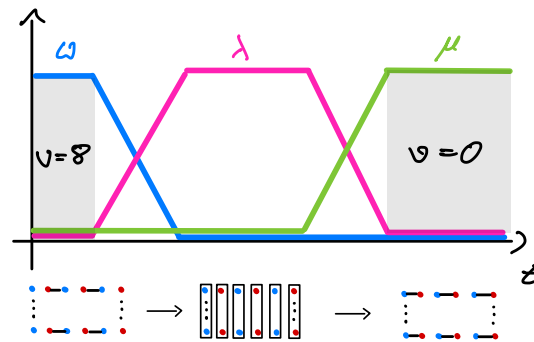
$$\hat{H}(\mu, w, \lambda) = \hat{H}_{\text{MC}}(\mu, w) + \lambda \sum_{n=1}^{2L} W_n \qquad (1.390)$$

with quartic interaction between the 8 chains

$$W_n = \gamma_n^1 \gamma_n^2 \gamma_n^3 \gamma_n^4 \pm \ldots \text{many more quartic terms} \qquad (1.391)$$

➲ Eq. (8) in Ref. [94] for the full term and its derivation.

Protocol:

On this continuous path …

- the bulk gap remains open (can be shown by exact diagonalization on a unit cell)

- and TRS is not broken (this is easily checked by inspection).

5. $\nu = 0$ and $\nu = 8$ are the same phases!

$\rightarrow$ $\mathbb{Z}$-index of **BDI** in $d = 1$ reduces to $\mathbb{Z}_8$-index
$\rightarrow$ With interactions there are not infinitely many top. superconductors in 1D but only 8.

For an overview how quartic interactions modify the periodic table in other dimensions/symmetry classes ➲ [88].

1.7 Topologically protected edge states in classical systems

> **† Note**
>
> In this lecture I will discuss a classical mechanics realization of topological bands derived from the quantum spin Hall effect that has been described and implemented by Süsstrunk & Huber [95]. There is also a review by Huber on the broader field of "topological mechanics" [96]. For more references on classical systems with topological bands, see the end of this section and Section 1.3.2 of my PhD thesis [66].

1.7.1 Review: Effects of topological bands

In this course we have studied various models that realize topological *quantum phases* at $T = 0$. The role of topology was to describe "twists" in the band structure that cannot be undone without closing the gap (or breaking a protecting symmetry). These topologially non-trivial band structures had observable, physical consequences:

- *Quantized Hall response:*
  Remember:

$$\sigma_{xy} \overset{\text{MB}}{=} -\frac{e^2 \nu}{2\pi\hbar} \quad \text{with} \quad \nu \overset{\text{SP}}{=} \sum_{n:\varepsilon_n < E_F} C^{[n]} \in \mathbb{Z} \qquad (1.392)$$

  $\rightarrow$ Requires filled bands
  $\rightarrow$ Many-body phenomenon (Fermi statistics!)

  $\rightarrow$ Genuine quantum effect!

  Note that $\hbar$ appears in the expression above, so quantum mechanics must play a role. (You can trace the $\hbar$ back to the Kubo formula and therefore to the propagator/path integral; it is not related to the Chern numer, that is, topology.)

- *Robust edge modes:*
  Remember:

  | Topological system in 2D w/ OBC | $\rightarrow$ | Gapless edge modes |
  | Topological system in 1D w/ OBC | $\rightarrow$ | Zero-energy boundary modes |

  $\rightarrow$ *Bulk-boundary correspondence*
  $\rightarrow$ Single-particle phenomenon (studying the band structure is sufficient)
  We do not need the Fock space / Slater determinants (= Fermi statistics) nor time-evolution operators / path integrals to understand the appearance of edge modes.

  $\rightarrow$ *Not* a quantum effect!

We conclude:

> Topological features of the *band structure* (= single-particle features) are *not* quantum effects!

Question: Can we translate edge modes to *classical* systems?

Note that because we will focus on single-particle features in the following, there is no sense in talking about topological *phases*— neither quantum nor classical. What we will study are topological *features* of classical systems that affect the behaviour of their finite-energy excitations.

1.7.2 Example: Topological mechanics and helical edge modes

This subsection is based on Ref. [95].

1. *Goal:* Realization of the helical edge modes of the QSHE (➲ Kane-Mele model) in a classical mechanics setup governed by Newton's equation

   Rationale: A "phononic topological insulator" would transmit energy (= vibrations) only along its surface but not through the bulk. The robustness of topological edge modes would allow for wave guides of arbitrary shape (in contrast to *wispering gallery modes* that delicately depend on geometry).

2. *Quantum system (QS):*
   ◁ SP Schrödinger equation

   $$\underbrace{i\hbar\dot{\Psi}_i^\alpha}_{\text{Quantum dynamics}} = H_{ij}^{\alpha\beta}\,\Psi_j^\beta \tag{1.393}$$

   i, j: sites
   α, β: spin
   H: SP Hamiltonian = Hermitian matrix

   Note that *states* in the SP Hilbert space have the form $|\Psi\rangle = \sum_{i,\alpha} \Psi_i^\alpha |i, \alpha\rangle$ where $|i, \alpha\rangle$ describes an electron on site i with spin α.

3. *Classical system (CS):*
   ◁ Newton's equation for N coupled oscillators (e.g., pendula coupled by springs)

   $$\underbrace{\ddot{x}_i}_{\text{Classical dynamics}} = -D_{ij}\,x_j \tag{1.394}$$

   (The masses of the oscillators are set to one or, equivalently, absorbed into D.)

   x_i: states of oscillators (in 3D it would be $i = 1, \ldots, 3N$)
   D: Dynamical coupling matrix = real, symmetric, positive semidefinite matrix

   First, D only contains spring constants, thus it is real. Next, Newton's third law (action-reaction law) demands the symmetry of D because D_{ij} (D_{ji}) encodes the force by pendulum j (i) on pendulum i (j). And last, the eigenvalues of D are the *frequencies squared* of the eigenmodes of the system and therefore must be positive (remember that for a single 1D pendulum $m\ddot{x} = -Dx$ leads to an eigenfrequency $\omega^2 = D/m$).

4. *Observation:*

   - QS characterized by *eigenstates* of H

   - CS characterized by *eigenmodes* of D (eigenmodes = eigenstates)

But: Edge modes are simply special eigenstates of H

Idea: Use H with edge modes (e.g., from QSHE) to construct D with edge modes!

Note that the *dynamics* of QS and CS are different (1st vs. 2nd order) but this has no effect on the existence of edge states/modes which is a property of the matrices H and D, respectively.

5. *Model construction:*

   a) ⊲ Two independent copies of the *Hofstadter model* (➔ Problemset 3) with spin-dependent flux $\alpha\hat{\Phi} = \pm p/q = \pm 1/3$:

$$H = \begin{pmatrix} H_\uparrow & 0 \\ 0 & H_\downarrow \end{pmatrix} \tag{1.395}$$

$$\text{with} \quad H_\alpha = \sum_{x,y} \left[\begin{matrix} |x, y+1, \alpha\rangle\langle x, y, \alpha| \\ +e^{-2\pi i\alpha\hat{\Phi}y} |x+1, y, \alpha\rangle\langle x, y, \alpha| \end{matrix} \right] + \text{h.c.} \tag{1.396}$$

$\alpha = \uparrow/\downarrow = +1/-1$: pseudo-spin index

H_α is given in Landau gauge.

   b) $q = 3 \to$ Three gapped, spin-degenerate bands:
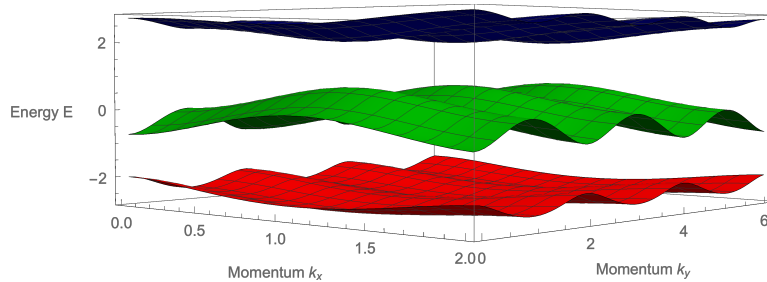
Chern numbers:

Red band:	$1 = 3s_1 + t_1 \Rightarrow s_1 = 0, t_1 = 1$	$\Rightarrow C_1 = t_1 - t_0 = 1$
Green band:	$2 = 3s_2 + t_2 \Rightarrow s_2 = 1, t_2 = -1$	$\Rightarrow C_2 = t_2 - t_1 = -2$
Blue band:	$3 = 3s_3 + t_3 \Rightarrow s_3 = 1, t_3 = 0$	$\Rightarrow C_3 = t_3 - t_2 = 1$

$\to$ TKNN invariant $\nu = C_1 = +1$ in red/green gap and $\nu = C_1 + C_2 = -1$ in green/blue gap

⊲ Finite sample with open boundaries (like a square):
$\to$ Two helical edge modes (opposite spin/group velocity) *in each gap*

Note that the situation in each of the two gaps is comparable to the Kane-Mele model with upper/lower bands of Chern number ± 1. In each spin sector, a TKNN invariant of $|\nu| = 1$ demands for a single conducting edge channel. Because the signs of ν are different for the two gaps, the edge modes (for a fixed spin) have opposite chiralities (➔ experimental results below).

   c) *Symmetries:*

   • *Time-reversal symmetry:* $T = i\sigma^y\mathcal{K}$ with $T^2 = -\mathbb{1}$ and

$$THT^{-1} = H \tag{1.397}$$

↑ Notes

since $H_\uparrow = H_\downarrow^*$

$\to$ **All** with $\mathbb{Z}_2$ Pfaffian index

- *Spin conservation:*

$$\sigma^z H \sigma^z = H \tag{1.398}$$

This is the same unitary symmetry that we encountered for the Kane-Mele model in the absence of a Rashba term. It allows for the expression of the Pfaffian invariant in terms of the Chern numbers of the spin-polarized bands [$\circleddash$ Eq. (1.234)] so that one can avoid the more complicated expressions we discussed in detail.

d) *Problem:* H is complex

Solution: Unitary rotation in Kramers-degenerate subspace:

$$D := U^\dagger H U = \begin{pmatrix} \operatorname{Re} H & \operatorname{Im} H \\ \operatorname{Im} H^T & \operatorname{Re} H \end{pmatrix} \quad \text{with} \quad U = \underbrace{\frac{1}{\sqrt{2}} \begin{pmatrix} 1 & -i \\ 1 & i \end{pmatrix}}_{u} \otimes \mathbb{1}_{\text{lattice}} \tag{1.399}$$

with $\operatorname{Re} H_\uparrow = \operatorname{Re} H_\downarrow \equiv \operatorname{Re} H$ and $\operatorname{Im} H_\downarrow = \operatorname{Im} H_\uparrow^* = \operatorname{Im} H_\uparrow^T \equiv \operatorname{Im} H^T$

Note that U is a *local unitary* in pseudo-spin-space so that edge modes of H remain edge modes of D.

$\to$ D real and symmetric
Positive semidefiniteness can always be achieved through shifting by a constant: $D \mapsto D + \text{const} \times \mathbb{1}$; clearly this does not affect the existence of edge modes.

e) *Transformed basis*:

$$\begin{pmatrix} X_{xy} \\ Y_{xy} \end{pmatrix} \equiv u^\dagger \begin{pmatrix} \psi_{xy\uparrow} \\ \psi_{xy\downarrow} \end{pmatrix} \tag{1.400}$$

(X_{xy}, Y_{xy}): Position of 2D harmonic oscillator on site (x, y) (pendula, $\circleddash$ below)

$\lhd$ Spin-up mode on site (x, y):

$$\Psi_{xy\uparrow}(t) = \Psi_0 \, e^{-i\omega t} \begin{pmatrix} 1 \\ 0 \end{pmatrix}_{xy} \tag{1.401}$$

$$\Rightarrow \quad u^\dagger \Psi_{xy\uparrow}(t) = \Psi_0 e^{-i\omega t} \underbrace{\frac{1}{\sqrt{2}} \begin{pmatrix} 1 \\ i \end{pmatrix}_{x,y}}_{\text{Jones vector}} \tag{1.402}$$

That is:

$$\Rightarrow \quad \operatorname{Re}\left[u^\dagger \Psi_{xy\uparrow}(t) \right] \propto \begin{pmatrix} \cos(\omega t) \\ \sin(\omega t) \end{pmatrix}_{xy} \tag{1.403}$$

$\to$

| Spin UP | $\leftrightarrow$ | LEFT circular polarization | (1.404) |
| Spin DOWN | $\leftrightarrow$ | RIGHT circular polarization | (1.405) |

f) Requirements on the *setup*:

- Hofstadter model with $q = 3 \rightarrow 3$ sites per magnetic unit cell
- Two-fold spin/polarization degeneracy per site
  $\rightarrow$ 2 harmonic oscillators (= 1D pendula) per site

$\rightarrow 6 \times$ 1D pendula per unit cell coupled by springs according to D:

- Re $H \rightarrow XX$- and YY-couplings
- Im $H \rightarrow XY$-couplings

6. *Experiment & Results:*
   The following figures are taken from Ref. [95].

   a) *Construction:*

   Array of $9 \times 15 = 135$ sites with 270 pendula, each of $500\,\text{mm}$ length and $500\,\text{g}$ heavy, coupled by springs and lever arms; the whole setup is suspended from the ceiling:
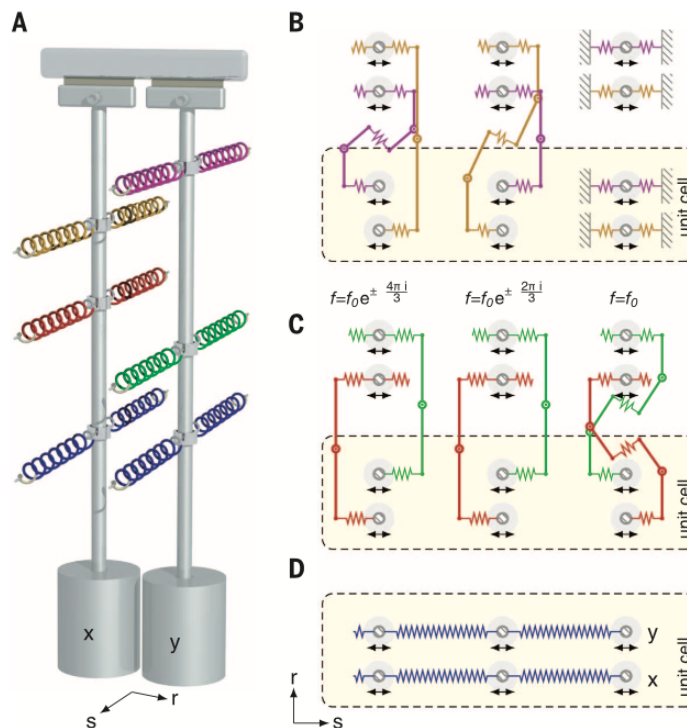
Coupling in $x(r)$-direction via lever arms:

- *One* lever arm $\rightarrow$ negative coupling
- *Two* lever arms $\rightarrow$ positive coupling

Note that because of Landau gauge there are only real, positive couplings in $y(s)$-direction which can be implemented by direct XX- and YY-spring couplings without lever arms.

➜ Video S3 on https://science.sciencemag.org/content/suppl/2015/07/01/349.6243.47.DC1
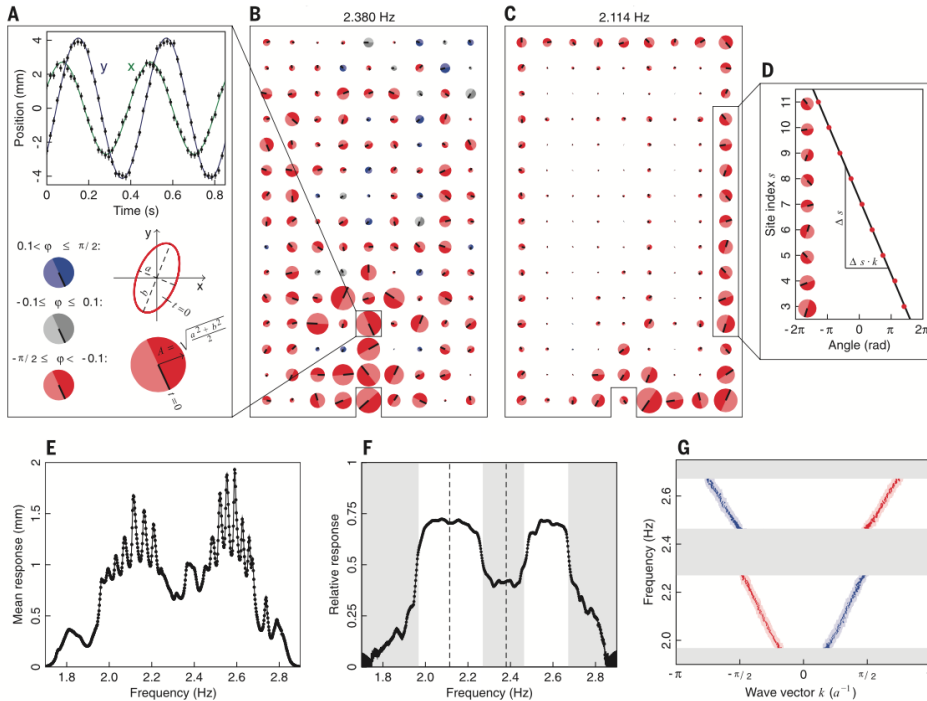
b) *Edge modes:*

i.   Drive system with circular polarization on edge

ii. Track $(X_{xy}(t), Y_{xy}(t))$ for every site after steady state is reached
     $\rightarrow$ Average amplitude A_{xy} (size of circle), polarization (color of circle)

iii. Strong response A_{xy} on edges in band gap $\rightarrow$ Edge modes

iv. Measure orientation/phase in X-Y-plane at fixed time on boundary (black lines in circles)
     $\rightarrow$ Dispersion of edge modes
     $\rightarrow$ Two helical edge modes in each band gap

$\rightarrow$ Videos S1/S2 on `https://science.sciencemag.org/content/suppl/2015/07/01/349.6243.47.DC1`

c) *Application:* Beam splitter
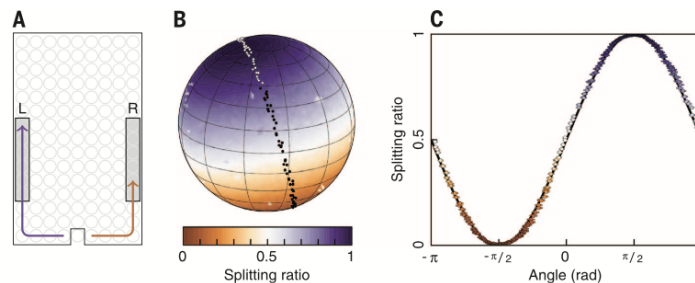
i.   Drive single site on boundary with *linear* (or any other) polarization
     $\rightarrow$ Superposition of left- and right circular polarization

ii. Helical edge modes
     $\rightarrow$ Right (left) circular polarized waves propagate to the left (right)

→ "Beam splitter" for phonons

For more applications of this setup ➲ Ref. [97].

d) *Robustness:*
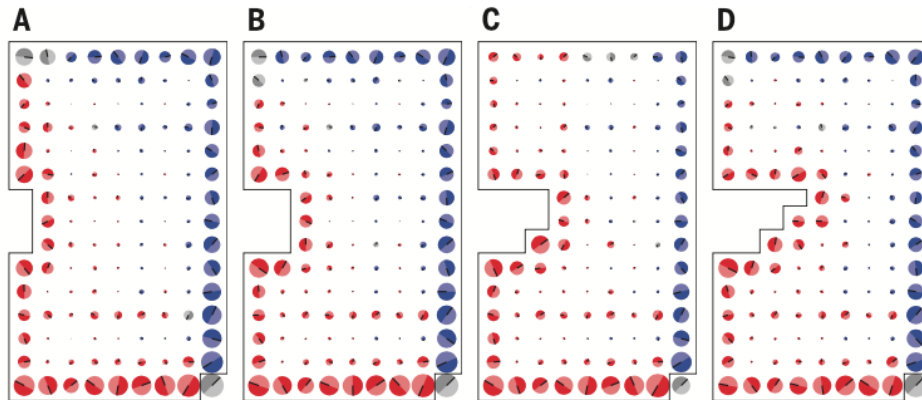
Note that this behaviour is very differnt from whispering gallery modes which are bound to *concave* surfaces and would scatter into the bulk when hitting a *convex* obstacle on the boundary.

Remember that the edge modes of the QSHE are protected by time-reversal symmetry:

$$H \overset{!}{=} THT^{-1} = U_T H^* U_T^\dagger = U_T (UU^\dagger HUU^\dagger)^* U_T^\dagger \qquad (1.406)$$

$$\Leftrightarrow \quad D = U^\dagger HU \overset{!}{=} (U^\dagger U_T U^*)D(U^{*\dagger}U_T^\dagger U) = S^\dagger DS \qquad (1.407)$$

(Here we assume that D is real-valued by construction.)

with unitary symmetry

$$S = U^{*\dagger}U_T^\dagger U = \begin{pmatrix} 0 & 1 \\ -1 & 0 \end{pmatrix} \qquad (1.408)$$

→

$$\text{with} \quad D = \begin{pmatrix} D_{XX} & D_{XY} \\ D_{YX} & D_{YY} \end{pmatrix} \quad \Rightarrow \quad \begin{matrix} D_{XX} \overset{!}{=} D_{YY} \\ \text{and } D_{XY} \overset{!}{=} -D_{YX} \end{matrix} \qquad (1.409)$$

Note that $D_{XX} = D_{YY} = \operatorname{Re} H$, $D_{XY} = \operatorname{Im} H$ and $D_{YX} = \operatorname{Im} H^T = \operatorname{Im} H^* = -\operatorname{Im} H$ satisfy these constraints. In addition, Newton's third law always imposes the constraint $D^T = D$ so that $D_{XY}^T = D_{YX}$ and therefore $D_{XY}^T = -D_{XY}$.

→ In particular, perturbations of the form

$$D' = D + \begin{pmatrix} \delta D & 0 \\ 0 & \delta D \end{pmatrix} \qquad (1.410)$$

do not destroy the edge modes!

Note that the spring strength on different sites *can* vary as there are no additional constraints imposed by S on δD. Thus to ensure the symmetry, a *local* tuning of parameters on each site is sufficient.

→ *Local* symmetry constraint

1.7.3 More classical systems

What follows is a brief (and incomplete) list of classical setups where topological edge modes have been proposed and/or experimentally realized. Many of these systems are studied with applications in mind (like efficient transport of signals or energy).

- *Topological mechanics* (Review ➔ [96]):

    - Pioneered by Kane and Lubensky who studied mechanical constructs called *isostatic lattices* [98]. These systems can exhibit robust zero-frequency modes of topological origin at boundaries ("floppy modes").

    - While zero-frequency "floppy modes" can influence the low-energy response of a mechanical system, topologically protected, chiral edge modes with non-zero frequency allow for robust and scattering-free excitations.

    - Time-reversal breaking Chern insulator [99] (realized as a gyroscopic phononic crystal [100])

    - Time-reversal protected quantum spin Hall insulator [95, 97]

    - Higher-order topological insulators with protected *corner* modes [101]

- *Topological acoustics*:

    - Rationale: transmit sound waves through robust, scattering-free edge modes [102]

    - Experimental demonstration of an "acoustic Chern insulator" [103]

- *Topological photonics* (Review ➔ [104]):

    - Kick-started by Haldane & Raghu [105, 106] who proposed a classical analog of the Chern insulator for photonic crystals

    - Time-reversal breaking, chiral edge modes with microwaves in magneto-optical photonic crystals [107]

    - Chiral edge modes without magnetic fields in a Floquet setting in the optical regime [108]

    - Symmetry-protected analogs of topological insulators in lattice of photonic resonators [109]

    - Application: "topological insulator lasers" [110–112]

- *Topoelectrical circuits* (Review ➔ [113]):

    - Electrical circuits (composed of "lumped elements" like inductors, capacitors, etc.) can exhibit symmetry-protected edge modes [114]

    - Higher-order topological insulators realized both in the microwave regime [115] and with "topoelectrical circuits" [116]

- *Topological fluid dynamics*:

    - Fluid dynamics on the surface of rotating spheres exhibits robust, chiral modes that are trapped at the equator and protected by non-zero Chern numbers [117]

    - Such modes have long been known to influence Earth's atmospheric and oceanic flow systems.

2 Symmetry-protected topological phases of interacting bosons

3 Intrinsic topological order

Bibliography

[1] X. Chen, Z.-C. Gu and X.-G. Wen, *Local unitary transformation, long-range quantum entanglement, wave function renormalization, and topological order*, Physical Review B **82**, 155138 (2010), **doi:**`10.1103/physrevb.82.155138`. (Cited on pages 10 and 15.)

[2] L. D. Landau, *Zur Theorie der Phasenumwandlungen I*, Physikalische Zeitschrift der Sowjetunion **11**, 26 (1937). (Cited on page 15.)

[3] L. D. Landau, *Zur Theorie der Phasenumwandlungen II*, Physikalische Zeitschrift der Sowjetunion **11**, 545 (1937). (Cited on page 15.)

[4] V. L. Ginzburg and L. D. Landau, *On the theory of superconductivity*, Journal of Experimental and Theoretical Physics (JETP) **20**, 1064 (1950). (Cited on page 15.)

[5] E. Witten, *Topological quantum field theory*, Communications in Mathematical Physics **117**(3), 353 (1988), **doi:**`10.1007/bf01223371`. (Cited on page 15.)

[6] X.-G. Wen, *Topological orders in rigid states*, International Journal of Modern Physics B **04**(02), 239 (1990), **doi:**`10.1142/s0217979290000139`. (Cited on page 15.)

[7] X. Chen, Z.-C. Gu and X.-G. Wen, *Classification of gapped symmetric phases in one-dimensional spin systems*, Physical Review B **83**, 035107 (2011), **doi:**`10.1103/physrevb.83.035107`. (Cited on page 15.)

[8] X. Chen, Z.-C. Gu, Z.-X. Liu and X.-G. Wen, *Symmetry protected topological orders and the group cohomology of their symmetry group*, Physical Review B **87**, 155114 (2013), **doi:**`10.1103/physrevb.87.155114`. (Cited on pages 15 and 110.)

[9] Z.-C. Gu and X.-G. Wen, *Symmetry-protected topological orders for interacting fermions: Fermionic topological nonlinear σ models and a special group supercohomology theory*, Physical Review B **90**, 115141 (2014), **doi:**`10.1103/physrevb.90.115141`. (Cited on page 15.)

[10] A. Kapustin, R. Thorngren, A. Turzillo and Z. Wang, *Fermionic symmetry protected topological phases and cobordisms*, Journal of High Energy Physics **2015**(12), 1 (2015), **doi:**`10.1007/jhep12(2015)052`. (Cited on page 15.)

[11] A. P. Schnyder, S. Ryu, A. Furusaki and A. W. W. Ludwig, *Classification of topological insulators and superconductors in three spatial dimensions*, Physical Review B **78**, 195125 (2008), **doi:**`10.1103/physrevb.78.195125`. (Cited on pages 15, 114, and 115.)

[12] A. Kitaev, *Periodic table for topological insulators and superconductors*, AIP Conference Proceedings **1134**(1), 22 (2009), **doi:**`10.1063/1.3149495`. (Cited on pages 15, 50, 109, 114, 115, 117, and 118.)

[13] X.-G. Wen and Q. Niu, *Ground-state degeneracy of the fractional quantum Hall states in the presence of a random potential and on high-genus Riemann surfaces*, Physical Review B **41**, 9377 (1990), **doi:**`10.1103/physrevb.41.9377`. (Cited on page 16.)

[14] D. Arovas, J. R. Schrieffer and F. Wilczek, *Fractional statistics and the quantum Hall effect*, Physical Review Letters **53**, 722 (1984), **doi:**`10.1103/physrevlett.53.722`. (Cited on page 16.)

[15] G. Moore and N. Read, *Nonabelions in the fractional quantum Hall effect*, Nuclear Physics B **360**(2), 362 (1991), **doi:**`10.1016/0550-3213(91)90407-o`. (Cited on page 16.)

[16] R. B. Laughlin, *Anomalous quantum Hall effect: An incompressible quantum fluid with fractionally charged excitations*, Physical Review Letters **50**, 1395 (1983), **doi:**`10.1103/physrevlett.50.1395`. (Cited on page 16.)

[17] X.-G. Wen, *Chiral Luttinger liquid and the edge excitations in the fractional quantum Hall states*, Physical Review B **41**, 12838 (1990), **doi:**`10.1103/physrevb.41.12838`. (Cited on page 16.)

[18] A. Zee, *Quantum Hall fluids*, In *Field Theory, Topology and Condensed Matter Physics*, pp. 99–153. Springer Berlin Heidelberg, **doi:**`10.1007/bfb0113369` (1995). (Cited on page 16.)

[19] K. v. Klitzing, G. Dorda and M. Pepper, *New method for high-accuracy determination of the fine-structure constant based on quantized Hall resistance*, Physical Review Letters **45**, 494 (1980), **doi:**`10.1103/physrevlett.45.494`. (Cited on page 19.)

[20] D. J. Thouless, M. Kohmoto, M. P. Nightingale and M. den Nijs, *Quantized Hall conductance in a two-dimensional periodic potential*, Physical Review Letters **49**, 405 (1982), **doi:**`10.1103/physrevlett.49.405`. (Cited on pages 19, 30, and 37.)

[21] M. Born and V. Fock, *Beweis des Adiabatensatzes*, Zeitschrift für Physik **51**(3-4), 165 (1928), **doi:**`10.1007/bf01343193`. (Cited on page 24.)

[22] M. V. Berry, *Quantal phase factors accompanying adiabatic changes*, Proceedings of the Royal Society of London. A. Mathematical and Physical Sciences **392**(1802), 45 (1984), **doi:**`10.1098/rspa.1984.0023`. (Cited on page 27.)

[23] J. von Bergmann and H. von Bergmann, *Foucault pendulum through basic geometry*, American Journal of Physics **75**(10), 888 (2007), **doi:**`10.1119/1.2757623`. (Cited on page 27.)

[24] M. Berry, *Anticipations of the geometric phase*, Physics Today **43**(12), 34 (1990), **doi:**`10.1063/1.881219`. (Cited on page 27.)

[25] D. Tong, *Lectures on the Quantum Hall Effect*, arXiv (1606.06687) (2016). (Cited on pages 30, 38, and 43.)

[26] B. A. Bernevig and T. L. Hughes, *Topological Insulators and Topological Superconductors*, Princeton University Press, ISBN 9780691151755 (2013). (Cited on pages 30, 66, and 96.)

[27] E. Fradkin, *Field Theories of Condensed Matter Systems*, Addison-Wesley Publishing Company (1991). (Cited on pages 30 and 38.)

[28] Q. Niu, D. J. Thouless and Y.-S. Wu, *Quantized hall conductance as a topological invariant*, Physical Review B **31**(6), 3372 (1985), **doi:**`10.1103/physrevb.31.3372`. (Cited on pages 30 and 38.)

[29] P. Mazur and S. de Groot, *On Onsager's relations in a magnetic field*, Physica **19**(1-12), 961 (1953), **doi:**`10.1016/s0031-8914(53)80108-4`. (Cited on page 37.)

[30] Y. Hatsugai, *Chern number and edge states in the integer quantum Hall effect*, Physical Review Letters **71**, 3697 (1993), **doi:**`10.1103/physrevlett.71.3697`. (Cited on page 41.)

[31] A. M. Essin and V. Gurarie, *Bulk-boundary correspondence of topological insulators from their respective Green's functions*, Physical Review B **84**, 125132 (2011), **doi:**`10.1103/physrevb.84.125132`. (Cited on page 41.)

[32] T. Fukui, K. Shiozaki, T. Fujiwara and S. Fujimoto, *Bulk-edge correspondence for Chern topological phases: A viewpoint from a generalized index theorem*, Journal of the Physical Society of Japan **81**(11), 114602 (2012), **doi:**`10.1143/jpsj.81.114602`. (Cited on page 41.)

[33] H. Nielsen and M. Ninomiya, *Absence of neutrinos on a lattice: (I). Proof by homotopy theory*, Nuclear Physics B **185**(1), 20 (1981), **doi:**`10.1016/0550-3213(81)90361-8`. (Cited on page 42.)

[34] H. Nielsen and M. Ninomiya, *Absence of neutrinos on a lattice: (II). Intuitive topological proof*, Nuclear Physics B **193**(1), 173 (1981), **doi:**`10.1016/0550-3213(81)90524-1`. (Cited on page 42.)

[35] C. Brouder, G. Panati, M. Calandra, C. Mourougane and N. Marzari, *Exponential localization of Wannier functions in insulators*, Physical Review Letters **98**, 046402 (2007), **doi:**`10.1103/physrevlett.98.046402`. (Cited on page 43.)

[36] M. B. Hastings and T. A. Loring, *Almost commuting matrices, localized Wannier functions, and the quantum Hall effect*, Journal of Mathematical Physics **51**(1), 015214 (2010), **doi:**`10.1063/1.3274817`. (Cited on page 43.)

[37] A. W. W. Ludwig, *Topological phases: Classification of topological insulators and superconductors of non-interacting fermions, and beyond*, Physica Scripta **2016**(T168), 014001 (2016), **doi:**`10.1088/0031-8949/2015/t168/014001`. (Cited on pages 44, 51, 109, 115, and 117.)

[38] X.-G. Wen, *Colloquium: Zoo of quantum-topological phases of matter*, Reviews of Modern Physics **89**, 041004 (2017), **doi:**`10.1103/revmodphys.89.041004`. (Cited on pages 45, 60, and 107.)

[39] L. Kong and X.-G. Wen, *Braided fusion categories, gravitational anomalies, and the mathematical framework for topological orders in any dimensions*, arXiv e-prints arXiv:1405.5858 (2014), `1405.5858`. (Cited on page 45.)

[40] D. S. Freed, *Short-range entanglement and invertible field theories* (2014), `1406.7278`. (Cited on page 45.)

[41] A. Kitaev and J. Preskill, *Topological entanglement entropy*, Physical Review Letters **96**, 110404 (2006), **doi:**`10.1103/physrevlett.96.110404`. (Cited on page 45.)

↑ Notes

[42] I. D. Rodríguez and G. Sierra, *Entanglement entropy of integer quantum Hall states*, Physical Review B **80**, 153303 (2009), **doi:**`10.1103/physrevb.80.153303`. (Cited on page 45.)

[43] S. Rachel, *Quantum phase transitions of topological insulators without gap closing*, Journal of Physics: Condensed Matter **28**(40), 405502 (2016), **doi:**`10.1088/0953-8984/28/40/405502`. (Cited on page 45.)

[44] S. Rachel, *Interacting topological insulators: a review*, Reports on Progress in Physics **81**(11), 116501 (2018), **doi:**`10.1088/1361-6633/aad6a6`. (Cited on page 45.)

[45] T. H. R. Skyrme, *A non-linear field theory*, Proceedings of the Royal Society of London. Series A. Mathematical and Physical Sciences **260**(1300), 127 (1961), **doi:**`10.1098/rspa.1961.0018`. (Cited on page 48.)

[46] L. Fu, C. L. Kane and E. J. Mele, *Topological insulators in three dimensions*, Physical Review Letters **98**(10), 106803 (2007), **doi:**`10.1103/physrevlett.98.106803`. (Cited on pages 50 and 80.)

[47] L. Fu and C. L. Kane, *Topological insulators with inversion symmetry*, Physical Review B **76**(4), 045302 (2007), **doi:**`10.1103/physrevb.76.045302`. (Cited on pages 50 and 66.)

[48] E. P. Wigner, *Gruppentheorie und ihre Anwendung auf die Quantenmechanik der Atomspektren*, Vieweg+Teubner Verlag, Wiesbaden, ISBN 978-3-663-00642-8, **doi:**`10.1007/978-3-663-02555-9` (1931). (Cited on page 51.)

[49] E. P. Wigner, *Über die Operation der Zeitumkehr in der Quantenmechanik* pp. 213–226 (1993), **doi:**`10.1007/978-3-662-02781-3_15`. (Cited on page 52.)

[50] J. E. Moore and L. Balents, *Topological invariants of time-reversal-invariant band structures*, Physical Review B **75**(12), 121306 (2007), **doi:**`10.1103/PhysRevB.75.121306`. (Cited on pages 54, 75, and 80.)

[51] X.-L. Qi, Y.-S. Wu and S.-C. Zhang, *Topological quantization of the spin hall effect in two-dimensional paramagnetic semiconductors*, Physical Review B **74**(8), 085308 (2006), **doi:**`10.1103/physrevb.74.085308`. (Cited on page 57.)

[52] F. D. M. Haldane, *Model for a quantum Hall effect without Landau levels: Condensed-matter realization of the "parity anomaly"*, Physical Review Letters **61**, 2015 (1988), **doi:**`10.1103/physrevlett.61.2015`. (Cited on page 60.)

[53] F. D. M. Haldane, *Nobel lecture* (2016). (Cited on page 60.)

[54] C. L. Kane and E. J. Mele, *Quantum spin Hall effect in graphene*, Physical Review Letters **95**, 226801 (2005), **doi:**`10.1103/physrevlett.95.226801`. (Cited on pages 66 and 69.)

[55] C. L. Kane and E. J. Mele, *Z_2 topological order and the quantum spin Hall effect*, Physical Review Letters **95**, 146802 (2005), **doi:**`10.1103/physrevlett.95.146802`. (Cited on pages 66, 69, 71, 77, 78, and 79.)

[56] L. Fu and C. L. Kane, *Time reversal polarization and aZ2adiabatic spin pump*, Physical Review B **74**(19), 195312 (2006), **doi:**`10.1103/PhysRevB.74.195312`. (Cited on pages 66 and 75.)

[57] M. Fruchart and D. Carpentier, *An introduction to topological insulators*, Comptes Rendus Physique **14**(9-10), 779 (2013), **doi:**`10.1016/j.crhy.2013.09.013`. (Cited on pages 66 and 75.)

[58] D. Carpentier, *Topology of bands in solids: From insulators to dirac matter*, In *Dirac Matter*, pp. 95–129. Springer, **doi:**`10.1007/978-3-319-32536-1_5` (2017). (Cited on page 66.)

[59] R. M. Kaufmann, D. Li and B. Wehefritz-Kaufmann, *Notes on topological insulators*, Reviews in Mathematical Physics **28**(10), 1630003 (2016), **doi:**`10.1142/S0129055X1630003X`. (Cited on page 66.)

[60] C. Nash and S. Sen, *Topology and Geometry for Physicists*, Dover Books on Mathematics. Dover Publications, ISBN 9780486318363 (2013). (Cited on page 66.)

[61] M. Nakahara, *Geometry, Topology and Physics*, CRC Press, ISBN 9781420056945 (2018). (Cited on page 66.)

[62] Y. A. Bychkov and E. I. Rashba, *Oscillatory effects and the magnetic susceptibility of carriers in inversion layers*, Journal of Physics C: Solid State Physics **17**(33), 6039 (1984), **doi:**`10.1088/0022-3719/17/33/015`. (Cited on page 70.)

[63] S. Ryu, A. P. Schnyder, A. Furusaki and A. W. W. Ludwig, *Topological insulators and superconductors: Tenfold way and dimensional hierarchy*, New Journal of Physics **12**(6), 065010 (2010), **doi:**`10.1088/1367-2630/12/6/065010`. (Cited on pages 80, 109, 114, and 115.)

[64] R. Roy, *Topological phases and the quantum spin hall effect in three dimensions*, Physical Review B **79**(19), 195322 (2009), **doi:**`10.1103/PhysRevB.79.195322`. (Cited on page 80.)

↑ Notes

[65] J. K. Asbóth, L. Oroszlány and A. P. Pályi, *A Short Course on Topological Insulators: Band Structure and Edge States in One and Two Dimensions*, Lecture Notes in Physics. Springer International Publishing, ISBN 3319256076 (2016). (Cited on page 83.)

[66] N. Lang, *One-Dimensional Topological States of Synthetic Quantum Matter*, Verlag Dr. Hut, München, ISBN 978-3-8439-4157-0 (2019). (Cited on pages 83, 96, 106, and 121.)

[67] W. P. Su, J. R. Schrieffer and A. J. Heeger, *Solitons in polyacetylene*, Physical Review Letters **42**, 1698 (1979), **doi:**10.1103/physrevlett.42.1698. (Cited on page 83.)

[68] J. Zak, *Berry's phase for energy bands in solids*, Physical Review Letters **62**, 2747 (1989), **doi:**10.1103/physrevlett.62.2747. (Cited on page 88.)

[69] M. Atala, M. Aidelsburger, J. T. Barreiro, D. Abanin, T. Kitagawa, E. Demler and I. Bloch, *Direct measurement of the Zak phase in topological Bloch bands*, Nature Physics **9**, 795 (2013), **doi:**10.1038/nphys2790. (Cited on page 89.)

[70] S. de Léséleuc, V. Lienhard, P. Scholl, D. Barredo, S. Weber, N. Lang, H. P. Büchler, T. Lahaye and A. Browaeys, *Observation of a symmetry-protected topological phase of interacting bosons with rydberg atoms*, Science **365**(6455), 775 (2019), **doi:**10.1126/science.aav9105. (Cited on page 94.)

[71] N. Lang and H. P. Büchler, *Topological networks for quantum communication between distant qubits*, npj Quantum Information **3**(1), 47 (2017), **doi:**10.1038/s41534-017-0047-x. (Cited on page 94.)

[72] A. Y. Kitaev, *Unpaired Majorana fermions in quantum wires*, Physics-Uspekhi **44**(10S), 131 (2001), **doi:**10.1070/1063-7869/44/10s/s29. (Cited on pages 96 and 102.)

[73] N. Lang, *Phase transitions and topological phases by driven dissipation*, Master's thesis, University of Stuttgart (2013). (Cited on page 96.)

[74] V. Mourik, K. Zuo, S. M. Frolov, S. R. Plissard, E. P. A. M. Bakkers and L. P. Kouwenhoven, *Signatures of Majorana fermions in hybrid superconductor-semiconductor nanowire devices*, Science **336**(6084), 1003 (2012), **doi:**10.1126/science.1222360. (Cited on page 97.)

[75] H. Zhang, C.-X. Liu, S. Gazibegovic, D. Xu, J. A. Logan, G. Wang, N. van Loo, J. D. S. Bommer, M. W. A. de Moor, D. Car, R. L. M. Op het Veld, P. J. van Veldhoven *et al.*, *Quantized Majorana conductance*, Nature **556**, 74 (2018), **doi:**10.1038/nature26142. (Cited on page 97.)

[76] M. R. Zirnbauer, *Particle–hole symmetries in condensed matter*, Journal of Mathematical Physics **62**(2), 021101 (2021), **doi:**10.1063/5.0035358. (Cited on page 101.)

[77] J. C. Budich and E. Ardonne, *Equivalent topological invariants for one-dimensional majorana wires in symmetry classD*, Physical Review B **88**(7), 075419 (2013), **doi:**10.1103/PhysRevB.88.075419. (Cited on page 103.)

[78] R. Wakatsuki, M. Ezawa, Y. Tanaka and N. Nagaosa, *Fermion fractionalization to majorana fermions in a dimerized kitaev superconductor*, Physical Review B **90**(1), 014505 (2014), **doi:**10.1103/PhysRevB.90.014505. (Cited on page 105.)

[79] S. Bravyi, B. M. Terhal and B. Leemhuis, *Majorana fermion codes*, New Journal of Physics **12**(8), 083039 (2010), **doi:**10.1088/1367-2630/12/8/083039. (Cited on page 108.)

[80] J. Alicea, Y. Oreg, G. Refael, F. von Oppen and M. P. A. Fisher, *Non-abelian statistics and topological quantum information processing in 1D wire networks*, Nature Physics **7**, 412 (2011), **doi:**10.1038/nphys1915. (Cited on page 108.)

[81] C. Nayak, S. H. Simon, A. Stern, M. Freedman and S. Das Sarma, *Non-abelian anyons and topological quantum computation*, Reviews of Modern Physics **80**, 1083 (2008), **doi:**10.1103/revmodphys.80.1083. (Cited on page 108.)

[82] L. Fu, *Topological crystalline insulators*, Physical Review Letters **106**, 106802 (2011), **doi:**10.1103/physrevlett.106.106802. (Cited on page 110.)

[83] C.-K. Chiu, H. Yao and S. Ryu, *Classification of topological insulators and superconductors in the presence of reflection symmetry*, Physical Review B **88**, 075142 (2013), **doi:**10.1103/physrevb.88.075142. (Cited on page 110.)

[84] T. Morimoto and A. Furusaki, *Topological classification with additional symmetries from Clifford algebras*, Physical Review B **88**, 125129 (2013), **doi:**10.1103/physrevb.88.125129. (Cited on page 110.)

[85] K. Shiozaki and M. Sato, *Topology of crystalline insulators and superconductors*, Physical Review B **90**, 165114 (2014), **doi:**10.1103/physrevb.90.165114. (Cited on page 110.)

↑ Notes

[86] P. Heinzner, A. Huckleberry and M. Zirnbauer, *Symmetry classes of disordered fermions*, Communications in Mathematical Physics **257**(3), 725 (2005), **doi:**`10.1007/s00220-005-1330-9`. (Cited on page 110.)

[87] S. Ryu, J. E. Moore and A. W. W. Ludwig, *Electromagnetic and gravitational responses and anomalies in topological insulators and superconductors*, Physical Review B **85**(4), 045104 (2012), **doi:**`10.1103/PhysRevB.85.045104`. (Cited on page 115.)

[88] T. Morimoto, A. Furusaki and C. Mudry, *Breakdown of the topological classification Z for gapped phases of noninteracting fermions by quartic interactions*, Physical Review B **92**(12), 125104 (2015), **doi:**`10.1103/PhysRevB.92.125104`. (Cited on pages 118 and 120.)

[89] S. Rachel, *Interacting topological insulators: a review*, Reports on Progress in Physics **81**(11), 116501 (2018), **doi:**`10.1088/1361-6633/aad6a6`. (Cited on page 118.)

[90] Q.-R. Wang and Z.-C. Gu, *Towards a complete classification of symmetry-protected topological phases for interacting fermions in three dimensions and a general group supercohomology theory*, Physical Review X **8**, 011055 (2018), **doi:**`10.1103/physrevx.8.011055`. (Cited on page 118.)

[91] L. Fidkowski and A. Kitaev, *Topological phases of fermions in one dimension*, Physical Review B **83**, 075103 (2011), **doi:**`10.1103/physrevb.83.075103`. (Cited on page 118.)

[92] A. M. Turner, F. Pollmann and E. Berg, *Topological phases of one-dimensional fermions: An entanglement point of view*, Physical Review B **83**, 075102 (2011), **doi:**`10.1103/physrevb.83.075102`. (Cited on page 118.)

[93] X. Chen, Z.-C. Gu and X.-G. Wen, *Complete classification of one-dimensional gapped quantum phases in interacting spin systems*, Physical Review B **84**, 235128 (2011), **doi:**`10.1103/physrevb.84.235128`. (Cited on page 118.)

[94] L. Fidkowski and A. Kitaev, *Effects of interactions on the topological classification of free fermion systems*, Physical Review B **81**, 134509 (2010), **doi:**`10.1103/physrevb.81.134509`. (Cited on pages 118 and 119.)

[95] R. Süsstrunk and S. D. Huber, *Observation of phononic helical edge states in a mechanical topological insulator*, Science **349**(6243), 47 (2015), **doi:**`10.1126/science.aab0239`. (Cited on pages 121, 122, 125, and 128.)

[96] S. D. Huber, *Topological mechanics*, Nature Physics **12**, 621 (2016), **doi:**`10.1038/nphys3801`. (Cited on pages 121 and 128.)

[97] R. Süsstrunk, P. Zimmermann and S. D. Huber, *Switchable topological phonon channels*, New Journal of Physics **19**(1), 015013 (2017), **doi:**`10.1088/1367-2630/aa591c`. (Cited on pages 127 and 128.)

[98] C. L. Kane and T. C. Lubensky, *Topological boundary modes in isostatic lattices*, Nature Physics **10**, 39 (2013), **doi:**`10.1038/nphys2835`. (Cited on page 128.)

[99] L. M. Nash, D. Kleckner, A. Read, V. Vitelli, A. M. Turner and W. T. M. Irvine, *Topological mechanics of gyroscopic metamaterials*, Proceedings of the National Academy of Sciences **112**(47), 14495 (2015), **doi:**`10.1073/pnas.1507413112`. (Cited on page 128.)

[100] P. Wang, L. Lu and K. Bertoldi, *Topological phononic crystals with one-way elastic edge waves*, Physical Review Letters **115**, 104302 (2015), **doi:**`10.1103/physrevlett.115.104302`. (Cited on page 128.)

[101] M. Serra-Garcia, V. Peri, R. Süsstrunk, O. R. Bilal, T. Larsen, L. G. Villanueva and S. D. Huber, *Observation of a phononic quadrupole topological insulator*, Nature **555**, 342 (2018), **doi:**`10.1038/nature25156`. (Cited on page 128.)

[102] Z. Yang, F. Gao, X. Shi, X. Lin, Z. Gao, Y. Chong and B. Zhang, *Topological acoustics*, Physical Review Letters **114**, 114301 (2015), **doi:**`10.1103/physrevlett.114.114301`. (Cited on page 128.)

[103] Y. Ding, Y. Peng, Y. Zhu, X. Fan, J. Yang, B. Liang, X. Zhu, X. Wan and J. Cheng, *Experimental demonstration of acoustic Chern insulators*, Physical Review Letters **122**, 014302 (2019), **doi:**`10.1103/physrevlett.122.014302`. (Cited on page 128.)

[104] L. Lu, J. D. Joannopoulos and M. Soljačić, *Topological photonics*, Nature Photonics **8**, 821 (2014), **doi:**`10.1038/nphoton.2014.248`. (Cited on page 128.)

[105] F. D. M. Haldane and S. Raghu, *Possible realization of directional optical waveguides in photonic crystals with broken time-reversal symmetry*, Physical Review Letters **100**, 013904 (2008), **doi:**`10.1103/physrevlett.100.013904`. (Cited on page 128.)

[106] S. Raghu and F. D. M. Haldane, *Analogs of quantum-Hall-effect edge states in photonic crystals*, Physical Review A **78**, 033834 (2008), **doi:**`10.1103/physreva.78.033834`. (Cited on page 128.)

[107] Z. Wang, Y. Chong, J. D. Joannopoulos and M. Soljačić, *Observation of unidirectional backscattering-immune topological electromagnetic states*, Nature **461**, 772 (2009), **doi:**`10.1038/nature08293`. (Cited on page 128.)

[108] M. C. Rechtsman, J. M. Zeuner, Y. Plotnik, Y. Lumer, D. Podolsky, F. Dreisow, S. Nolte, M. Segev and A. Szameit, *Photonic Floquet topological insulators*, Nature **496**, 196 (2013), **doi:**`10.1038/nature12066`. (Cited on page 128.)

[109] M. Hafezi, S. Mittal, J. Fan, A. Migdall and J. M. Taylor, *Imaging topological edge states in silicon photonics*, Nature Photonics **7**, 1001 (2013), **doi:**`10.1038/nphoton.2013.274`. (Cited on page 128.)

[110] B. Bahari, A. Ndao, F. Vallini, A. El Amili, Y. Fainman and B. Kanté, *Nonreciprocal lasing in topological cavities of arbitrary geometries*, Science **358**(6363), 636 (2017), **doi:**`10.1126/science.aao4551`. (Cited on page 128.)

[111] G. Harari, M. A. Bandres, Y. Lumer, M. C. Rechtsman, Y. D. Chong, M. Khajavikhan, D. N. Christodoulides and M. Segev, *Topological insulator laser: Theory*, Science **359**, eaar4003 (2018), **doi:**`10.1126/science.aar4003`. (Cited on page 128.)

[112] M. A. Bandres, S. Wittek, G. Harari, M. Parto, J. Ren, M. Segev, D. N. Christodoulides and M. Khajavikhan, *Topological insulator laser: Experiments*, Science **359**, eaar4005 (2018), **doi:**`10.1126/science.aar4005`. (Cited on page 128.)

[113] C. H. Lee, S. Imhof, C. Berger, F. Bayer, J. Brehm, L. W. Molenkamp, T. Kiessling and R. Thomale, *Topolectrical circuits*, Communications Physics **1**(1), 39 (2018), **doi:**`10.1038/s42005-018-0035-2`. (Cited on page 128.)

[114] J. Ningyuan, C. Owens, A. Sommer, D. Schuster and J. Simon, *Time- and site-resolved dynamics in a topological circuit*, Physical Review X **5**, 021031 (2015), **doi:**`10.1103/physrevx.5.021031`. (Cited on page 128.)

[115] C. W. Peterson, W. A. Benalcazar, T. L. Hughes and G. Bahl, *A quantized microwave quadrupole insulator with topologically protected corner states*, Nature **555**, 346 (2018), **doi:**`10.1038/nature25777`. (Cited on page 128.)

[116] S. Imhof, C. Berger, F. Bayer, J. Brehm, L. W. Molenkamp, T. Kiessling, F. Schindler, C. H. Lee, M. Greiter, T. Neupert and R. Thomale, *Topolectrical-circuit realization of topological corner modes*, Nature Physics **14**(9), 925 (2018), **doi:**`10.1038/s41567-018-0246-1`. (Cited on page 128.)

[117] P. Delplace, J. B. Marston and A. Venaille, *Topological origin of equatorial waves*, Science **358**(6366), 1075 (2017), **doi:**`10.1126/science.aan8819`. (Cited on page 128.)

↑ Notes